NORSK **KLIMA**SERVICE**SENTER**

NCCS report 1/2024

Sea-Level Rise and Extremes in Norway:

Observations and Projections Based on IPCC AR6

M.J.R. Simpson, A. Bonaduce, H.S. Borck, K. Breili, Ø. Breivik, O.R. Ravndal and K. Richter

Meteorologisk institutt
NVE
NORCE
Kartverket
BJERKNES CENTRE for Climate Research

The following institutions have contributed to this report and its associated data products:

Authors:

Matthew J.R. Simpson[1], Antonio Bonaduce[2,3], Hilde S. Borck[4], Kristian Breili[1], Øyvind Breivik[5], Oda R. Ravndal[4], Kristin Richter[3,6].

Affiliations:

1. Geodetic Institute, Norwegian Mapping Authority, 3507 Hønefoss, Norway.
2. Nansen Environmental and Remote Sensing Center.
3. Bjerknes Centre for Climate Research, Bergen, Norway.
4. Hydrographic Service, Norwegian Mapping Authority, 4021 Stavanger, Norway.
5. The Norwegian Meteorological Institute.
6. NORCE Norwegian Research Centre, Bergen, Norway.

Citation:

Simpson, M.J.R., Bonaduce, A., Borck, H.S., Breili, K., Breivik, Ø., Ravndal, O.R., Richter, K., 2024. Sea-Level Rise and Extremes in Norway: Observations and Projections Based on IPCC AR6. Norwegian Centre for Climate Services report 1/2024, ISSN 2704-1018, Oslo, Norway.

Corresponding author:

Matt Simpson (matthew.simpson@kartverket.no)

URL:

This report can be downloaded at www.klimaservicesenter.no

Commissioned by:

Miljø-
direktoratet

The Norwegian Centre for Climate Services (NCCS) is a collaboration between the Norwegian Meteorological Institute, the Norwegian Water Resources and Energy Directorate, the Norwegian Mapping Authority, NORCE, and the Bjerknes Centre for Climate Research. The main purpose of NCCS is to provide decision makers in Norway with relevant information for climate change adaptation. In addition to the partners, the Norwegian Environment Agency is represented on the Board. The NCCS report series includes reports where one or more authors are affiliated to the Centre, as well as reports initiated by the Centre. All reports in the series have undergone a professional assessment by at least one expert associated with the Centre. They may also be included in a report series from the institutions to which the authors are affiliated.

Title Sea-Level Rise and Extremes in Norway: Observations and Projections Based on IPCC AR6	Date 08.04.2024
ISSN nr. 2704-1018	**Report no.** No. 1/2024
Author(s) M.J.R. Simpson, A. Bonaduce, H.S. Borck, K. Breili, Ø. Breivik, O.R. Ravndal and K. Richter	**Classification** ● Free ○ Restricted
Client(s) Norwegian Environment Agency	**Client's reference** M-2748|2024

Abstract

Greenhouse gas emissions from human activity, primarily resulting from the burning of fossil fuels, are causing our climate to warm. As a result of this, glaciers and the Greenland and Antarctic ice sheets are losing mass and the oceans are warming, causing global sea-level rise. This represents a growing risk that coastal countries, including Norway, will have to adapt to.

Owing to vertical land uplift, Norway has long had falling or stable relative sea levels. However, results from this report show that sea-level rise is starting to push up water levels in some parts of the coast, most notably in Western and Southern Norway. Owing to global warming, Norway is transitioning from a country with on average falling or stable relative sea level, to one with rising relative sea levels. Measured coastal average geocentric (the ocean surface) sea-level rise is 2.3 ± 0.3 mm/yr for the period 1960-2022, i.e., an increase of 14 ± 2 cm over that time.

Projections based on IPCC AR6 show Norway's coastal average relative sea-level change for 2100, compared to the period 1995-2014, will range from 0.13 m (*likely* -0.12 to 0.41 m) for the very low emissions scenario (SSP1-1.9) to 0.46 m (*likely* 0.21 to 0.79 m) for the very high emissions scenario (SSP5-8.5). Projected local sea-level change will deviate from Norway's coastal average largely because of geographical differences in vertical land motion.

For the very high emissions scenario (SSP5-8.5), and a low-likelihood high-impact storyline of rapid ice-sheet mass loss, coastal average relative sea-level change for Norway could approach between 1 and 1.5 m by 2100. Shortly after 2100, massive ice loss from Antarctica could rapidly increase Norway's coastal average relative sea level to between 4.5 and 5 m by 2150. This is a storyline that cannot be ruled out and is particularly relevant for users with low risk tolerance.

Sea-level rise will increase flood risk in Norway by pushing up the height of sea level extremes (the combination of tides, storm surges, and waves) which will reach higher and further inland. Sea-level rise will also drive sharp increases in flooding frequency; this means that, unless timely adaptation measures are taken, flooding will develop into a chronic problem.

Projected changes to the strength and frequency of storms suggest that some of the most extreme wave and storm surge events will become more severe in future. However, there is low confidence in these projected changes. Projections also indicate that the wave climate in the Barents Sea and along the coasts of Northern Norway will become more severe as a result of Arctic sea ice retreat (a robust finding).

Keywords
Sea-level rise, tide gauges, altimetry, vertical land motion, projections, extreme still water levels, extreme value analysis, storm surges, waves

Disciplinary signature

Responsible signature

Sammendrag på Norsk

Menneskeskapte klimaendringer gjør at havnivået stiger flere steder i verden. Havnivåstigningen er dessuten akselererende. Dette innebærer en økende risiko som kystnasjoner må tilpasse seg, også Norge.

På grunn av havets og innlandsisens lange responstid på et varmere klima, gjør dagens klimagassutslipp at havnivåstigningen vil fortsette i flere hundre til tusener av år. Havnivåstigning er derfor en langsiktig utfordring som må håndteres over flere generasjoner. For å unngå de mest dramatiske konsekvensene i fremtiden, må dagens utslipp reduseres kraftig. Store utslippskutt vil begrense ytterligere akselerasjon i havnivåstigningen og redusere risikoen for at innlandsisen på Grønland og i Antarktis krysser vippepunkter som vil føre til flere meter med havnivåstigning. En slik økning i havnivået vil være permanent, det vil si irreversibel på menneskelige tidsskalaer, og svært vanskelig å tilpasse seg.

Formålet med denne rapporten er å gi et kunnskapsgrunnlag for politikere og beslutningstakere som arbeider med utslippsreduserende tiltak og tilpasningsstrategier for kystplanlegging i Norge. Endringer i havnivå og ekstreme vannstandsnivåer vil få konsekvenser for hvordan havet påvirker kystsonen og representerer en økende risiko for mennesker og naturmiljøet.

Det er flere faktorer som teller i Norges favør når man vurderer eksponering og sårbarhet for havnivåstigning. Kysten er generelt bratt og steinete, og landheving etter siste istid motvirker havnivåstigningen. Dette innebærer at Norge gjennom historien har hatt ganske stabilt eller til og med fallende relativt havnivå. I motsetning til mange andre kystnasjoner, har derfor Norge til nå ikke erfart konsekvensene av havnivåstigning. Faren er at dette kan skape en falsk trygghetsfølelse, der den langsiktige risikoen ikke er tilstrekkelig forstått eller til og med ignorert.

Resultatene fra denne rapporten viser at havnivåstigningen allerede påvirker vannstanden i enkelte deler av landet, særlig på Vest- og Sørlandet. På grunn av global oppvarming, er Norge i ferd med å gå fra å være et land med gjennomsnittlig fallende eller stabilt havnivå til et land med stigende havnivå. Jo høyere oppvarming desto raskere havnivåstigning, og mer av landet vil oppleve netto relativ havnivåstigning.

Havnivåstigning vil føre til at flom skapt av ekstrem vannstand når høyere og lenger inn på land. Selv om bratt topografi ofte begrenser flom fra havet, gjør Norges lange og varierte kystlinje at forholdsvis store områder likevel kan være utsatt. Kystbyer og en betydelig mengde infrastruktur er i faresonen. Havnivåstigning vil også føre med seg en kraftig økning i flomfrekvens: En havnivåstigning på eksempelvis 0,1 m vil føre til en tredobling av flomrisikoen mange steder. Dette betyr at hvis ikke

tilpasningstiltak iverksettes i tide, så vil flom utvikle seg til å bli et hyppig forekommende problem.

Kunnskapsgrunnlaget om havnivåstigning blir stadig forbedret og anslagene for framtidig havnivåstigning er derfor også i utvikling. Imidlertid er det fortsatt vanskelig å tallfeste enkelte usikkerheter fordi de bakenforliggende prosessene ikke er godt forstått (gjerne referert til som dyp usikkerhet knyttet til prosesser på og i ytterkant av innlandsisen). Alt dette taler for å ha en fleksibel tilnærming, der kunnskapsgrunnlaget er i stadig utvikling og der vi er i stand til å håndtere potensielle overraskelser fra klimasystemet. I den forbindelse er det viktig å opprettholde og forbedre både nasjonal og global overvåking av havnivået. Forbedret overvåking av havnivået og systemer for tidlig varsling er viktig for å styrke kystsoneplanleggingen og utvikle tilpasningsstrategier i områder der havnivået øker.

De viktigste funnene i denne rapporten er:

Observert havnivå

- På grunn av global oppvarming fortsetter havnivået (havoverflaten) å stige langs norskekysten. Dette kalles det *geosentriske* havnivået og tar ikke hensyn til landheving. I gjennomsnitt har det geosentriske havnivået langs norskekysten steget med 2,3 ± 0,3 mm/år for perioden 1960-2022 og 3,3 ± 0,9 mm/år for perioden 1993-2022. Dette stemmer godt overens med den observerte globale gjennomsnittlige havnivåstigningen.
- *Landheving*, som følge av at isen trakk seg tilbake etter siste istid, reduserer virkningen av den geosentriske havnivåstigningen i ulik grad langs kysten. Målinger av vannstand langs norskekysten fra 1960 til 2022 viser at den relative havnivåendringen er negativ rundt Oslofjorden (med minimum -2,3 mm/år i Oslo hvor landhevingen er høy) og langs deler av kysten av Trøndelag og Nordland, og positiv langs deler av Vest- og Sørlandet (med maksimalt 1,3 mm/år i Måløy hvor landhevingen er lav). Rundt 60 % av kysten opplevde ingen vesentlig endring.

Framskrivninger av havnivået

- *Framskrivninger* eller *klimaprojeksjoner* forteller hvordan klimaet vil respondere på framtidige utslipp av klimagasser. For et scenario med svært lave utslipp (SSP1-1.9), viser framskrivninger basert på den sjette hovedrapporten fra FNs klimapanel (IPCC AR6) at det relative havnivået i Norge i gjennomsnitt vil være 0,13 m (-0,12 til 0,41 m) høyere i 2100 enn i perioden 1995-2014. For et svært høyt utslippsscenario (SSP5-8.5) vil det relative havnivået stige med 0,46 m (0,21 til 0,79 m) over tilsvarende periode. Denne økningen er mellom 40 % og 70 % lavere enn det anslåtte globale gjennomsnittet; en forskjell som kan forklares med pågående landheving i Norge og nærhet til Grønland og arktiske isbreer.

- Lokalt vil havnivåendringene avvike fra gjennomsnittet hovedsakelig som følge av geografiske forskjeller i landheving. Anslåtte relative havnivåendringer for 2100 på seks utvalgte steder er:

Framskrevet havnivåendring for 2100	SSP1-1.9 Median (Sannsynlig utfallsrom)	SSP1-2.6 Median (Sannsynlig utfallsrom)	SSP3-7.0 Median (Sannsynlig utfallsrom)	SSP5-8.5 Median (Sannsynlig utfallsrom)	SSP5-8.5 Lav sannsynlighet - stor konsekvens
Oslo	-0.05 (-0.30 to 0.23)	0.01 (-0.19 to 0.25)	0.21 (-0.02 to 0.50)	0.32 (0.07 to 0.64)	0.84 og 1.56
Stavanger	0.28 (0.02 to 0.57)	0.33 (0.10 to 0.60)	0.55 (0.30 to 0.85)	0.65 (0.38 to 0.99)	1.19 og 1.92
Bergen	0.25 (-0.02 to 0.53)	0.30 (0.08 to 0.56)	0.51 (0.26 to 0.81)	0.61 (0.35 to 0.94)	1.14 og 1.85
Heimsjø	0.07 (-0.17 to 0.35)	0.12 (-0.11 to 0.37)	0.30 (0.06 to 0.60)	0.41 (0.15 to 0.73)	0.93 og 1.60
Tromsø	0.14 (-0.12 to 0.42)	0.16 (-0.07 to 0.43)	0.34 (0.09 to 0.65)	0.44 (0.18 to 0.77)	0.96 og 1.59
Honningsvåg	0.19 (-0.04 to 0.45)	0.20 (-0.03 to 0.47)	0.39 (0.15 to 0.69)	0.49 (0.24 to 0.81)	1.01 og 1.65

Tabell 3.1 fra kapittel 3: Framskrevet relativ havnivåendring (oppgitt i meter) fram mot 2100 i forhold til perioden 1995-2014. Median (50 %) og sannsynlig utfallsrom (17-83 %; det vil si de midtre to tredjedeler av utfallsrommet) er gitt for framskrivninger med middels faglig sikkerhet og for ulike utslippsscenarioer. For det svært høye utslippsscenarioet SSP5-8.5 vises også tall for et utfall med lav sannsynlighet, men stor konsekvens, som innebærer raskere istap fra innlandsisen i Antarktis (gitt som 83 og 95 prosentiler av fremskrivningene med lav faglig sikkerhet).

- For det lave utslippsscenarioet (SSP1-2.6) vil store deler av Vest- og Sør-Norge, samt en liten del av Nord-Norge, sannsynligvis (17-83 prosentiler av utfallsrommet) oppleve relativ havnivåstigning fram mot 2100. For de resterende to tredjedeler av kysten, er det en mulighet for at havnivået vil holde seg stabilt under dette scenarioet. For scenarier med høyere klimagassutslipp enn SSP1-2.6, vil det meste av kysten sannsynligvis oppleve relativ havnivåstigning fram mot 2100. (Dette er framskrivninger med middels faglig sikkerhet.)
- For 2150 viser framskrivningene at det relative havnivået i Norge i gjennomsnitt vil stige med 0,16 m (-0,24 til 0,61 m) for SSP1-1.9 til 0,73 m (0,25 til 1,38 m) for SSP5-8.5. (Framskrivninger med middels faglig sikkerhet, gitt som median og 17 og 83 prosentiler.)

- For et scenario med lav sannsynlighet, men stor konsekvens, der svært høye utslipp (SSP5-8.5) kombineres med raskt istap i Antarktis, kan den gjennomsnittlige relative havnivåstigningen i Norge nærme seg mellom 1 og 1.5 m fram til 2100. Noen steder langs kysten, særlig Stavanger og Bergen, kan man oppleve nær 2 m havnivåstigning (se tabell 3.1). Kort tid etter 2100 kan massivt istap fra Antarktis raskt øke Norges gjennomsnittlige havnivåstigning til mellom 4,5 og 5 m innen 2150. Dette er et scenario som ikke kan utelukkes og er spesielt relevant for brukere med lav risikotoleranse. (Dette er framskrivninger med lav faglig sikkerhet, gitt som 83 og 95 prosentiler.)
- Ut fra dagens kunnskapsgrunnlag, kan vi ikke utelukke at raskt istap fra Antarktis også kan utløses av mindre utslippsintensive scenarier enn SSP5-8.5. Imidlertid er prosesser som gir et betydelig tap fra innlandsisen usannsynlig for SSP1-1.9 eller SSP1-2.6, i det minste innenfor tidsrammen fram til 2100. (Dette er framskrivninger med lav faglig sikkerhet.)
- For 2300 viser framskrivninger at den relative havnivåstigningen i Norge i gjennomsnitt vil stige med 0,35 m (-0,75 til 1,4 m) for SSP1-2.6 til 4,15 m (0,4 til 16 m) for SSP5-8.5. (Framskrivninger med lav faglig sikkerhet, gitt som median og 17 og 83 prosentiler.)

Fremtidig flomrisiko som følge av havnivåstigning

- Havnivåstigning vil bidra til å øke flomrisikoen i Norge ved at de ekstreme vannstandsnivåene blir høyere. Flom fra hav vil dermed nå høyere og lengre inn på land.
- Det er små forskjeller (0,3 til 0,6 m avhengig av sted) mellom vannstandsnivåer som inntreffer årlig og vannstandsnivåer som inntreffer i snitt hvert to-hundrede år. Dette viser at bare noen få desimeter havnivåstigning er nok til å gjøre dagens 200-årsnivåer til årlige for deler av kysten. Havnivåstigning vil derfor føre til at historisk sett sjeldne vannstandsnivåer nås hyppigere, til og med årlig eller enda hyppigere i fremtiden.
- Når og hvordan flomfrekvensen endrer seg, er avhengig av hvordan havnivåstigningen utvikler seg. For høyere utslippsscenarier, og dermed raskere og større fremtidig havnivåstigning, vil flomfrekvensen endres tidligere og være mer utbredt. Det er Vestlandet og Sørlandet som først vil oppleve økning i flomfrekvens.

Framskrivninger av stormflo og bølger

- Framskrivingene av ekstreme vannstandnivåer bestemmes først og fremst av framskrivingene av gjennomsnittlige endringer i havnivå. Endringer i stormenes styrke og hyppighet er av underordnet betydning. Mens framskrivninger viser at middelvinden for norskekysten kan avta, kan variansen bli større. Dette antyder at noen av de mest ekstreme bølge- og stormflohendelsene vil kunne bli mer alvorlige i fremtiden. Det er imidlertid lav faglig sikkerhet knyttet til disse anslåtte endringene.

- Framskrivninger tyder på at bølgeklimaet i Barentshavet og langs kysten av Nord-Norge vil bli mer kraftfullt. Dette er et resultat av tilbaketrekning av arktisk havis og dermed økt strøklengde (eng. fetch), noe som betyr at bølger kan bygge seg opp over et større område (større strøklengde).

Summary and key findings

Greenhouse gas emissions from human activity, primarily resulting from the burning of fossil fuels, are causing our climate to warm. As a result of this, global sea levels are rising. Furthermore, the rate of global sea-level rise is increasing; that is, it is accelerating. This represents a growing risk that coastal countries, including Norway, will have to adapt to.

Because of the long response times of the oceans and ice sheets to warming, today's greenhouse gas emissions have implications for future sea-level rise over hundreds to thousands of years. Sea-level rise is a long-term challenge that will have to be managed over multiple generations. Crucially, however, we can reduce the long-term risks by acting now, and implementing rapid and deep emission cuts. Major emission cuts will rein in further sea level acceleration, and reduce the risk that thresholds for the stability of the large ice sheets in Greenland and Antarctica are crossed; which would commit us to multiple metres of sea-level rise. These increases in sea level would be permanent, that is, irreversible on human timescales, and would present a profound adaptation challenge. Furthermore, some ice sheet tipping mechanisms can potentially drive rapid sea-level rise (multiple metres over hundred year timescales).

The purpose of this report is to provide a knowledge base for policy and decision makers working with mitigation and adaptation strategies for coastal planning in Norway. Changes to sea level and sea level extremes will lead to changes in coastal impacts. These changes represent a changing risk to human and natural systems.

There are several factors that count in Norway's favour when considering its exposure and vulnerability to sea-level rise. The coast is generally steep and rocky, and upwards vertical land motion acts against sea-level rise, meaning Norway has historically had rather stable or falling relative sea levels. Unlike other coastal countries, Norway is therefore yet to feel the impacts of sea-level rise. The danger is that this can foster a false sense of security, where the long-term risks are not understood or ignored.

The results from this report show that sea-level rise is starting to push up water levels in some parts of the country, most notably in Western and Southern Norway. Owing to global warming, Norway is transitioning from a country with on average falling or stable sea levels, to one with rising sea levels. For increasing levels of warming, sea-level rise will become faster, and more of the country will transition to relative sea-level rise.

Sea-level rise will cause flooding from sea level extremes to reach higher and further inland. Although flooding is often very localised, because of the steep topography, the sheer length and complexity of the coast means that in sum, quite a large area can be exposed. Coastal towns and cities, and a considerable amount of infrastructure, are at potential risk. Sea-level rise will also drive sharp increases in flooding frequency: A 0.1 m sea-level rise will lead to a *tripling* of the flood risk in many locations. This means that, unless timely adaptation measures are taken, flooding will develop into a chronic problem.

As understanding of sea level and sea level extremes improves and evolves, our knowledge base, and therefore climate change projections, will change over time. Improved understanding will lead to better constrained projections and hopefully narrower uncertainties. Some uncertainties, however, remain difficult to quantify because the processes are not well understood (referred to as deep uncertainty and associated with ice sheet processes). This all speaks to having a flexible approach to adaptation; where you have an evolving knowledge base and need to be able to react to potential surprises from the climate system. In this regard, it is important to maintain and improve monitoring of sea level. Improved monitoring and the establishment of early warning systems, both globally and nationally, are a vital part of developing adaptation strategies and better planning for sea-level rise.

The key findings from this report are:

Sea-level observations

- Because of global warming, geocentric sea level (the ocean surface) continues to rise along the Norwegian coast. Norway's coastal average geocentric sea-level rise is 2.3 ± 0.3 mm/yr for the period 1960-2022 and 3.3 ± 0.9 mm/yr for the period 1993-2022. This agrees well with the observed global mean sea-level rise.
- Vertical land uplift from glacial isostatic adjustment acts against geocentric sea-level rise to various degrees over the coastline: For the period 1960-2022, relative sea-level change from the national tide gauge network ranges from a fall around the Oslofjord and along parts of the coast of Trøndelag and Nordland (with a minimum of -2.3 mm/yr in Oslo) to a rise for parts of Western and Southern Norway (with a maximum of 1.3 mm/yr in Måløy). Around 60% of the coast experienced no significant change.

Sea-level projections

- Projections based on IPCC AR6 show Norway's coastal average relative sea-level change for 2100, relative to the period 1995-2014, will range from 0.13 m (*likely* -0.12 to 0.41 m) for the very low emissions scenario (SSP1-1.9) to 0.46 m (*likely* 0.21 to 0.79 m) for the very high emissions scenario (SSP5-8.5). This rise is between 40% and 70% lower than the projected global average; a difference that can be explained by ongoing vertical land motion in Norway and the close proximity of Greenland and Arctic glaciers. (*Medium confidence* projections given with median values and *likely* ranges.)

- Projected local sea-level change will deviate from Norway's coastal average largely because of geographical differences in vertical land motion. Projected relative sea-level changes for 2100 at six key locations are:

Projected sea-level change for 2100	SSP1-1.9 Median (*Likely* range)	SSP1-2.6 Median (*Likely* range)	SSP3-7.0 Median (*Likely* range)	SSP5-8.5 Median (*Likely* range)	SSP5-8.5 Low-likelihood high-impact
Oslo	-0.05 (-0.30 to 0.23)	0.01 (-0.19 to 0.25)	0.21 (-0.02 to 0.50)	0.32 (0.07 to 0.64)	0.84 and 1.56
Stavanger	0.28 (0.02 to 0.57)	0.33 (0.10 to 0.60)	0.55 (0.30 to 0.85)	0.65 (0.38 to 0.99)	1.19 and 1.92
Bergen	0.25 (-0.02 to 0.53)	0.30 (0.08 to 0.56)	0.51 (0.26 to 0.81)	0.61 (0.35 to 0.94)	1.14 and 1.85
Heimsjø	0.07 (-0.17 to 0.35)	0.12 (-0.11 to 0.37)	0.30 (0.06 to 0.60)	0.41 (0.15 to 0.73)	0.93 and 1.60
Tromsø	0.14 (-0.12 to 0.42)	0.16 (-0.07 to 0.43)	0.34 (0.09 to 0.65)	0.44 (0.18 to 0.77)	0.96 and 1.59
Honningsvåg	0.19 (-0.04 to 0.45)	0.20 (-0.03 to 0.47)	0.39 (0.15 to 0.69)	0.49 (0.24 to 0.81)	1.01 and 1.65

Table 3.1 from Chapter 3: Projected relative sea-level changes for 2100, relative to the period 1995-2014. Median values (50%) and *likely* ranges (17-83%; the central two-thirds of the probability distribution) are given for the *medium confidence* projections and for a selection of emission scenarios. For the very high emissions scenario SSP5-8.5, a low-likelihood high-impact storyline of rapid ice-sheet mass loss is shown (the 83rd and 95th percentiles of the *low confidence* projections). Units are in metres.

- For the low emissions scenario (SSP1-2.6), projections show large parts of Western and Southern Norway, as well as a small part of Northern Norway will *likely* experience relative sea-level rise for 2100. For the remaining two-thirds of the coast, sea levels have a chance of being kept stable under SSP1-2.6. For scenarios with higher greenhouse gas emissions than SSP1-2.6, a majority of the coast will *likely* experience relative sea-level rise for 2100. (*Medium confidence* projections.)
- For 2150, projections show coastal average relative sea-level change for Norway will range from 0.16 m (-0.24 to 0.61 m) under SSP1-1.9 to 0.73 m (0.25 to 1.38 m) under SSP5-8.5. (*Medium confidence* projections given with median values and 17-83% ranges.)
- For the very high emissions scenario (SSP5-8.5), and a low-likelihood high-impact storyline of rapid ice-sheet mass loss, coastal average relative

sea-level change for Norway could approach between 1 and 1.5 m by 2100. Some locations along the coast, notably Stavanger and Bergen, could experience close to 2 m (Table 3.1). Shortly after 2100, massive ice loss from Antarctica could rapidly increase Norway's coastal average sea level to between 4.5 and 5 m by 2150. This is a storyline that cannot be ruled out and is particularly relevant for users with low risk tolerance. (*Low confidence* projections given with 83rd and 95th percentiles.)

- Due to limited scientific understanding, we cannot rule out that rapid ice mass loss from Antarctica could also be triggered by emission scenarios below SSP5-8.5. However, processes that can drive rapid ice-sheet mass loss are unlikely to be significant for SSP1-1.9 or SSP1-2.6, at least within the timeframe of 2100. (*Low confidence* projections.)
- For 2300, projections show coastal average sea-level change for Norway will range from 0.35 m (-0.75 to 1.4 m) under SSP1-2.6 to 4.15 m (0.4 to 16 m) under SSP5-8.5. (*Low confidence* projections given with median values and 17-83% ranges.)

Future flood risk due to projected sea-level rise

- Sea-level rise will increase flood risk in Norway by pushing up the height of sea level extremes, which will reach higher and further inland.
- Small height differences (0.3 to 0.6 m depending on location) separate the 1-in-200 year extreme still water level and the once-a-year event. This shows that, in some areas of the coast, only a few decimeters of sea-level rise are required to drive a 200-fold increase in flooding frequency. Sea-level rise will therefore cause the height of historically rare extreme sea level events to be reached annually or more frequently in the future.
- There are large differences in the timing and extent of flooding frequency changes depending on projected sea level. For higher emission scenarios, and thus faster and larger future sea-level rises, flooding frequency increases occur earlier and are more widespread. Western and Southern Norway will experience increases in flooding frequency first.

Storm surge and wave projections

- Projected changes to sea level extremes are primarily determined by the projected mean sea-level change. Changes to the strength and frequency of storms are of secondary importance. While projections show that the mean wind speed for the Norwegian coast may decrease, the variance can get larger. This suggests that some of the most extreme wave and storm surge events will become more severe in future. However, there is low confidence in these projected changes.

- Projections indicate that the wave climate in the Barents Sea and along the coasts of Northern Norway will become more severe. This is a result of Arctic sea ice retreat and hence increased fetch, which means waves can build up over a larger stretch of water.

Contents

1 Introduction

Sea level is a key indicator of climate change. As the climate has warmed due to human activity, global mean sea level (GMSL) has risen too. The main drivers of GMSL rise are mass loss from glaciers and ice sheets, and ocean thermal expansion. It is a long-term change that indicates that we live in a warming world. Indeed, sea-level rise is one of the most obvious and visually striking signs of global warming.

On human timescales recent global sea-level rise is anomalous. The Sixth Assessment Report from the International Panel for Climate Change (IPCC AR6) concluded that GMSL rise during the past 100 years was faster than any other century in at least the last 3000 years (Fox-Kemper et al., 2021). Furthermore, the rate of global sea-level rise is increasing, that is, sea-level rise is accelerating. And because of the long response times of the oceans and ice sheets to warming, we expect global sea-level rise will continue beyond 2100 and for centuries to millennia to come.

GMSL rose around 0.2 m over the period 1901 to 2018 (Fox-Kemper et al., 2021). For this national report for Norway, we are mainly interested in local sea-level changes, and how they vary along the coast (Box 1.1). This requires an understanding of relative sea-level (RSL) change, which is the change in local sea surface heights with respect to the Earth's surface. Changes in RSL can be significantly different from the global mean because of vertical land motion (VLM) and other physical processes. RSL change is typically measured using tide gauges and is important for adaptation planning.

Box 1.1: Processes contributing to sea-level change and sea level extremes

Useful terms and abbreviations used in this report and adapted from Gregory et al. (2019) and Fox-Kemper et al. (2021).

Global mean sea level (GMSL) is the sea level averaged in time, to remove unwanted variability, and then averaged over the oceans. The main drivers of GMSL rise are mass loss from glaciers and ice sheets, and ocean thermal expansion.

Local sea-level change will deviate from the GMSL change due to processes acting on different time- and spatial scales (Fig. 1.1). Processes driving local sea-level change can be in the ocean, cryosphere, Earth, and atmosphere. **Relative sea-level (RSL)** change is the change in local sea surface heights with respect to the Earth's surface. RSL change is typically measured using tide gauges and is important for adaptation planning.

Geocentric sea-level change is the change in local mean sea surface height with respect to a terrestrial reference frame. This is the sea-level change as measured by satellites.

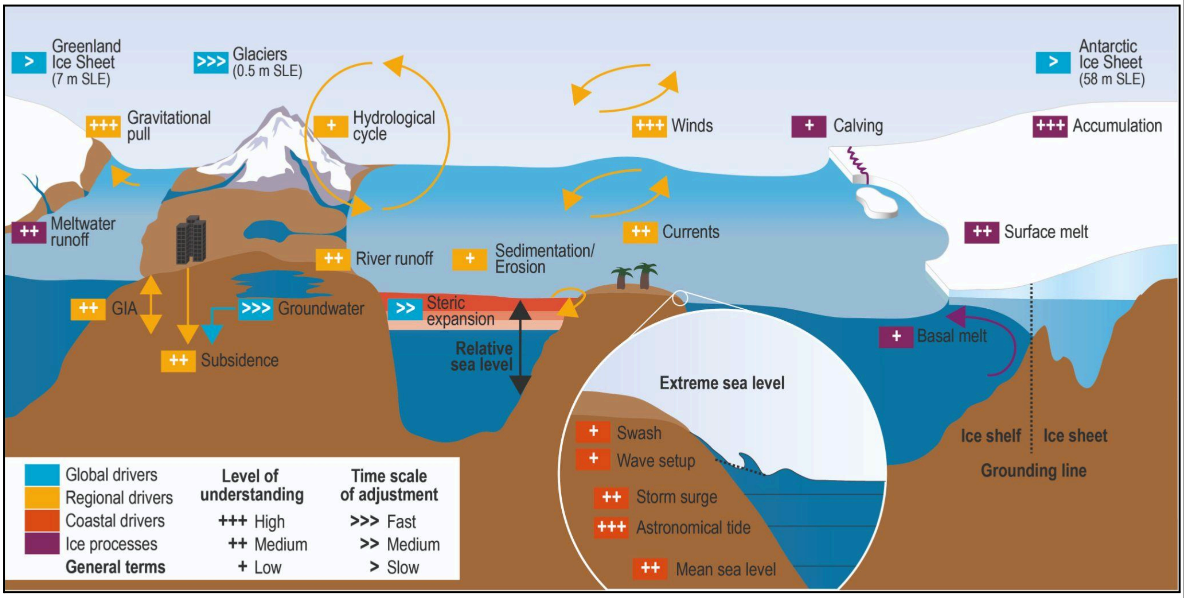

Figure 1.1: Processes contributing to sea-level change and sea level extremes. Figure taken from Oppenheimer et al. (2019).

Gravitation, rotation, and deformation (GRD) effects result from the movement of mass between terrestrial sources and the oceans. For an ice sheet losing mass, the weakening of the gravitational pull results in a relative sea-level fall within ~2000 km. GRD effects explain why Norway will receive a RSL change substantially less than the global average due to Greenland ice mass loss. Conversely, Norway will receive a RSL change above the global average due to Antarctic ice mass loss (see Chapter 3).

Glacial isostatic adjustment (GIA) is the ongoing GRD response to past ice mass changes. This is of special importance for Norway, where the Earth is still responding to the loss of the Northern European ice sheets ~10,000 years ago.

Vertical land motion (VLM) is the change in height of the Earth's surface. The broad pattern of regional VLM in Norway is caused by GIA. On local scales, however, processes like subsidence due to groundwater removal or sediment compaction can cause significant VLM changes.

Extreme sea level is a general description of the occurrence of exceptionally high local sea-surface heights from short-term effects (the combination of tides, storm surges, and waves). **Extreme still water levels (ESWLs)** are the combination of RSL change, tides, and storm surges. They do not include the effect of waves. Estimates of the return frequencies of ESWLs (e.g. the 1-in-100 year event) are a standard approach in coastal planning decisions.

Across many coastlines in the world, increases in RSL have acted to push up the heights of extreme sea levels (i.e., tides, storm surges, and waves) (Fox-Kemper et al., 2021). This has caused extreme sea levels to reach higher and further inland, thereby increasing our exposure to such events. Furthermore, areas already exposed to flooding have experienced more frequent inundation because of RSL rise (see e.g. Sweet et al. (2022) and references therein). As a rule of thumb, a 0.1 m increase in sea level will cause a *tripling* of the flooding frequency, meaning sea-level rise exponentially increases flooding frequency.

For coastal planning, the heights of extreme sea levels are typically estimated from tide gauge measurements using extreme value analysis. They are commonly expressed as return frequencies of extreme still water levels (ESWLs), which are the combination of RSL change, tides, and storm surges. ESWLs do not include the effects of waves (without waves they are quiet or still, hence the name). Following Norwegian planning law, residential buildings, for example, need to be built above or protected from the 1-in-200 year ESWL. A 1-in-200 year ESWL has a 0.5% annual probability or an expected rate of 0.005 events/year.

1.1 This national report and its associated data products

The purpose of this report is to provide a knowledge base for policy and decision makers working with mitigation and adaptation strategies in coastal planning for Norway. Changes to sea level and sea level extremes will lead to changes in coastal impacts. This represents a changing risk to human and natural systems. Secondly, the report provides input to the national climate assessment “Klima i Norge 2100”.

This report and its associated data products deal with the physical science of sea-level rise and extreme sea levels (e.g. how fast is sea level projected to rise?). The report is geographically limited to mainland Norway. The previous national report for Norway (Simpson et al., 2015; hereafter SLC2015) was based on IPCC AR5 (Church et al., 2013). The current report, hereafter SLR2024, is based on IPCC AR6. Where possible, we try to stick to the terminology used in IPCC AR6 and that by Gregory et al. (2019). Publications deemed relevant to this report and published post-AR6 have been included up until May 2023.

The report is broadly structured into three topics: Sea-level change, tides and storm surges, and waves. Waves were not included in SLC2015 so this is new to this report. Each topic is further divided into historical observations and projections. The sea-level projections are based on IPCC AR6. Projected changes to storm surges and waves are, however, largely based on literature review and/or IPCC AR5.

The report covers our understanding of sea-level rise and extreme sea levels for Norway, whereas the associated data products have a more practical application. For coastal municipalities, there are two main data products for planning that can be used “off-the-shelf” and are available as DOK (Det offentlige kartgrunnlaget - publicly available geodata for use in planning) datasets:

1. Sea level allowances based on IPCC AR6 projections.
2. Updated ESWLs for the return frequencies used in Norwegian planning law (1-in-20, 1-in-200, and 1-in-1000 year ESWLs corresponding to the F1, F2, and F3 safety classes). A new addition to this dataset is an estimated high-end ESWL (øvre estimat vannstand).

There is also a modelled historical wave climate product that can be used for coastal planning (Breivik et al., 2022). However, users should be aware that this wave product is for the open ocean, and therefore will need translating for use along the coast.

Data products for coastal municipality planning and for other applications are described in Chapter 8. Guidelines for how to use these data products in municipal planning will be given in a separate document and are the responsibility of The Norwegian Directorate for Civil Protection (DSB).

This national report represents the most up to date knowledge of sea-level rise and extreme sea levels for Norway. That said, it is important that users are aware of the following limitations of the report and its associated data products:

1. The IPCC AR6 based sea-level projections used in this report are based on climate model output (CMIP6) for a range of greenhouse gas emission scenarios (SSPs). The projections are therefore limited by the SSPs explored (Box 1.2), and the limitations and assumptions in the underlying climate and ice models (Box 1.3 and Chapter 3).
2. Local sea-level change can deviate significantly from the IPCC AR6 based projections because of missing processes. Processes like compaction and groundwater extraction can cause very localised VLM changes that have not been considered in IPCC AR6, nor in this report, meaning local RSL change can deviate from the projections.
3. The ESWLs presented in this report and used in Norwegian planning law assume that the causes of extreme sea levels (tides, storm surges, and waves) do not change over time. This ignores, for example, possible future changes to the strength and frequency of storms, which will in turn impact storm surges and waves. See Chapters 5 and 6 for discussion.
4. The available wave products are for the open ocean and need translating for use along the coast (Breivik et al., 2022). Local wave conditions are dependent on very local factors like the shape of the coastline, sheltering from islands, and the local wind field.
5. Possible interactions between sea level, storm surges, tides, and waves are not assessed in this report. For example, sea-level rise leads to increased water depths. This can cause changes to the way storm surges, tides, and waves interact along the coast (e.g., Arns et al., 2017).
6. Compound events, multiple hazards occuring at the same time, are not assessed in this report. An example of a compound event would be storm surge co-occurring with flooding from high rainfall at a river estuary location (e.g., Bevacqua et al., 2019).
7. Processes like erosion and human activities that cause changes to the coast are not accounted for in this report.

Box 1.2: Shared Socioeconomic Pathways (SSPs) and emission scenarios

Increasing amounts of greenhouse gases in the atmosphere will lead to more heat being trapped in the climate system. Shared Socioeconomic Pathways (SSPs) are the greenhouse gas emission scenarios explored in IPCC AR6 and referenced throughout this report (Table 1.1). They represent the climate forcing used to produce the sea-level projections. The five scenarios are referred to as SSPx-y, where x refers to the SSP pathway (SSP1 sustainability, SSP2 middle-of-the-road, SSP3 regional rivalry, SSP4 inequality, SSP5 fossil fuel-intensive) and y the radiative forcing (Watts/m^2) in 2100.

SSP	Emissions scenario	Best estimate of warming (2081-2100)	*Very likely* range (2081-2100)
SSP1-1.9	Very low emissions: Implies net zero emissions around 2050.	1.4 °C	1.0 to 1.8 °C
SSP1-2.6	Low emissions: Implies net zero emissions in the second half of the 21st century.	1.8 °C	1.3 to 2.4 °C
SSP2-4.5	Intermediate emissions: Current emissions remain stable until 2050, then fall but do not reach net zero by 2100.	2.7 °C	2.1 to 3.5 °C
SSP3-7.0	High emissions: Current emissions double by 2100.	3.6 °C	2.8 to 4.6 °C
SSP5-8.5	Very high emissions: Current emissions triple by 2075.	4.4 °C	3.3 to 5.7 °C

Table 1.1: Projected global warming for the Shared Socioeconomic Pathways and future greenhouse gas emission scenarios. Temperature increases are relative to the baseline period 1850-1900. Table adapted from IPCC (2021).

Box 1.3 Understanding the IPCC AR6-based sea-level projections presented in SLR2024

IPCC assessments use specific terms and language which are also used in this report for Norway. To help understand the findings of SLR2024, the IPCC's uncertainty language and its relevance for the sea-level projections are explained below.

IPCC reports use a calibrated uncertainty language where confidence is determined based on an assessment of the available evidence and agreement between different lines of evidence. If there is sufficient *confidence*, then a quantitative evaluation of the *likelihood* is made, expressed as probabilities (Box 1, Chen et al., 2021; Slangen et al., 2023). The text is italicised when referring to the IPCC's calibrated uncertainty language.

There are two sets of sea-level projections presented in this report and based on IPCC AR6 (see also Chapter 3):

- The *medium confidence* sea level projections which extend to 2150. These comprise of physical processes in whose projection there is at least *medium confidence*. The projections have a *likely* range, which refers to at least 66% probability (the range is typically expressed as the outer 17^{th}-83^{rd} percentiles). This range can be thought of as characterising the central two-thirds of the probability distribution under a given emissions scenario. In other words, there may be up to 34% probability that processes in which there is *medium confidence* can cause future sea level to lie outside the *likely* range.
- The *low confidence* sea level projections which extend to 2300. These projections are assessed as *low confidence* because of limited evidence and/or lack of agreement in that evidence. Subsequently no probability, that is, likelihood is evaluated (i.e. there is no *likely* range). Due to deep uncertainty in ice sheet processes it is not possible to ascribe a robust and meaningful probability to the AR6 *low confidence* projections. The *low confidence* sea level projections are new to the IPCC reports and include potential high-end ice sheet contributions. They represent useful planning scenarios for users with low risk tolerance to explore vulnerabilities and adaptation options. The *low confidence* projections are presented as a **low-likelihood, high-impact** storyline of rapid ice-sheet mass loss in the summary of this report.

1.2 Differences between this national sea level report (SLR2024) and the previous (SLC2015)

SLR2024 is based on IPCC AR6 (Fox-Kemper et al., 2021). Whereas, the previous national report, SLC2015 (Simpson et al., 2015), is based on IPCC AR5 (Church et al., 2013). The key differences between these reports, focussing on the sea-level projections and ESWLs, the two main data products for coastal planning, are summarised below.

1.2.1 Sea-level projections

SLR2024 is based on IPCC AR6, which uses CMIP6 climate model output and the SSP emission scenarios (Box 1.2). Whereas, SLC2015 is based on IPCC AR5, which uses CMIP5 climate model output and the RCP (Representative Concentration Pathways) emission scenarios. Comparing SLR2024 and SLC2015, there are differences between the emission scenarios, climate models, and methods used to project sea level (Slangen et al., 2023; Chapter 3). Key differences in the properties of the projections are summarised in Table 1.2 below:

	SLC2015 (based on IPCC AR5)	SLR2024 (based on IPCC AR6)	Notes
Reference period	1986-2005	1995-2014	
Type and length of projections	*Medium confidence* projections to 2100.	*Medium confidence* projections to 2150. *Low confidence* projections to 2300.	SLR2024 projections extend further into the future and include *low confidence* information.
Likely range	Given as the 5-95% model spread but interpreted as about 17-83% probabilities.	Central part of the distribution with at least two-thirds probability; encompassing 17-83% range.	Definition of *likely* range in AR5 and AR6 is broadly similar (representing central two-thirds of probability distribution) but not exactly the same.
Format	Given as one (or a few) numbers per coastal municipality.	Grid format (approximately 9 x 9 km).	See Chapter 8 for details.

Table 1.2: Key differences between the properties of the sea-level projections given in SLC2015 and SLR2024.

Results from Chapter 3.9 show projected *likely* sea level for Norway in SLR2024 is generally slightly higher than in the previous report SLC2015. Differences between the reports are less 0.1 m for 2090 and these differences are within uncertainties (comparison made using the same reference period 1995-2014). The projected *likely* ranges in SLR2024 and SLC2015 are therefore broadly similar.

SLR2024 includes *low confidence* sea-level projections which extend to 2300. These projections are presented as a low-likelihood, high-impact storyline of rapid ice-sheet mass loss. SLC2015 includes sea-level projections that account for an emerging Antarctic ice sheet collapse, but only up until 2100, and as an extra contribution of some tens of centimetres. What is new in SLR2024, therefore, is that under very high emissions (SSP5-8.5), the *low confidence* sea-level projections show massive Antarctic ice loss post-2100 could rapidly increase Norway's coastal average sea level to between 4.5 and 5 m by 2150 (see Chapter 3 for details). This is a key difference between SLR2024 (IPCC AR6) and SLC2015 (IPCC AR5).

1.2.2 Extreme still water levels

Present-day ESWLs are estimated using statistical analysis (extreme value analysis) of the tide gauge data (Chapter 4). Comparing SLR2024 and SLC2015, the same statistical method is used to calculate the ESWLs. From a user perspective, however, a major change is that the 2024 ESWLs are provided in the tidal zone format, whereas, in 2015, the ESWLs were given as one (or a few) numbers per coastal municipality.

Results from Chapter 4.3.1 show there are generally very small changes in the ESWLs between the 2015 and 2024 updates. The change in the 1-in-200 year ESWL at the tidal zones is generally less than ±0.05 m (Fig. 4.2 and 4.3). An exception to this is the area close to the Andenes tide gauge, which shows a reduction in the height of the 1-in-200 year ESWL of between 0.10 and 0.15 m. Differences in the ESWLs between 2015 and 2024 can be explained by (1) having 8 years of additional data for the extreme value analysis and (2) improvements to the observations and model used to quantify the tidal regime in areas away from the permanent tide gauges.

Users have raised the need for a high-end extreme still water level (øvre estimat vannstand). This is of relevance for buildings and infrastructure that are important for regional or national emergency response and preparedness. We therefore provide a high-end ESWL for use in planning; an estimate of a very rare event when the maximum tide coincides with a very large surge. This new estimate is a key difference between SLR2024 and SLC2015.

1.3 Norway's exposure to sea-level rise and use of this report in policy and decision making.

This report does not deal with questions around Norway's vulnerability and exposure to extreme sea levels and sea-level rise, which depend on things like topography, land use, and other factors. Nor does it address how the numbers in this report are used in risk assessment and adaptation planning (as mentioned above, guidelines for how to deal with sea-level rise in municipal planning are given by DSB). That said, we make the following clarifications for context and for the framing of this report.

Norway is generally less exposed and vulnerable to sea-level rise than other coastal nations (Aunan and Romstad, 2008; Breilli et al., 2020). On one hand, the coast is largely characterised by steep topography and an exposed bedrock that is resistant to erosion. On the other hand, the coastline is relatively long, being around 105,000 km in length, with fjords, inlets, and many thousands of islands. Flood mapping has shown many parts of the coast are vulnerable to local-scale flooding (Breili et al., 2020). Coastal towns and cities, and a considerable amount of infrastructure, are at risk over the long and complex coastline. Sea-level rise will cause an increase in the area, number of buildings, and length of roads exposed to storm surges (Table 1.3).

	Area (km^2)	Buildings	Roads (km)
Today	517	118,000	563
2090	767	151,000	1454
Increase	+250	+33,000	+891

Table 1.3: Exposure of Norway to a 1-in-200 year storm surge event today and in 2090. For 2090, sea-level projections are taken from SLC2015 (95th percentile of RCP8.5) and are equivalent to a GMSL rise of 0.82 m. Numbers of the area, buildings, and roads exposed are calculated following Breili et al. (2020) and updated as of January 2022.

To bridge the gap between those working with sea-level science and the end users of that information, it is important that there is a common understanding of the scientific knowledge-base and the needs of the users. Users should be involved from the start of the process, with co-production of the knowledge base, involving both sea level scientists and the users (e.g. Hinkel et al., 2019; Kopp et al., 2019). In an effort to do this, there has been an ongoing two-way dialogue between the report authors and the users; represented by the relevant directorates and municipalities in a reference group.

Coastal climate adaptation decisions are informed by the time horizon of interest and the uncertainty tolerance of the users (Hinkel et al., 2019). In general, because of the uncertain nature of climate change, coastal climate adaptation can benefit from a flexible or adaptive approach to decision making (e.g. Haasnoot et al., 2013;

Ranger et al., 2013; Haasnoot et al., 2020). New Zealand is an example of such an adaptive approach applied at a national level (Lawrence et al., 2018).

In particular, we highlight the different decision making frameworks that can be applied to coastal climate adaptation (see e.g. Hinkel et al., 2019; Kopp et al., 2019). These studies show that in some cases it may be more appropriate to apply a "decision first" framework to coastal adaptation - rather than a more traditional approach of starting with sea level science. There has been little focus on such decision making frameworks in Norway.

In finding an appropriate planning response for Norway, we suggest that new developments in coastal climate adaptation are looked at. However, any guidelines should also acknowledge Norway's specific exposure and vulnerabilities, and other aspects such as the ease of use of such information, and the resources available to planners.

2 Sea-level observations

In this chapter we first give updated estimates of vertical land movement in Norway. Following this, observed RSL changes from Norway's tide gauge network are analysed. Estimates of geocentric sea-level rise are also given and compared to results from satellite altimetry. Finally, the contributions to sea-level rise in Norway and the role of natural variability are discussed.

2.1 Key points

- Because of global warming, geocentric sea level (the ocean surface) continues to rise along the Norwegian coast.
- Vertical land uplift from glacial isostatic adjustment acts against sea-level rise to various degrees over the coastline: For the period 1960-2022, *relative* sea-level change from the national tide gauge network ranges from -2.3 mm/yr in Oslo to a rise of 1.3 mm/yr in Måløy.
- Geographical differences in relative sea-level change over 1960 to 2022 show that; areas around Oslofjord and parts of the coast of Trøndelag and Nordland underwent relative sea-level fall, whereas parts of Western and Southern Norway experienced a rise. Around 60% of the coast experienced no significant change (i.e., geocentric sea-level rise and vertical land motion have been in balance).
- Coastal average relative sea-level change is -0.3 mm/yr (-1.1 to 0.4) (66% range) for 1960 to 2022 and 0.7 mm/yr (-0.5 to 1.8) (66% range) for 1993 to 2022. Coastal average relative sea level has therefore been stable over the past ~60 years.
- Norway's coastal average geocentric sea-level rise estimated from the national tide gauge network is 2.3 ± 0.3 mm/yr (1960-2022) and 3.3 ± 0.9 mm/yr (1993-2022). For the latter period, this estimate agrees with independent observations from satellites.
- Coastal average geocentric sea-level rise over the past ~50 and ~30 years agrees well with the observed global mean sea-level rise. On shorter time scales, however, the impact of natural variability can lead to large deviations from global mean sea-level rise.
- While global mean sea-level rise has accelerated throughout the last century and recent decades, results for Norway are less conclusive. This is mainly due to the increased importance of natural variability on regional to local scales, masking the global signal, as well as Norway's proximity to Greenland and Arctic glaciers, making it less sensitive to ice mass loss from those regions.

2.2 Vertical land movement and glacial isostatic adjustment

When assessing RSL change it is important to account for vertical land motion. VLM can be caused by a number of processes that operate over different spatial- and timescales.

In Norway, the broad pattern of regional VLM is caused by the ongoing response of the Earth to the loss of the Northern European ice sheets ~10,000 years ago (a process known as Glacial Isostatic Adjustment, GIA). The Earth is still adjusting to the removal of this ice and, over century timescales, it can be assumed to have a near constant rate (a reasonable assumption for mainland Norway). Observations from precise levelling and GNSS (Global Navigation Satellite System) and modelling of VLM show that all of Norway is uplifting (Fig. 2.1, left panel; Vestøl et al., 2019), although deviations from this regional pattern can be expected on local scales (Box 2.1). Geographical differences in VLM largely explain why RSL change varies along the coastline.

As well as VLM, or deformation, there are gravitation and rotation effects associated with GIA that are also important for sea level (collectively known as GRD effects). These changes to the gravity field are largely driven by the movement of mantle material from the edges back towards the centre of the former ice sheet as the region uplifts. The movement of mass acts to increase gravitational attraction which, in turn, causes sea surface heights to increase. These changes are typically between 5 and 10% of the VLM signal so this is a relatively small effect (Fig. 2.1, central panel).

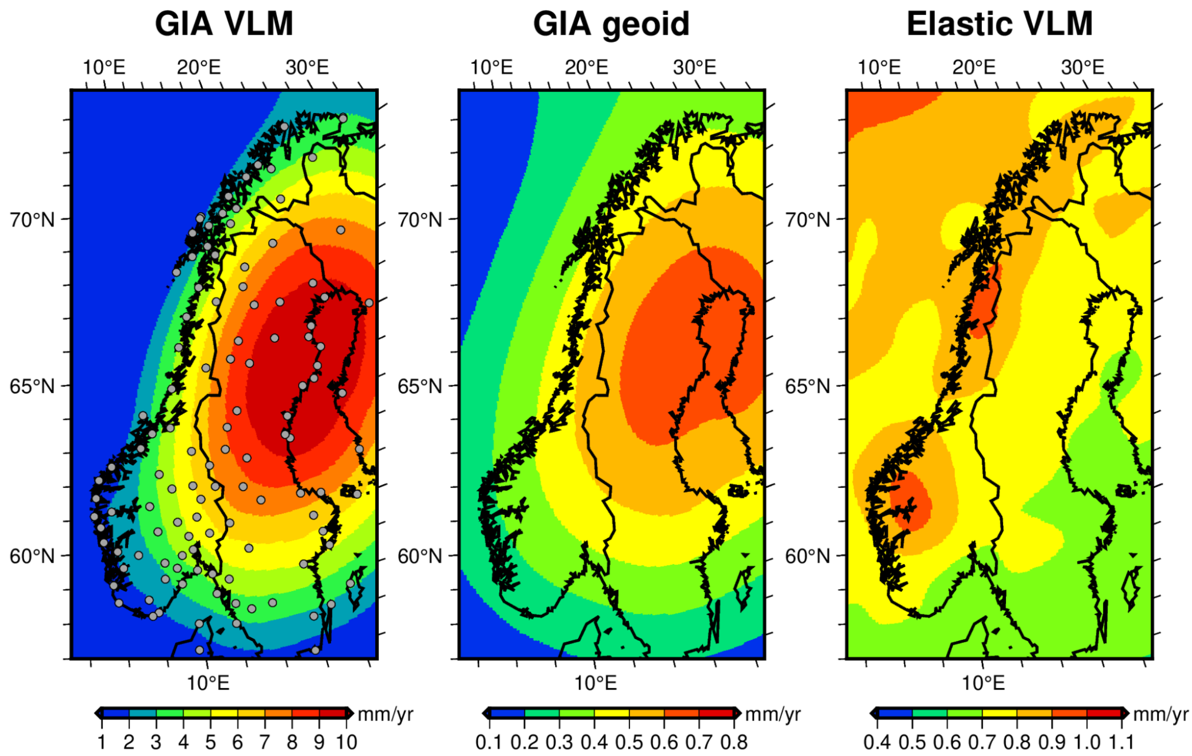

Figure 2.1: Left panel: Vertical land movement based on the semi-empirical NKG2016LU_abs model (Vestøl et al., 2019). Grey dots show the permanent GNSS network (Kierulf et al., 2021). Central panel: Modelled geoid changes associated with GIA. The sea surface approximately follows the geoid and, therefore, positive values indicate rising sea levels. Right panel: Elastic VLM driven by contemporary mass changes over the period 2000 to 2015, taken from Kierulf et al. (2021). Note that each panel has a different colorbar scale. GIA vertical land motion rates are an order of magnitude larger than geoid or elastic VLM processes.

Recent research has suggested a small but significant component of VLM in Norway is driven by present-day surface mass changes (e.g. Coulson et al., 2021; Kierulf et al., 2021; Ludwigsen et al., 2022). This elastic Earth response to a changing load is very fast (instantaneous) and therefore varies in its pattern and over time in accordance with the surface mass changes. The study of Kierulf et al. (2021) indicates that elastic VLM rates in Norway were up to 1 mm/yr over the period 2000 to 2015 (Fig. 2.1, right panel). These uplift rates are largely driven by Greenland and local glacier ice melt.

In this report, VLM estimates from the semi-empirical NKG2016LU model (Vestøl et al., 2019) are used to analyse the historical tide gauge observations (Section 2.3) and to build regional sea-level projections (Chapter 3). That is, it is assumed that the observed VLM rates were the same during the tide-gauge period, and will remain constant in the future. The total GIA contribution to RSL change is the sum of (1) the observed VLM field (Fig. 2.1, left panel) and (2) modelled GRD effects associated with GIA (Fig. 2.1, central panel). Elastic VLM is presumed to be included in the observed VLM field and we opt not to try and separate this effect. Rates of the GIA contribution to RSL change range between about 1 and 5 mm/yr along the coast. The coastal average GIA contribution to RSL change is -2.6 ± 1.0 mm/yr (1-sigma).

The NKG2016LU model provides uncertainties for the VLM rates but not for the modelled geoid change. Uncertainties for the VLM field are typically smaller than ±0.25 mm/yr for where we have observations and for mainland Norway. Uncertainties on the modelled geoid changes are neglected as they are much smaller. The VLM rates are given in the international terrestrial reference frame ITRF2008 (Altamimi et al., 2011). A review concluded that ITRF is stable along each axis to better than 0.5 mm/yr and has a scale error of less than 0.3 mm/yr (Collilieux et al., 2014). For the total error budget for the GIA contribution the NKG2016LU VLM and ITRF uncertainties are added in quadrature, under the assumption that they are independent.

While the regional pattern of VLM in Norway is dominated by GIA, there are other processes which can contribute to vertical land movement. These can cause significant deviations from the regional GIA contribution, especially on local scales. In the Ranafjord area, for example, neotectonics are thought to play a role in crustal deformation (Olesen et al., 2013; Kierulf, 2017). Furthermore, some coastal cities have highly localised areas of subsidence owing to compaction and/or groundwater changes (see Box 2.1).

Box 2.1: Vertical land motion and local deformations from InSAR

Vertical land motion can be caused by a number of processes that operate over different spatiotemporal scales and can be caused by human activity, natural processes, or climate change. While the regional pattern of VLM in Norway largely reflects GIA, there are other important processes that contribute to substantial vertical land movement. For example; GRD effects (see e.g. elastic GRD effects in Fig. 2.1), tectonics, volcanism, subsidence owing to groundwater or hydrocarbon removal, or sediment compaction.

Interferometric synthetic aperture radar (InSAR) is a technique which uses satellite radar to measure VLM with millimetre accuracy. InSAR can image the pattern of VLM and has good spatial coverage, allowing users to identify local areas of deformation. Users can access InSAR products for Norway using a webtool (Fig. 2.2).[1] Users should familiarise themselves with the background information, including the limitations of InSAR, before making any interpretations of the data.

[1] InSAR Norge (https://insar.ngu.no/) is a webtool hosted by The Geological Survey of Norway (NGU)

For example, in the context of sea level and climate adaptation work, it is important to be aware that InSAR is a *relative* technique and therefore VLM is measured relative to a local point. This is not the same as the GNSS data used to produce the NKG2016LU model, which are given in a geocentric reference frame and can be considered *absolute*.

InSAR has been successfully used to identify local subsidence along several parts of the Norwegian coast. Fig. 2.2 shows subsidence of around 10 mm/yr in the harbour area of Trondheim, thought to be caused by land reclamation over the past ~150 years. Subsidence acts to increase the rate of RSL rise. Furthermore, such local deformations are not included in the regional NKG2016LU model, meaning local sea-level change can deviate significantly from the projections given in this report.

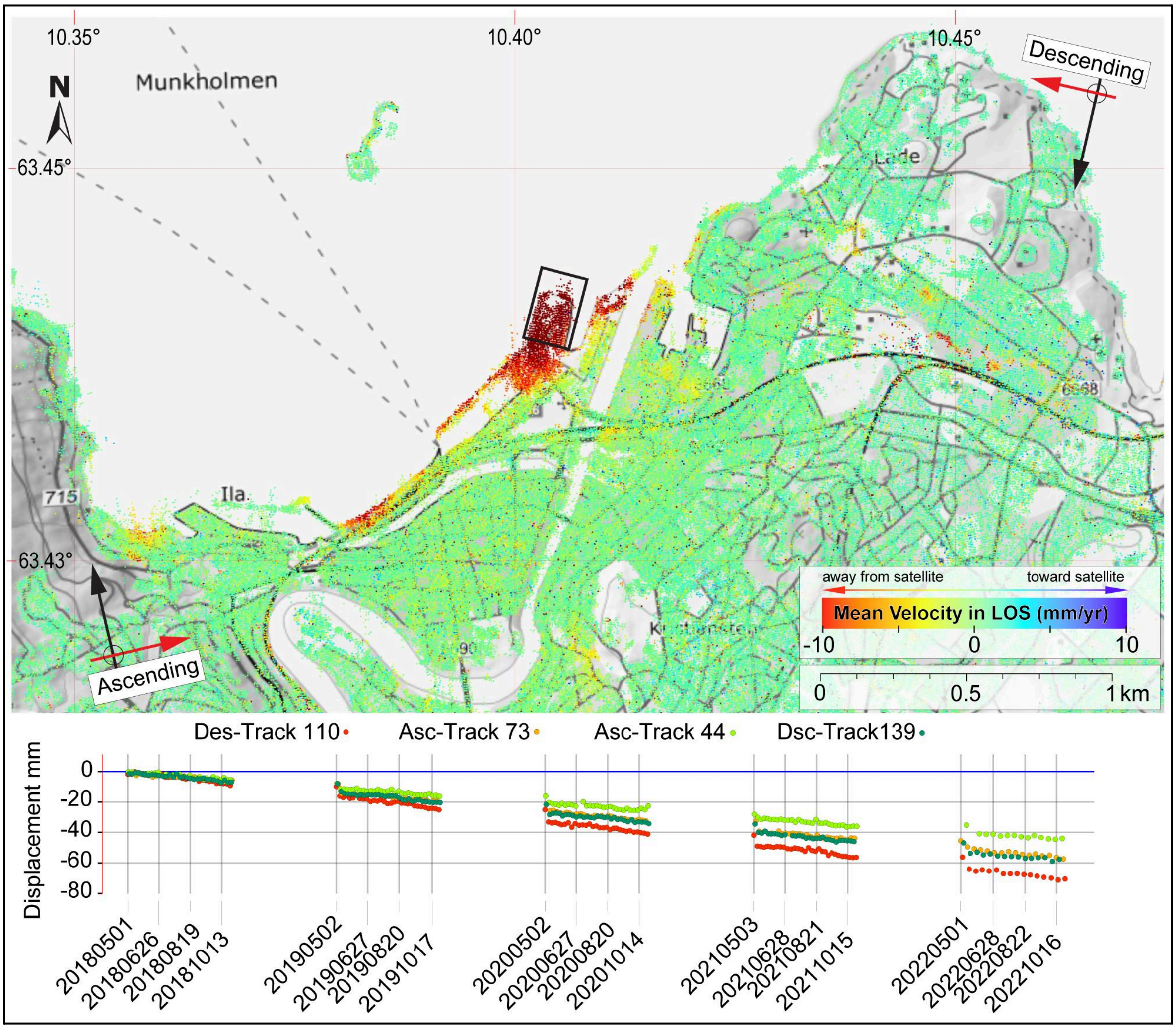

Figure 2.2: InSAR measurements used to identify local subsidence in the harbour area of Trondheim.

2.3 Observed sea-level changes

In this subchapter we present and analyse sea-level observations from tide gauges and satellite altimetry. We present all available data but the main trend analysis is performed for periods 1960-2022 and 1993-2022. We chose 1960-2022 as we have good data coverage from the tide gauge network from the start of this period and an understanding of the contributions to sea-level rise. We chose 1993-2022 to compare observations from tide gauges with altimetry, as well as to assess sea-level changes over the past 30 years. These choices also give some continuation from SLC2015 which analysed similar periods. However, for comparison with estimates of GMSL rise and other published estimates, we will adjust the periods whenever necessary. This will be made clear in the text.

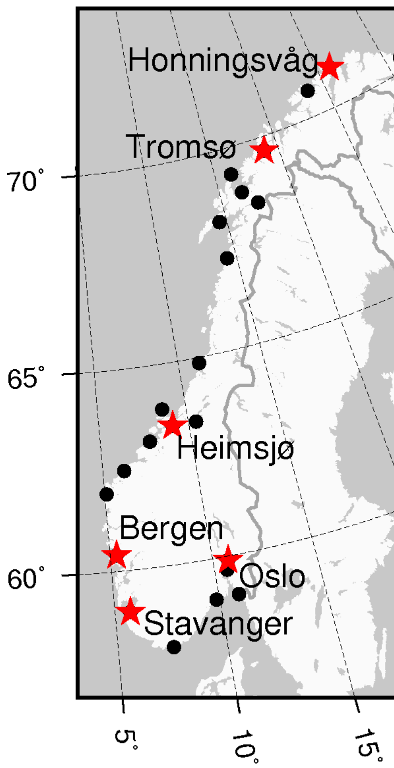

Figure 2.3: Location of tide gauges with at least 30 years of data. Named locations marked with a red star indicate the sites chosen as key locations in Chapter 3.

2.3.1 Analysis of tide gauge data

The Norwegian tide gauge network consists of 23 tide gauges that provide observations of RSL for varying periods of at least 30 years. The earliest observations date back to the end of the 19th century, but in this report we limit ourselves to measurements starting from 1960, when a reasonable coverage of the entire Norwegian coast is available. The locations of the tide gauges are shown in Fig. 2.3. Monthly sea level observations were obtained from the Permanent Service for Mean Sea Level (PSMSL) (Holgate et al. 2013) except for Mausund. Data from Mausund was at the time not yet available at PSMSL but was directly downloaded from the Norwegian Mapping Authority.

As this report is concerned with long-term changes in sea level, we did not analyse the seasonal cycle but removed it from the monthly data prior to analysis. Linear trends were computed using a simple linear regression model

$$z(t) = a + bt + \varepsilon(t)$$

where z(t) is the observation at time t, *a* is the intercept of the model, *b* is the rate (equivalent to the trend) and ε is the error. This is a simpler regression model than used in SLC2015, and we do not account for autocorrelation of the residuals. This might result in an underestimation of the standard errors. However, comparison with SLC2015 and Breili (2022) shows that the standard errors are similar for comparable periods. Linear trends were only computed when data was available for at least 80% of the considered period.

The study by Breili (2022) is the most comprehensive analysis of sea-level trends as observed by tide gauges since SLC2015. In the remainder of the chapter, results from that study will be presented when appropriate.

2.3.1.1 Estimates of sea-level trends from tide gauges along the coast of Norway

Fig. 2.4 shows observed annual sea level as well as the linear trends over the period 1960/1993 to 2022 for all operating tide gauges along the Norwegian coast. The trends are largely governed by the pattern of VLM as discussed in Section 2.2 (see also Fig. 2.5).

Due to relatively high VLM rates, RSL is falling in the southeast (Oscarsborg, Oslo) and along the coast of Trøndelag and Nordland (from Heimsjø to Narvik). The RSL decrease in Narvik is more pronounced as the tide gauge is located towards the head of a fjord further inland, and where land uplift rates are larger. At the tide gauges along the western coast (Stavanger to Ålesund), geocentric sea-level rise is larger than the relatively low land uplift rates. In this area RSL has therefore risen over the period 1960-2022. Note that trend estimates are dependent on the period examined. For tide gauges where the data extends back to the early 1900s or earlier there is a slightly different picture. For example, at the station in Bergen, the linear trend over the entire observational period (1916-2022) is 0 ± 0.2 mm/yr as opposed to 1.0 ± 0.3 mm/yr for the period 1960-2022. RSL rates have therefore been somewhat negative in the start of the record but positive after the 1960s.

It is worth noting that, at all stations in Fig. 2.4, the highest mean annual sea level this century occurred in 2020. At Tregde, Stavanger, Bergen and Måløy this was the highest observed annual sea level on record. February 2020 also saw a series of new record-high sea level extremes along western Norway.[2] This is an example of how interannual variability can lead to deviations from long-term trends (Section 2.5).

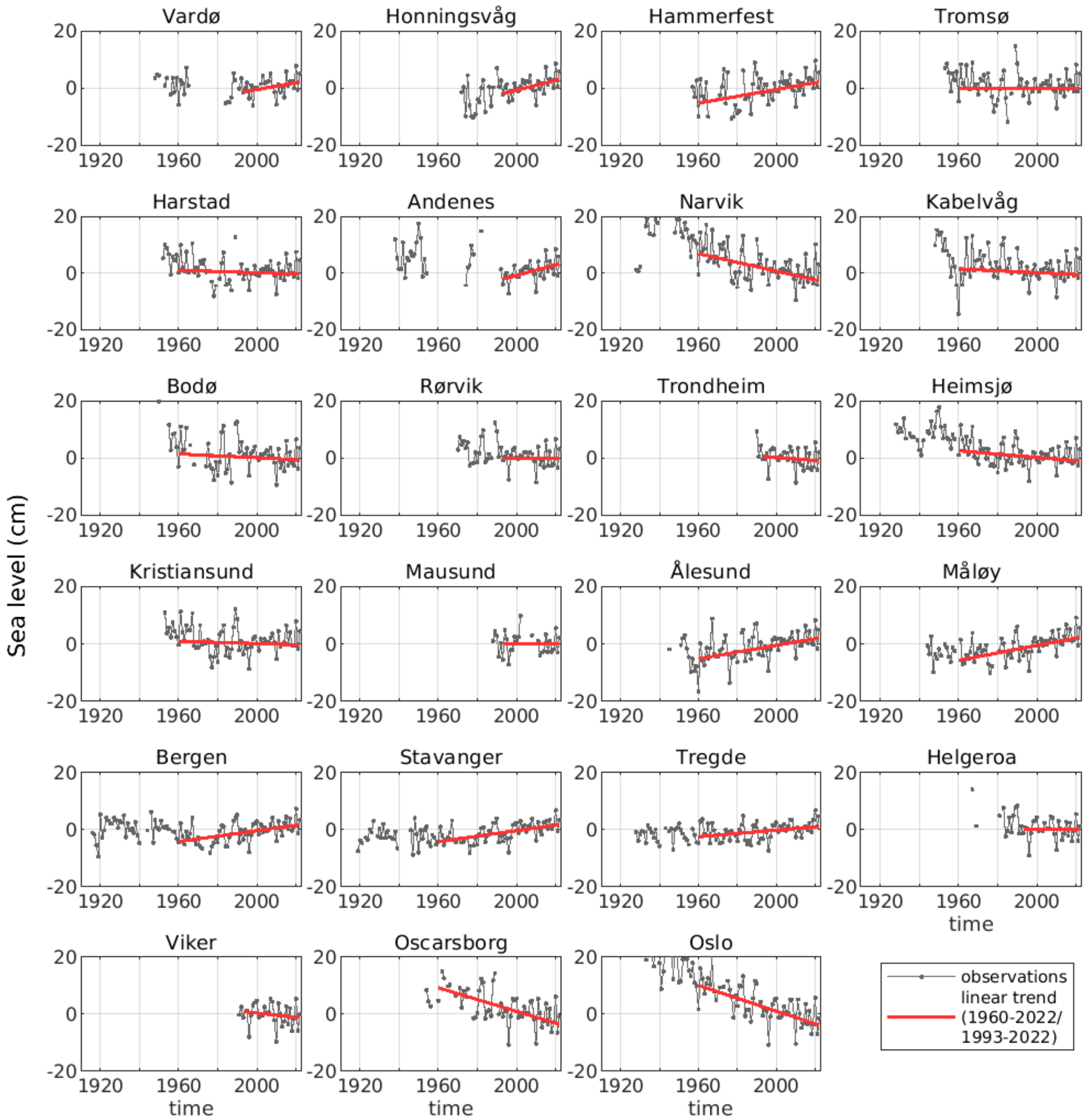

Figure 2.4: Time series of observed relative sea level for 23 tide gauges along the Norwegian coast. The red line in each panel represents the linear trend for the period 1960-2022 or - if not enough data is available 1993-2022 (see also Table 2.1). The reference period is 1995-2014, for consistency with the projections in Chapter 3.

---

[2] Record-high extreme sea level on 11th February 2020 at Måløy can be viewed here.

Tide gauge	1960-2022		1993-2022		1993-2021
	RSL (mm/yr)	Geocentric (mm/yr)	RSL (mm/yr)	Geocentric (mm/yr)	Altimetry (mm/yr)
Vardø	-	-	1.2 ± 1.0	3.9 ± 1.3	4.4 ± 0.9
Honningsvåg	-	-	1.7 ± 0.9	3.9 ± 1.2	4.1 ± 0.9
Hammerfest	1.2 ± 0.4	3.5 ± 0.8	1.8 ± 1.0	4.1 ± 1.2	4.0 ± 0.9
Tromsø	0.0 ± 0.3	2.5 ± 0.8	1.0 ± 1.0	3.6 ± 1.2	3.7 ± 0.9
Andenes	-	-	1.9 ± 0.9	3.2 ± 1.2	3.9 ± 0.9
Harstad	-0.2 ± 0.3	2.5 ± 0.8	1.0 ± 0.9	3.7 ± 1.2	4.0 ± 1.0
Narvik	-1.5 ± 0.4	2.5 ± 0.8	-0.6 ± 1.1	3.4 ± 1.3	4.1 ± 1.1
Kabelvåg	-0.3 ± 0.4	1.8 ± 0.9	1.1 ± 1.0	3.2 ± 1.3	4.2 ± 1.0
Bodø	-0.3 ± 0.4	3.2 ± 0.8	-0.5 ± 1.1	3.0 ± 1.3	4.2 ± 0.8
Rørvik	-	-	0.0 ± 1.0	3.7 ± 1.3	4.0 ± 0.8
Trondheim	-	-	-0.5 ± 1.0	3.7 ± 1.2	4.0 ± 0.8
Heimsjø	-0.6 ± 0.3	2.3 ± 0.8	0.9 ± 1.0	3.7 ± 1.2	4.0 ± 0.8
Kristiansund	-0.2 ± 0.3	1.7 ± 0.8	1.6 ± 1.0	3.5 ± 1.2	4.0 ± 0.8
Mausund	-	-	0.0 ± 1.1	2.1 ± 1.3	-
Ålesund	1.2 ± 0.3	2.4 ± 0.8	1.9 ± 1.0	3.2 ± 1.2	3.8 ± 0.8
Måløy	1.3 ± 0.3	2.3 ± 0.8	2.6 ± 0.9	3.6 ± 1.2	3.8 ± 0.8
Bergen	1.0 ± 0.3	2.5 ± 0.8	1.5 ± 0.8	3.0 ± 1.1	3.7 ± 0.7
Stavanger	1.0 ± 0.3	2.3 ± 0.8	1.7 ± 0.8	3.1 ± 1.1	3.7 ± 0.7
Tregde	0.6 ± 0.2	2.0 ± 0.8	1.4 ± 0.7	2.9 ± 1.0	3.7 ± 0.8
Helgeroa	-	-	0.0 ± 1.0	3.3 ± 1.2	3.6 ± 1.0
Viker	-	-	-0.7 ± 1.2	3.2 ± 1.4	3.6 ± 1.1
Oscarsborg	-2.1 ± 0.5	2.2 ± 0.9	-0.8 ± 1.4	3.4 ± 1.5	3.7 ± 1.0
Oslo	-2.3 ± 0.5	2.4 ± 0.8	-1.0 ± 1.4	3.6 ± 1.6	3.5 ± 1.0

Table 2.1: Relative (RSL) and geocentric (GIA-corrected) sea-level trend estimates from tide gauge observations along the Norwegian coast for the periods 1960-2022 and 1993-2022. For the latter period, trend estimates from satellite altimetry are also given over the period 1993-2021 when data was available at the time of writing.

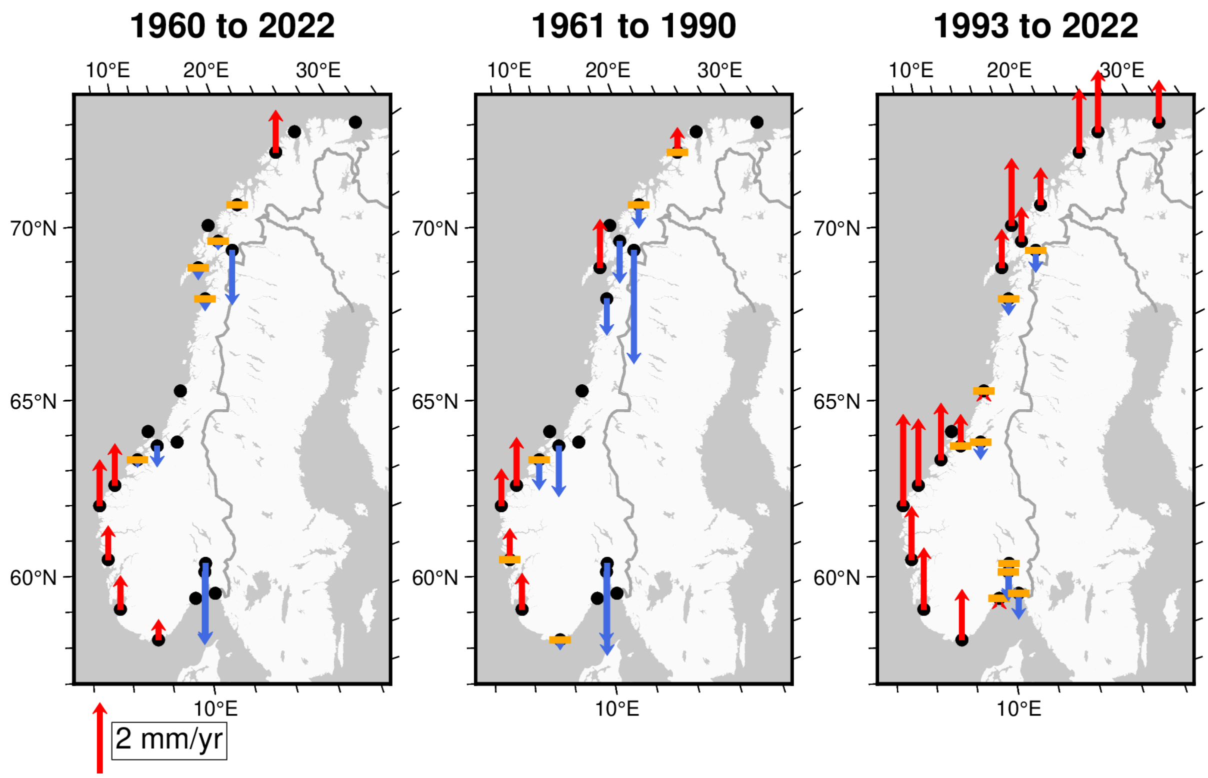

Figure 2.5: Relative sea-level rates at Norwegian tide gauges for the periods 1960-2022, 1961-1990 and 1993-2022. Rates that are not significantly different from zero are marked with an orange bar.

2.3.1.2 Coastal average geocentric and relative sea-level change

To obtain the geocentric sea-level change that can be compared to GMSL change and the sea level measured using altimetry from space, the tide gauge observations are corrected for GIA (Chapter 2.2). This results in positive geocentric sea-level trends, i.e. a sea-level rise, in all locations (Table 2.1). Compared to RSL trends, the rise is also more uniform along the Norwegian coast suggesting that it is meaningful to calculate the coastal average geocentric sea-level change for comparison with GMSL rise.

From the GIA-corrected observations the geocentric sea-level change along the entire Norwegian coast is estimated by performing a Principal Component Analysis (PCA). This analysis allows for extracting spatial patterns and their temporal evolution from a dataset consisting of different locations. Data gaps are filled randomly prior to the analysis and this process is repeated 100 times to account for the uncertainties introduced by missing data. The resulting range in the estimate of coastal mean sea level is very small (grey shading in Figure 2.6).

The coastal average geocentric sea-level rise along the Norwegian coast over the period 1960-2022 is 2.3 ± 0.3 mm/yr, higher than the trend estimated in SLC2015 for the period 1960-2010 (1.9 ± 0.6 mm/yr). Table 2.2 summarises how the mean trend along the Norwegian coast varies depending on the period considered and how it compares to SLC2015, as well as global trend estimates from the 6th Assessment Report by the IPCC. For 1971-2018, the trend in Norwegian mean sea level agrees with the trend in global mean sea level within uncertainties. This is also true for the shorter period 1993-2018. For the even shorter 13-yr period 2006-2018 Norwegian mean sea-level rise is smaller than GMSL rise (2.5 ± 3.0 versus 3.7 ± 0.5 mm/yr, respectively), however, extending the period to 2020 (by only two years) yields a sea-level rise of 3.9 ± 2.5 mm/yr along the Norwegian coastline. This emphasises the importance of natural climate variability (Chapter 2.5): On short time scales (years to 1-2 decades) it can have a significant impact on the trend estimates leading to large deviations from the global mean on regional to local scales. The uncertainties on the sea-level trends given in Table 2.2 reflect the growing importance of natural variability on shorter time scales (uncertainties are larger the shorter the chosen period) and over smaller spatial scales (uncertainties are larger on regional compared to global scales).

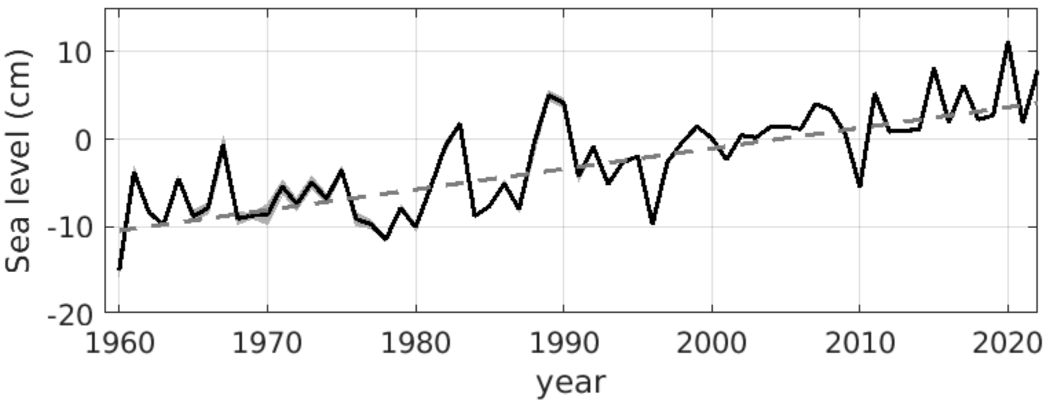

Figure 2.6: Coastal average geocentric sea-level change along the Norwegian coast inferred from Principal Component Analysis (PCA). The first Principal component is shown. It consists of a long-term trend and interannual variability representative for the entire Norwegian coast. The linear trend over the period 1960-2022 is also shown. For clarity, the data are presented as annual averages.

	1960-2010 (1960-2022)	1971-2018	1984-2014	1993-2018 (1991-2020)	1993-2022	2006-2018 (2006-2020)
NO-SLR2024 -TG	2.1 ± 0.4 (2.3 ± 0.3)	2.5 ± 0.4	2.3 ± 0.9	3.2 ± 1.1 (3.3 ± 0.9)	3.3 ± 0.9	2.5 ± 3.0 (3.9 ± 2.5)
NO-SLC2015 -TG	1.9 ± 0.6	-	2.4 ± 0.6	-	-	-
glob-AR6	-	2.3 ± 0.7	-	3.3 ± 0.4	-	3.7 ± 0.5
Breili (2022)	2.4 ± 0.4	-	-	(3.3 ± 0.4)	-	-

Table 2.2: Comparison of observed Norwegian mean sea-level trends for different periods and from different sources with observed global mean sea-level trends (glob-AR6). Trends have been corrected for glacial isostatic adjustment. NO-SLR2024 and NO-SLC2015 refer to mean Norwegian sea-level trends from this and the previous report, respectively.

To estimate coastal RSL change along the entire coastline instead of only at tide gauge locations, we add the geocentric sea-level trend (Fig. 2.6) to the GIA contribution along the coast. This assumes a uniform geocentric sea-level rise along the Norwegian coast which is reasonable as the variations in regional RSL change are dominated by the GIA contribution. Estimated coastal average RSL change is -0.3 mm/yr (-1.1 to 0.4) (66% range) for 1960 to 2022 and 0.7 mm/yr (-0.5 to 1.8) (66% range) for 1993 to 2022. Coastal average RSL change has therefore been somewhat stable, but as shown in Fig. 2.7, there are areas of the coast that have undergone significant RSL fall and rise.

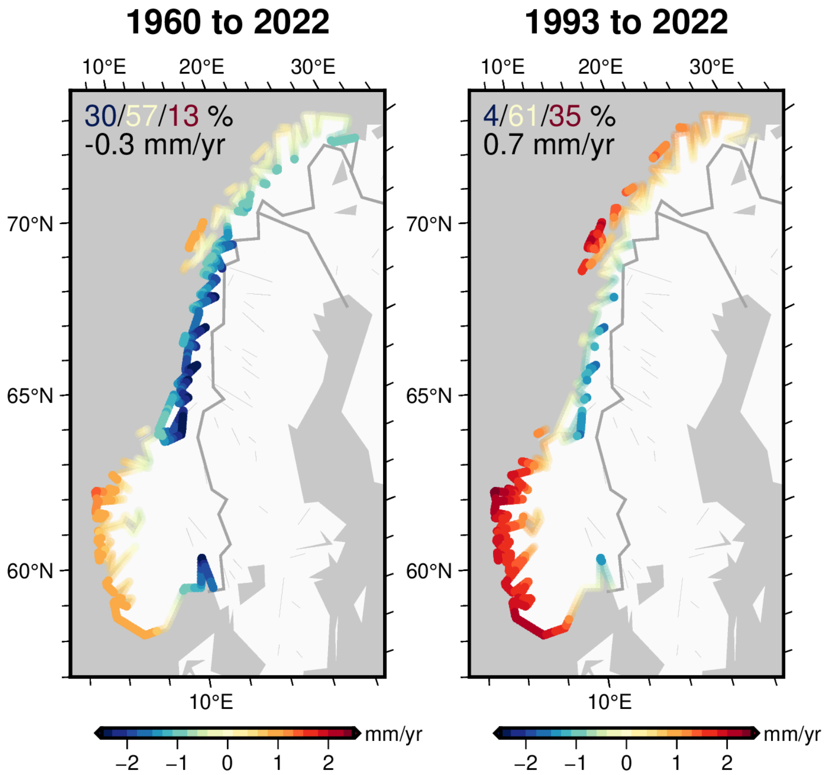

Figure 2.7: Estimated RSL rates along the Norwegian coast. The percentage splits in the top left corners indicate areas of the coast undergoing negative/no significant change/positive RSL change, where no significant change indicates percentage of coast where rate uncertainties overlap with zero. Estimated coastal average RSL change (mm/yr) is displayed in the top left.

2.3.1.3 Evolution of 30-yr trends and acceleration

The derived sea-level trends depend on the period examined and are generally not stationary. They may vary significantly over shorter periods of time when the influence of year-to-year and decade-to-decade natural variability is large compared to the long-term trend (e.g., Palmer et al, 2020). Additionally, the rate of global mean sea-level rise has increased throughout the last century and recent decades (Fox-Kemper et al., 202; Table 2.2) with a growing contribution from the Greenland and Antarctic ice sheets.

Here, we first look at the observed variability in the 30-yr trends and then go on to discuss a potential acceleration of sea-level rise along the Norwegian coast. The sensitivity of trends to the study period was shown in SLC2015. Fig. 2.8 is a reproduction of Figure 3.6 in SLC2015 but with additional data (shown in red) available since the previous report. It shows estimated sea-level trends for a 30-yr moving window shifted by 1-year from 1961 (or earliest available observations) to 1993 at tide gauges with sufficient data coverage. That is, the first and last dots in each panel represent the trends for the earliest available 30-yr period and 1993-2022, respectively.

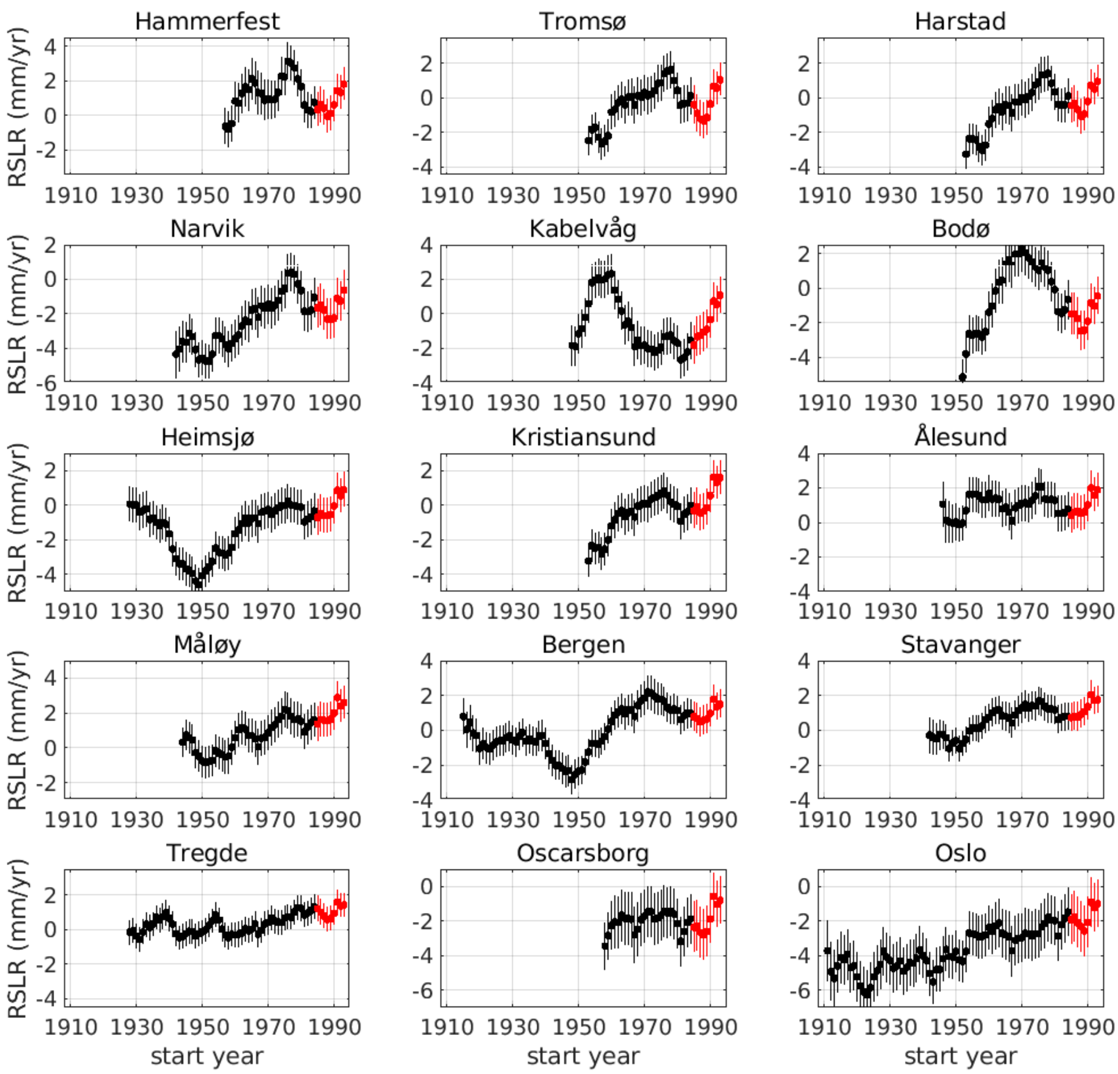

Figure 2.8: Relative sea-level rates (RSLR) from tide gauge observations, computed for 30-yr moving windows shifted by 1 year for start years ranging from 1910 to 1993; that is, the first and last dots in each panel represent the rates for the period 1910-1939 (if available) and 1993-2022, respectively. Red dots show new data since SLC2015. The error bars represent the 95% confidence interval of the standard error. The limits of the y-axis differ, however, the range is the same (8 mm/yr).

Moving the window by just 1 year can change the 30-yr trends by more than 1 mm/yr. The total range of 30-yr trends can be up to 5 mm/yr. SLC2015 showed rising rates at all stations (black dots in Fig. 2.8) pointing to an acceleration. However, rates decreased (e.g. Tromsø, Oslo) or stabilised (e.g. Bergen, Ålesund) for several years before all stations show a jump in rates for the most recent three 30-yr periods. At some stations (Heimsjø, Kristiansund, Måløy, Oscarsborg, Oslo) those rates are the highest ever observed, though still negative (but not statistically different from zero) in Oslo and Oscarsborg. Whether this is part of an ongoing long-term trend, natural variability or - most likely - a combination of both remains to be seen. It is however striking that - for the latest 30-yr period - sea-level rates are either positive or not significantly different from zero at all stations. This is not the case for any of the previous 30-yr periods considered. For example, only four stations show a statistically significant RSL rise while six stations show a fall (Fig. 2.5) for the period 1961-1990.

Breili (2022) investigated whether a significant acceleration could be detected at Norwegian tide gauges by performing a nonlinear trend analysis. Similar to the estimation of linear trends, he found that the magnitude of accelerations strongly depended on the time period considered. This underlines the dominant role of natural variability on shorter (decadal) time scales. In their analysis, Breili (2022) partly accounted for this variability by correcting the observations for sea-level changes related to changes in sea-level pressure and local winds. They found significant positive accelerations for the period 1960-2020 for most Norwegian tide gauges ranging from 0.021 (Tregde) to 0.059 (Heimsjø) mm/yr^2, with a coastal average of 0.030 ± 0.004 and 0.036 ± 0.005 mm/yr^2 for the raw and corrected data, respectively. When only considering a more recent period (1991-2020), no significant acceleration was detected at any of the individual tide gauges, neither for the raw nor the corrected observations. However, the coastal mean of the corrected observations showed a deceleration of -0.027 +- 0.004 mm/yr^2. A thorough discussion of potential causes for the recent declining sea-level rates can be found in Breili (2022). Essentially, both natural variability as well as changes in the relative importance of the contributions to global mean sea-level change may play a role. With respect to the latter, an increasing relative contribution from the Greenland ice sheet will, due to its proximity and GRD effects, lead to a smaller sea-level rise along the Norwegian coast compared to other regions (see also Chapter 2.4) and global mean sea-level rise.

2.3.1.4 Estimate of sea-level trends from satellite altimetry along the coast of Norway

For Norway, tide gauges provide observations of sea level relative to the solid Earth, some of which for more than a century but with a coarse and inhomogeneous spatial resolution. Satellite altimetry observes the range between the satellite and the sea surface (Cazenave and Nerem, 2004) with a higher spatial coverage but spanning approximately only three decades. To make both kinds of observations comparable, various corrections have to be applied: Tide-gauge observations have to be corrected for vertical land movements (see Section 2.2) and several geophysical corrections are needed to obtain geocentric sea-level change from altimeters (e.g. Taburet et al., 2019). Once the two signals are physically consistent it is important to evaluate how well they agree with each other.

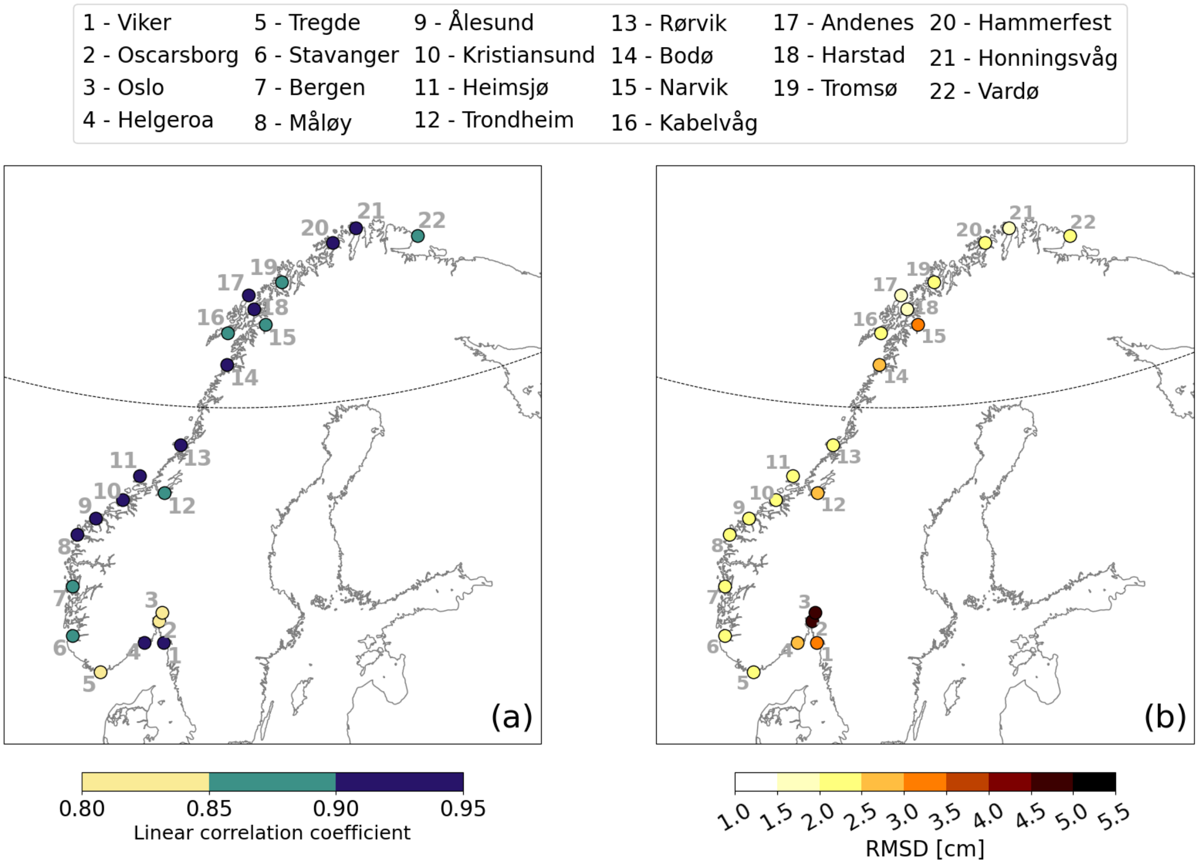

Figure 2.9: Comparison between coastal sea-level signals from in-situ and remote-sensing. The panels show the linear correlation coefficient (A) and RMSD (B) between the detrended and deseasoned monthly mean SLA from satellite altimetry and tide gauge data (1993-2020) at each tide gauge location. The black, dashed line indicates the 66°N parallel (updated from Mangini et al., 2022).

Fig. 2.9 shows a comparison between satellite altimetry retrievals (CMEMS, 2023), and tide gauge data along the coast of Norway (1993-2021) with all the necessary corrections applied. There is very good agreement along the west coast of Norway expressed by high linear correlation coefficients exceeding 0.90 and small errors (root mean square deviations, RMSD) ranging between 1.5 and 2.5 cm, compared to the variability of the sea-level signal gathered by tide-gauges. In more sheltered regions like the Trondheim fjord or the Oslofjord, the altimetric signal might not resolve the local sea-level variations accurately, for example due to land reflection (Gómez-Enri et al., 2010; Abulaitijiang et al., 2015). This is expressed by larger RMSDs up to around 5 cm along with a smaller but still significant correlation between the two signals (down to 0.8).

Fig. 2.10 shows geocentric sea-level trend estimates and their uncertainties at each tide-gauge location (upper panel) as well as the coastal average geocentric sea-level change (lower panel) obtained from altimetry and tide gauges. Both datasets return a similar spatial dependence of the geocentric sea-level trend along the Norwegian coast, with the lowest values found in the Skagerrak and the Oslofjorden (between 3 and 4 mm/yr) and the highest to the north of Bergen (> 4 mm/yr). Moreover, the two datasets return a similar uncertainty of the sea-level trend at each tide-gauge location. Satellite altimetry tends to overestimate the sea-level rates compared to those calculated from the tide gauges locally, in particular moving northward along the Norwegian coast, where the differences between the trend estimates are the largest (e.g. up to 1 mm/yr in Vardø). This suggests that sea-level trend estimates obtained from conventional altimetry data are more representative of changes over larger spatial scales and that at the high latitudes (e.g. > 66°N) they can be affected by the lesser number of satellite missions covering those geographical areas.

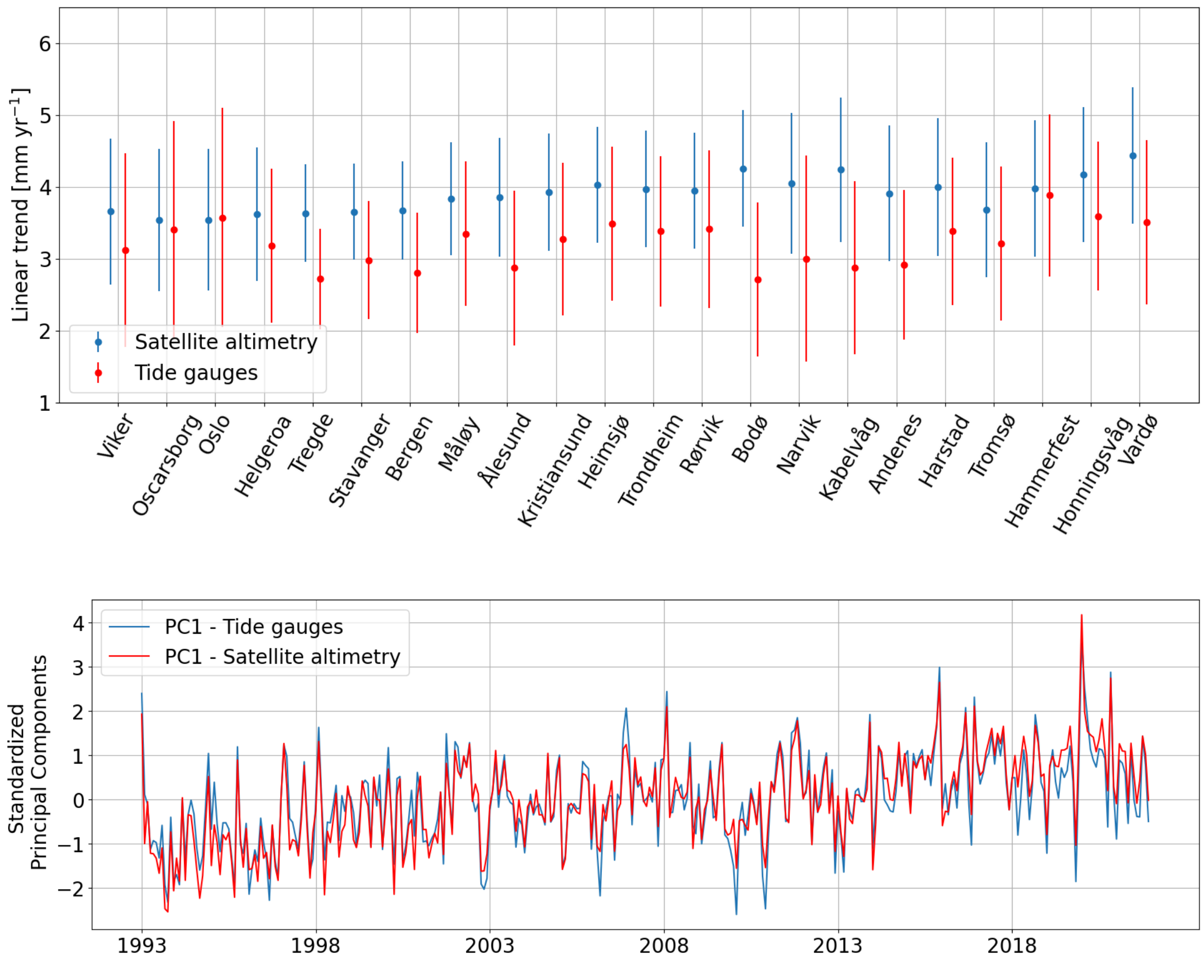

Figure 2.10: Top: Sea-level trend estimates from satellite altimetry measurements (blue) and tide gauges records (red) over the period from 1993 to 2021. The error bars show the 95th confidence intervals of the sea-level trend at each tide gauge location. Bottom: Leading modes of variability obtained from tide-gauge (blue) and satellite altimetry (red) records (seasonal signal removed). The figure shows the first principal component (PC1) obtained

from each data-set over the period 1993-2021, representative of the sea-level variability and trend over the entire coast of Norway.

In terms of coastal average geocentric sea-level change, estimates from altimetry and tide gauges agree very well (correlation coefficient > 0.9) emphasising the growing importance of satellite altimetry for monitoring coastal sea-level changes. Recent studies have explored the potential of coastal altimetry retrievals (Benveniste et al., 2020), which increase the accuracy of the sea-level signals obtained from remote-sensing in coastal areas and could bring valuable information where in-situ data are not reliable or missing. These enhanced altimetry retrievals should make part of national and regional sea-level assessments in the future.

2.4 Contributions to sea-level rise in Norway

Various contributions to sea-level variability and trends for Norway were discussed in SLC2015. Vertical land motion is the most influential contribution to the long-term trends and largely explains their spatial pattern. Sea-level rise is being driven partly by on-shelf ocean warming, which contributed up to 1 mm/yr over the period 1960-2010 (Richter et al., 2012). Other contributions (wind, melting of land-based ice, terrestrial water storage, ocean mass redistribution) have been estimated and discussed in the literature (e.g. Frederikse et al., 2016, Mangini et al., 2021). Since SLC2015 a few studies have looked at the components of sea-level change along the Norwegian coast and they are summarised below.

Frederikse et al (2016) studied regional sea level budgets on the Northwestern European shelf over the period 1958-2014, including long-term trends and decadal variability in the North Sea (including Tregde and Stavanger) and on the Norwegian shelf (from Bergen northward). They considered the mass contribution of glaciers, Greenland and Antarctic ice sheets, and terrestrial water storage as well as VLM and solid earth deformation. The combined impact of ocean density and dynamic changes (sterodynamic changes) was approximated by the steric (contribution from sea water density changes) height averaged over the deeper ocean in the Bay of Biscay. It has been shown that the variability in this region is highly representative of variability on the shelf further north. This is because sea-level anomalies travel as coastally trapped waves northward along the continental shelf. The advantage with this approach is that changes in the deeper ocean that indirectly impact coastal sea-level changes (see below) are also represented. The disadvantage is that local steric changes are ignored. On longer time scales, however, local changes are believed to be comparatively small.

Fredrikse et al. (2016) showed that the sterodynamic signal explained the bulk of the observed variability on decadal time scales. Due to the proximity of Greenland and many glacierized regions in the Arctic, the GRD contribution to long-term trend from melting land ice was found to be relatively small (0.2 mm/yr but showing an acceleration over the past two decades). The trend from the sterodynamic contribution was larger (0.75 mm/yr) and close to the global average. Both GRD effects and the sterodynamic sea-level rise were largely offset by vertical land uplift due to GIA.

Recently, Mangini et al (2022) compared different altimetry products over a 15-yr period (2003-2018) – on such time scales, natural variability is still large, potentially masking a long-term anthropogenic trend. Similarly to Richter et al. (2012) and as shown in SLC2015, they used hydrographic stations on the Norwegian shelf to assess the steric contribution. They found large regional differences with steric trends ranging from -1 mm/yr (Sognesjøen) to 2.5 mm/yr (Lista, Ingøy). Interestingly, on those time scales ocean density trends are not necessarily dominated by sea water temperature (as on longer scales discussed above) but to a large degree also by salinity.

Note that the local steric signal close to the coast is limited due to the relatively shallow depth of the continental shelves (~200 to 300 m) when compared to the deep open ocean (1000s of metres). Yet, steric changes that happen in the deeper layers of the open ocean (i.e. below shelf depth) due to warming of the deep ocean will indirectly contribute to sea-level rise at the coast through a coastward redistribution of sea water. This effect will play a major role in future sea-level rise on shallow continental shelves worldwide (Richter et al., 2013).

2.5 Natural Variability

As discussed in Section 2.3.1.3, sea-level trends are strongly impacted by natural variability on shorter time scales (years to decades). Along the Norwegian coast, two factors play a leading role: i) atmospheric variability (as also discussed in SLC2015) and ii) changes in the Norwegian Atlantic Current.

A persistent wind can pile up water along the coast and release it once it ceases blowing. Low air pressure raises the sea surface while high pressure depresses it. Those factors create storm surges (see Chapter 4) but – when sustained over a longer period of time – can also contribute to interannual and decadal variability. The dominating atmospheric regime in the Northern North Atlantic region is characterised by westerly winds the strength of which is measured by the North Atlantic Oscillation (NAO). Positive/negative NAO phases are associated with stronger/weaker storm tracks shifted northward/southward. In addition, the NAO is modified by secondary large-scale atmospheric patterns which, in combination, give rise to interannual to decadal-scale sea level changes (see Chafik et al., 2017 and

Mangini et al., 2021 for a summary of the dominating atmospheric patterns and their effect on coastal sea level).

The Norwegian Atlantic Current carries warm and saline water along the continental shelf through the Nordic Seas towards the Arctic. Although not in direct contact with the coast, changes in the temperature and/or salinity of the off-shore Atlantic water layer can be communicated to the shelf and the coast via wind and across-shelf redistribution of water masses. As those anomalies are thought to originate further upstream in the subpolar gyre there may be potential for decadal sea-level predictions for the Northern European shelf (Chafik et al, 2019). However, this remains to be investigated.

To assess the effect of natural variability on the observed sea-level rates, Breili (2022) assumed that a large part of the year-to-year and decade-to-decade variability is driven by atmospheric variability and fitted various regression models to the observed time series: the simplest model presented a simple linear regression (without taking atmospheric forcing into account) while more comprehensive models included various observed atmospheric variables such as sea-level pressure and wind speed closest to the stations. The results showed that for the 61-yr period 1960-2020, the trends estimated from observed sea level alone and those including atmospheric forcing, agreed within uncertainties. This was also true for the shorter period 1991-2020, but the difference between the two estimates was somewhat larger, underlining the importance of natural variability on shorter time scales.

Natural variability can be viewed as noise in the climate system. Variability around the underlying long-term trend can act to exacerbate or dampen sea-level rise. Figure 2.11 shows that annual sea levels can deviate from a long-term mean by up to ±10 cm or more at some tide gauge locations. Over short-timescales, for example for users interested in the next few decades, variability could be an important consideration (see also Chapter 3.6). As shown and discussed earlier in this chapter, variability can have a common cause and near uniform signal along the Norwegian coast.

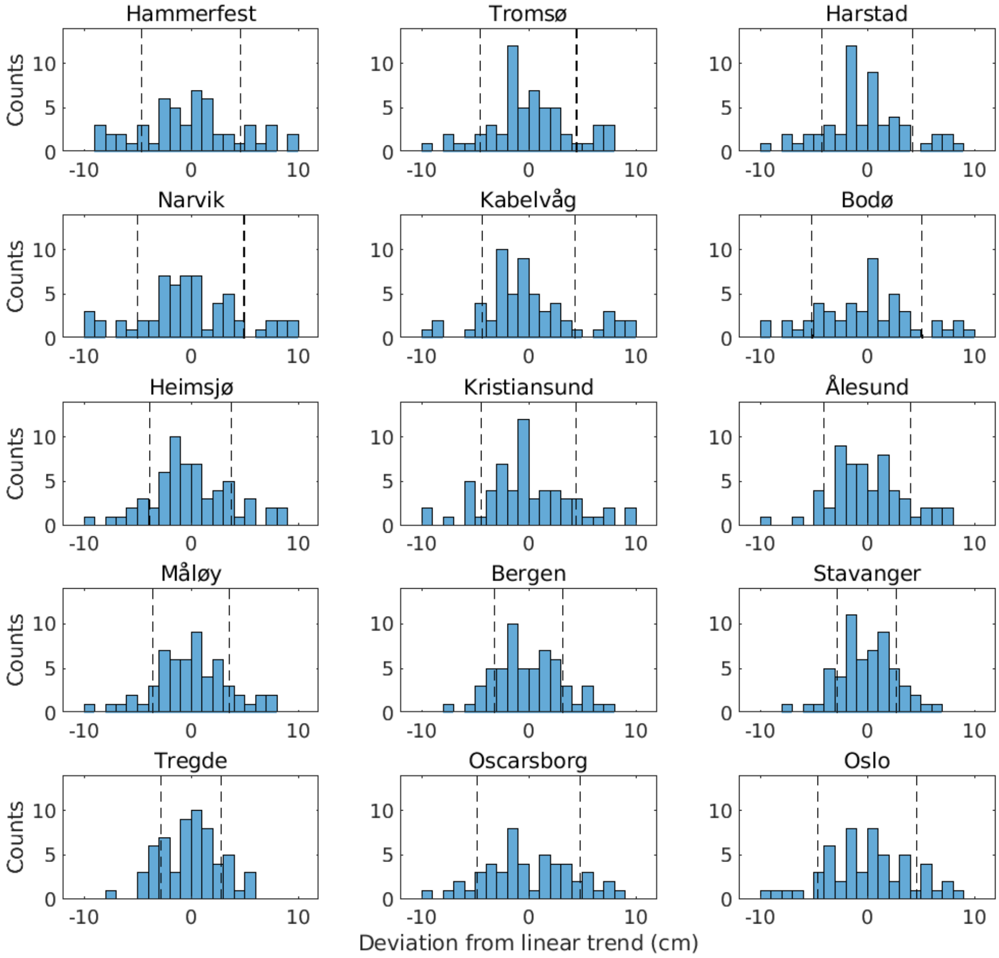

Figure 2.11: Deviation of annual sea-level observations from a linear trend and the frequency of their occurrence. Observations covering the period 1961-2020 have been used. The dashed lines represent one standard deviation.

3 Sea-level projections

In this chapter, the IPCC AR6 based sea-level projections are tailored to the Norwegian coast using regional estimates of GIA. Projected sea-level changes are shown as coastal averages, as well as regional and local RSL projections. Uncertainties on the projections are discussed. In the short-term, i.e., the next few decades, differences between the process-based AR6 projections and a simple extrapolation of observed sea-level change rates are presented. The long-term implications of sea-level rise are briefly discussed. Finally, the IPCC AR6-based projections are compared to the previous national report (SLC2015) which was based on IPCC AR5.

3.1 Key points

- Projections based on IPCC AR6 show Norway's coastal average relative sea-level change for 2100, relative to the period 1995-2014, will be between 0.13 m for the very low emissions scenario SSP1-1.9 (*likely* -0.12 to 0.41 m) and 0.46 m for the very high emissions scenario SSP5-8.5 (*likely* 0.21 to 0.79 m). This rise is between 40% and 70% lower than the projected global average; a difference that can be explained by ongoing vertical land motion in Norway and the close proximity of Greenland and Arctic glaciers. (*Medium confidence* projections.)
- Projected local sea-level change will deviate from Norway's coastal average largely because of geographical differences in vertical land motion. Projected relative sea-level changes for 2100 at six key locations are:

Projected sea-level change for 2100	**SSP1-1.9** Median (*Likely* range)	**SSP1-2.6** Median (*Likely* range)	**SSP3-7.0** Median (*Likely* range)	**SSP5-8.5** Median (*Likely* range)	**SSP5-8.5** Low-likelihood high-impact
Oslo	-0.05 (-0.30 to 0.23)	0.01 (-0.19 to 0.25)	0.21 (-0.02 to 0.50)	0.32 (0.07 to 0.64)	0.84 and 1.56
Stavanger	0.28 (0.02 to 0.57)	0.33 (0.10 to 0.60)	0.55 (0.30 to 0.85)	0.65 (0.38 to 0.99)	1.19 and 1.92
Bergen	0.25 (-0.02 to 0.53)	0.30 (0.08 to 0.56)	0.51 (0.26 to 0.81)	0.61 (0.35 to 0.94)	1.14 and 1.85
Heimsjø	0.07 (-0.17 to 0.35)	0.12 (-0.11 to 0.37)	0.30 (0.06 to 0.60)	0.41 (0.15 to 0.73)	0.93 and 1.60
Tromsø	0.14 (-0.12 to 0.42)	0.16 (-0.07 to 0.43)	0.34 (0.09 to 0.65)	0.44 (0.18 to 0.77)	0.96 and 1.59
Honningsvåg	0.19 (-0.04 to 0.45)	0.20 (-0.03 to 0.47)	0.39 (0.15 to 0.69)	0.49 (0.24 to 0.81)	1.01 and 1.65

Table 3.1: Projected relative sea-level changes for 2100, relative to the period 1995-2014. Median values (50%) and *likely* ranges (17-83%; the central two-thirds of the probability distribution) are given for the *medium confidence* projections and for a selection of emission scenarios. For the very high emissions scenario SSP5-8.5, a low-likelihood high-impact storyline of rapid ice-sheet mass loss is shown (the 83rd and 95th percentiles of the *low confidence* projections). Units are in metres.

- For the low emissions scenario SSP1-2.6, projections show a third of the coastline will *likely* experience relative sea-level rise (Western and Southern Norway, as well as parts of Northern Norway) for 2100. For the remainder of the coast, sea levels have a chance of being kept stable under SSP1-2.6. For emission scenarios above SSP1-2.6, a majority of the coast will *likely* experience relative sea-level rise for 2100. (*Medium confidence* projections.)
- For 2150, projections show coastal average sea-level change for Norway will range from 0.16 m (-0.24 to 0.61 m) under SSP1-1.9 to 0.73 m (0.25 to 1.38 m) under SSP5-8.5. (*Medium confidence* projections given with median values and 17-83% ranges.)
- For the very high emissions scenario SSP5-8.5, and a low-likelihood high-impact storyline of rapid ice-sheet mass loss, coastal average relative sea-level change for Norway could approach between 1 and 1.5 m by 2100. Some locations along the coast could experience close to 2 m. Shortly after 2100, massive ice loss from Antarctica could rapidly increase Norway's coastal average sea level to between 4.5 and 5 m by 2150. This is a storyline that cannot be ruled out and is particularly relevant for users with low risk tolerance. (*Low confidence* projections.)
- Due to limited scientific understanding, we cannot rule out that rapid ice mass loss from Antarctica could also be triggered by emission scenarios below SSP5-8.5. However, processes that can drive rapid ice-sheet mass loss are unlikely to be significant for SSP1-1.9 and SSP1-2.6, at least within the timeframe of 2100. (*Low confidence* projections.)
- In the next few decades projected sea-level change is similar across the SSPs. For 2050, projected coastal average relative sea-level changes are ~0.1 m (*likely* -0.05 to 0.26 m) across the SSPs. We suggest near-term future sea level will be somewhere between our extrapolation-based projections and the IPCC AR6 based projections. (*Medium confidence* projections.)
- For 2300, projections show coastal average relative sea-level change for Norway will range from 0.35 m (-0.75 to 1.4 m) under SSP1-2.6 to 4.15 m (0.4 to 16 m) under SSP5-8.5. (*Low confidence* projections given with 83rd and 95th percentiles.)
- Projected likely sea level for Norway in this national report (SLR2024; based on IPCC AR6) is generally slightly higher than in the previous report (SLC2015; based on IPCC AR5). Differences between the reports are less 0.1 m for 2090, using the same reference period 1995-2014, and changes are within

uncertainties. The projected *likely* ranges in SLR2024 and SLC2015 are therefore broadly similar. (*Medium confidence* projections.)

3.2 Some background on the IPCC AR6 sea level projections

IPCC AR6 uses a different method to project sea level than in earlier IPCC reports: AR6 makes use of an emulator approach, where sea level projections are consistent with the assessment of equilibrium climate sensitivity and projected global surface air temperature change. However, the resultant GMSL projections in IPCC AR6 are broadly similar to the projections presented in IPCC AR5 (Slangen et al., 2023).

There are two sets of sea level projections presented in IPCC AR6 (Box 1.3). Both sets of projections are provided at 1030 tide gauge locations from across the world, as well as a 1 x 1 degree global grid. The projections start in 2020 and have 10-year increments:

- The *medium confidence* sea level projections extend to 2150. These comprise of physical processes in whose projection there is at least *medium confidence*. The projections have a *likely* range, which refers to *at least* 66% probability (the range is typically expressed as the outer 17th-83rd percentiles). In other words, there may be up to 34% probability that processes in which there is *medium confidence* can cause future sea level to lie outside the *likely* range.
- The *low confidence* sea level projections extend to 2300 and are only available for a subset of the SSPs (SSP1-2.6, SSP2-4.5, and SSP5-8.5). These projections are assessed as *low confidence* because of limited evidence and/or lack of agreement in that evidence. Subsequently no probability, that is, *likelihood* is evaluated (i.e. there is no *likely* range). The *low confidence* sea level projections are new to the IPCC reports and include potential high-end ice sheet contributions.

The *low confidence* projections include information from structured expert judgement (Bamber et al., 2019) and from a single Antarctic ice sheet model that accounts for marine ice cliff collapse (Deconto et al., 2021), a process that is generally not included in ice sheet models. The *low confidence* projections were presented as a low-likelihood high-impact storyline in AR6 (see also Box 3.1). Due to deep uncertainty in ice sheet processes it is not possible to ascribe a robust and meaningful probability to the AR6 *low confidence* projections. However, they represent useful planning scenarios for users with low risk tolerance to explore vulnerabilities and adaptation options.

Box 3.1: A low-likelihood high-impact storyline of rapid ice-sheet mass loss

Potential instabilities in the climate system could lead to a rapid and irreversible loss of some parts of the large ice sheets in Greenland and Antarctica. This would drive a high-end sea-level rise. The processes driving these instabilities are, however, not well understood and are characterised by deep uncertainty (Fox-Kemper et al., 2021). The timing and amounts of these potential ice sheet contributions are therefore very uncertain.

The *medium confidence* sea level projections from AR6 are given with a *likely* range. This range can be thought of as characterising the central two-thirds of the probability distribution under a given climate change scenario. The absence of information on the upper tail of the probability distribution (i.e. the high-end of sea level projections) presents a problem for their use in practical applications, especially in risk-based frameworks. Understanding of low probability but high-end sea-level rise is important for adaptation planning and for users with low risk tolerance. To address this need, AR6 also includes *low confidence* sea-level projections, which includes potential high-end ice sheet contributions associated with self-sustaining instability processes. These *low confidence* projections can be thought of as a storyline. This storyline shows that, if ice sheet instabilities are triggered, future sea-level rise can be significantly higher than the *likely* ranges.

Both the Greenland and Antarctic ice sheets have potential instabilities that can lead to high-end sea-level rise. That said, owing to GRD effects, the regional pattern of sea-level change from ice sheet mass loss will vary considerably. As Norway is in the “near field” of Greenland, it will experience a sea-level rise somewhere between -40% and 10% of the global average sea-level rise owing to ice mass loss there (Simpson et al., 2017). On the other hand, ice mass losses in Antarctica will produce an above average sea-level rise along the Norwegian coast (~110%). Antarctica is therefore of most concern when considering potential high-end sea-level rise for Norway.

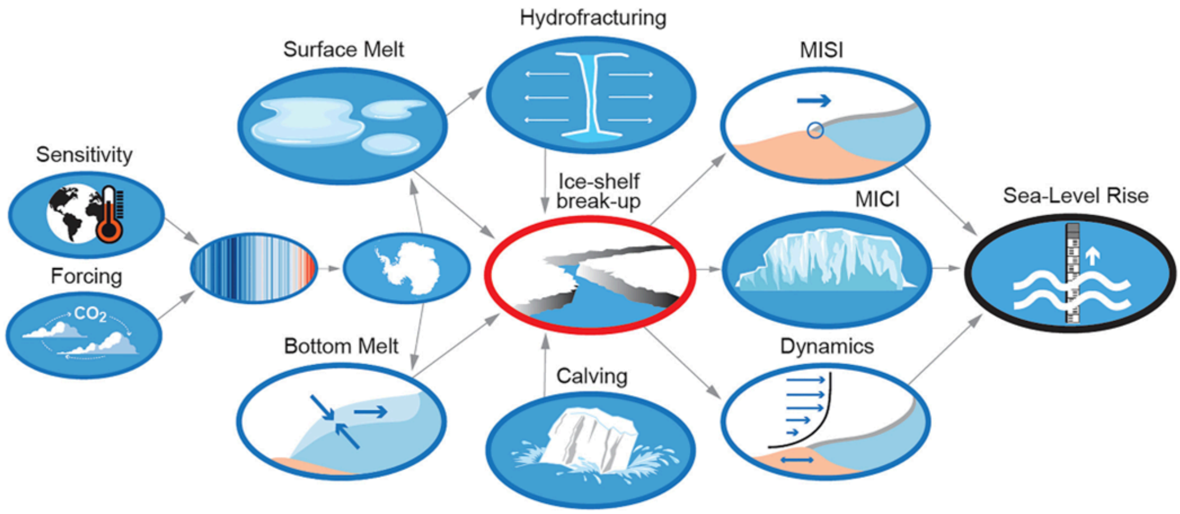

Figure 3.1: Processes that could cause Antarctica to contribute to a high-end sea-level rise. Figure taken from van de Wal et al. (2022).

AR6 describes in some detail how a storyline of rapid Antarctic ice loss would drive a high-end sea-level rise assuming a very high emissions scenario (see Box 9.4 in Fox-Kemper et al. (2021)). The storyline considers an early break-up of the ice shelves surrounding Antarctica. After this, processes called Marine Ice Cliff Instability (MICI) and Marine Ice Sheet Instability (MISI) lead to an abrupt loss of some portions of the marine based ice (Fig 3.1). For this storyline, and as explained later in this chapter, projected coastal average relative sea-level change for Norway could approach ~1 to 1.5 m in 2100 and ~4.5 to 5 m in 2150 (83^{rd} and 95^{th} percentile of the *low confidence* projections for SSP5-8.5). Local sea-level change would deviate from these numbers mainly because of differences in VLM.

As AR6 has recently assessed the evidence for high-end sea-level rise (and includes *low confidence* sea-level projections) it is not necessary to repeat the exercise for this national report. After the release of AR6, several studies of high-end sea-level rise have been published. We highlight the study by van de Wal et al. (2022) which looks at the physical evidence for high-end sea-level rise. The authors also look at the perspective of decision makers (i.e. people who have to use sea level information in practice). Using AR6 and van de Wal et al. (2022) we summarise the most important points for users of this report when considering high-end sea-level rise from Antarctica:

- The timing of ice shelf collapse around Antarctica is the precursor for a potential high-end sea-level rise. The timing of collapse is highly uncertain because of limited scientific understanding.
- There is currently no evidence that ice shelf collapse and major loss of marine based ice could occur before 2100. That said, there is some limited

evidence that under the very high emissions scenario (SSP5-8.5), ice shelf collapse and major ice loss could start to occur shortly after 2100 (Deconto et al., 2021).

- For the low emissions scenario (SSP1-2.6), van de Wal et al. (2022) estimate a global high-end sea-level rise of up to 0.9 m in 2100 and up to 2.5 m in 2300. For SSP5-8.5, they estimate up to 1.6 m in 2100 and up to 10.4 m in 2300. Their estimate of 1.6 m for SSP5-8.5 in 2100 is close to the 83rd percentile of the AR6 *low confidence* projections used in this report (the Antarctic contributions are also the same ~0.6 m). We therefore suggest that the 83rd percentile could be used as a plausible physical based estimate of high-end sea-level rise for 2100. This estimate is based on our current knowledge, and with the caveat that "unknown unknowns" in the climate system could drive a higher sea-level rise by 2100.
- It is very difficult to provide a robust high-end sea-level rise estimate for 2150 as the driving processes are poorly understood and constrained. That said, for 2150, the AR6 projections give some guidance for users with low risk tolerance and those interested in longer planning horizons. Users may want to consider a range of plausible estimates.
- A significant caveat with both AR6 and van de Wal (2022) is that, owing to lack of evidence, high-end sea-level rise is only assessed for a subset of the SSPs. There is generally low agreement on how emission scenarios relate to future Antarctic mass change (Fox-Kemper et al., 2021). Given this, we cannot rule out that rapid ice mass loss from Antarctica could also be triggered by emission scenarios below SSP5-8.5. However, processes that can drive rapid ice-sheet mass loss are unlikely to be significant for SSP1-1.9 and SSP1-2.6, at least within the timeframe of 2100.

3.3 Method for tailoring the IPCC AR6 sea-level projections to Norway

The Framework for Assessing Changes to Sea Level (FACTS) (Kopp et al., 2023) is the framework used to generate the IPCC AR6 sea-level projections.[3] FACTS is also a tool designed to support scientists doing national assessments.

[3] The FACTS model code and software can be found here: https://github.com/radical-collaboration/facts.

For this national report we tailor the IPCC AR6 projections to the Norwegian coast. This is done by replacing the vertical land motion component in the IPCC AR6 projections with the semi-empirical model NKG2016LU (Vestøl et al., 2019). For Norway, VLM is an important component of RSL change, and largely explains spatial differences in sea-level change along the coast. It is therefore important to treat this contribution carefully.

In the IPCC AR6 projections VLM is estimated as a constant background rate from the tide gauge records, which is then extrapolated to a global coverage using a GIA model and statistical approach (Kopp et al., 2014). We make use of the semi-empirical model NKG2016LU to estimate VLM and associated geoid changes (Vestøl et al., 2019). The advantages of using the NKG2016LU solution are: (1) it is based on geodetic observations of VLM rather than inferring land motion from the tide gauge records; (2) it provides better coverage of the observed VLM signal and is less reliant on spatial interpolation.

The projections could be further refined by looking at other contributions. For example, global climate models have a relatively coarse resolution, and it is unclear whether they are suited to projecting ocean dynamic sea-level changes along the coast. One study that looked at simulations of ocean dynamic sea-level change on the European shelf found sea level projections based on dynamical downscaling were up to ~15 cm smaller than those from global climate models (Hermans et al., 2020).

Instead of using the FACTS software, we make use of the IPCC AR6 projections without the background VLM component dataset (Kopp, 2021). To combine the IPCC AR6 projections with our VLM grid and their respective uncertainties we take a simple sampling approach. Here we sample 100,000 times over the IPCC AR6 projections in a manner that allows us to reproduce the skewed probability distribution and its given quantiles. Secondly, we sample over the VLM field the same number of times assuming a normal distribution of the uncertainties. The uncertainties on the IPCC AR6 projections and the VLM field are assumed to be uncorrelated.

The semi-empirical NKG2016LU model (Vestøl et al., 2019) is provided with uncertainties for the VLM rates but not for the modelled geoid change. Uncertainties for the VLM field are typically smaller than ±0.25 mm/yr (1σ) for where we have observations and for mainland Norway. Uncertainties on the modelled geoid changes are neglected as they are an order of magnitude smaller than the VLM uncertainties. The VLM rates are given in the international terrestrial reference frame ITRF2008 (Altamimi et al., 2011). A review concluded that the ITRF is stable along each axis to better than 0.5 mm/yr and has a scale error of less than 0.3 mm/yr

(Collilieux et al., 2014). For the total error budget for the GIA contribution we add the NKG2016LU VLM and ITRF uncertainties in quadrature.

The IPCC AR6 projections are on 1 x 1 degree grid and are interpolated to the NKG2016LU model grid which has a finer resolution. (The NKG2016LU model has a horizontal resolution of 1/12 degree latitude and 1/6 degree longitude, which is approximately 9 x 9 km.) Projected coastal average RSL change for Norway is calculated by averaging over a coarse coastline file using a 10 km spacing.

3.4 Projected coastal average relative sea-level changes

Projected coastal average RSL change for Norway is summarised in Fig. 3.2 and Tables 3.2 and 3.3. Up until 2050, the projections show considerable overlap across the SSPs but then begin to diverge. For 2050, *medium confidence* projected coastal average relative sea-level changes are ~0.1 m (*likely* -0.05 to 0.26 m) across the SSPs. *Low confidence* projections suggest that coastal average relative sea level could approach 0.3 m by 2050.

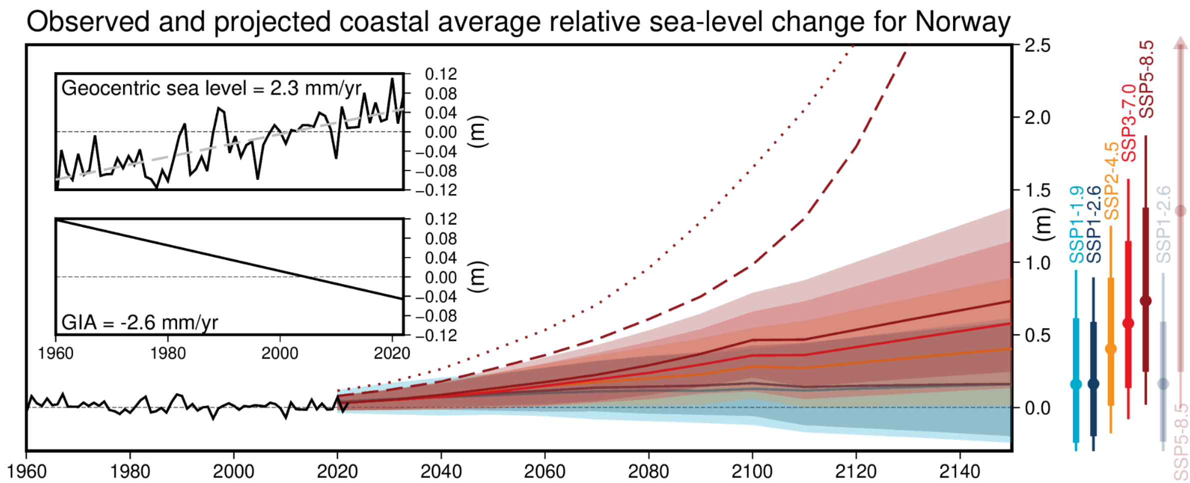

Figure 3.2: Observed and projected coastal average relative sea-level change for Norway. Geocentric sea-level rise has been in balance with GIA over the period 1960 to 2022, meaning coastal average RSL has been stable. On the main graph; *medium confidence* projections of relative sea-level change and their *likely* ranges (17-83%) are shown as lines and shading. *Low confidence* projections under SSP5-8.5 are shown for the 83rd percentile (dashed line) and 95th percentile (dotted line). To the right; bars show the 17-83% (thick bars) and 5-95% (thinner lines) for the *medium confidence* (solid colours) and *low confidence* (lightly shaded) projections for 2150. Baseline period is 1995-2014.

For 2100, the *medium confidence* projections show coastal average RSL change will be between 0.13 m for SSP1-1.9 (*likely* -0.12 to 0.41 m) and 0.46 m for SSP5-8.5 (*likely* 0.21 to 0.79 m). The big picture, therefore, is that the higher the emission scenario and thus global warming, the larger the future sea-level rise.

Projected median values show that coastal average RSL change for Norway will be positive for all emission scenarios. For scenarios above SSP1-2.6, the *likely* ranges show projected coastal average sea-level change for 2100 will be positive (i.e. for these SSPs the average sea-level change in Norway will *likely* be a rise rather than stable or falling sea levels). Another way of looking at this is that for the very low and low emission scenarios (SSP1-1.9 and SSP1-2.6), the average sea-level rise will be small with a chance of keeping sea levels stable over the 21st century. The median of the *medium confidence* projections shows that Norway will receive somewhere between 30% (SSP1-1.9) and 60% (SSP5-8.5) of the projected global mean rise by 2100. This is largely due to VLM and GRD effects which strongly influence relative sea-level change along Norway's coast (Simpson et al., 2014; 2015; 2017).

		Projected coastal average relative sea-level change (m)			
		2050	2100	2150	2300
Medium confidence	**SSP1-1.9**	0.08 (-0.05 to 0.23)	0.13 (-0.12 to 0.41)	0.16 (-0.24 to 0.61)	-
	SSP1-2.6	0.10 (-0.02 to 0.22)	0.17 (-0.06 to 0.43)	0.16 (-0.2 to 0.59)	-
	SSP2-4.5	0.11 (0 to 0.24)	0.28 (0.06 to 0.55)	0.40 (0.01 to 0.89)	-
	SSP3-7.0	0.11 (-0.01 to 0.23)	0.36 (0.11 to 0.66)	0.58 (0.13 to 1.15)	-
	SSP5-8.5	0.13 (0.01 to 0.26)	0.46 (0.21 to 0.79)	0.73 (0.25 to 1.38)	-
Low confidence	**SSP1-2.6**	0.09 (-0.04 to 0.22)	0.15 (-0.13 to 0.43)	0.16 (-0.23 to 0.59)	0.35 (-0.75 to 1.43)
	SSP5-8.5	0.13 (-0.01 to 0.27)	0.55 (0.16 to 0.98)	1.36 (0.25 to 4.47)	4.15 (0.37 to 15.89)

Table 3.2: Projected coastal average RSL change (m) under the different SSP scenarios. Baseline period is 1995-2014. Projected median values are shown with the *medium confidence* (*likely* range) and *low confidence* (17 to 83 percentile spread).

Under the very high emission scenario (SSP5-8.5), the median value of the *low confidence* projections starts to deviate from the equivalent *medium confidence* projections around 2100. The median value of the *low confidence* projections under SSP5-8.5 is 0.55 m in 2100 (around 0.1 m higher than the median of the *medium confidence* projections). This increases to 1.36 m in 2150 (over 0.6 m higher than *medium confidence*). This systematic difference is due to the *low confidence* projections, in contrast to the *medium confidence* projections, including ice sheet processes characterised by deep uncertainty (see Box 3.1).

The *low confidence* projections show that future sea-level rise can be considerably higher than the *likely* ranges. Projected coastal average sea-level change for Norway could approach ~1 to 1.5 m in 2100 and ~4.5 to 5 m in 2150 (83rd and 95th percentile of the *low confidence* projections for SSP5-8.5). Ice sheet processes characterised by deep uncertainty can therefore lead to a sea-level rise in Norway exceeding the *likely* ranges by some 10s of centimetres, perhaps up to around 1 m by 2100. The spread in the *low confidence* projections increases considerably after 2100 (see Table 3.2).This high-impact low-likelihood sea-level rise above the *likely* ranges is described as a storyline "we cannot rule out" (IPCC, 2021). For such a storyline, Norway would receive 60-70% of the GMSL rise by 2100, but over 90% by 2150. This pattern of change can be explained by the timing and partitioning of ice mass loss from Greenland and Antarctica. Ice mass loss from Antarctica leads to a sea-level rise in Norway that is above the global average owing to GRD effects (e.g. Mitrovica et al., 2009).

		Projected coastal average relative sea-level rate (mm/yr)			
		2050	2100	2150	2300
Medium confidence	SSP1-1.9	0.9 (-0.5 to 3.2)	0.9 (-1.6 to 4.4)	0.6 (-1.5 to 3.8)	-
	SSP1-2.6	1.4 (-0.9 to 4.8)	0.6 (-1.5 to 3.9)	0.2 (-1.7 to 3.1)	-
	SSP2-4.5	2.7 (0.3 to 5.8)	3.3 (0.8 to 7.3)	2.6 (0 to 6.9)	-
	SSP3-7.0	2.8 (0.4 to 6.1)	4.8 (0.6 to 10.5)	4.9 (1.2 to 10)	-
	SSP5-8.5	3.4 (0.2 to 7.7)	6.7 (2.7 to 12.9)	5.8 (1.7 to 11.9)	-
Low confidence	SSP1-2.6	1.4 (-1.1 to 4.8)	0.5 (-2.7 to 4.1)	0.9 (-4.4 to 6.8)	0.3 (-9.6 to 11.8)
	SSP5-8.5	3.6 (0.2 to 9.6)	11.8 (2.4 to 34.1)	23 (-0.4 to 102)	13.4 (-12.2 to 62.7)

Table 3.3: Projected coastal average RSL rates (mm/year) under the different SSP scenarios. Baseline period is 1995-2014. Projected median values are shown with the *medium confidence* (*likely* range) and *low confidence* (17 to 83 percentile spread).

Rates of coastal average sea-level change for the *medium confidence* projections are between 0.9 mm/year for SSP1-1.9 (*likely* -1.6 to 4.4 mm/year) and 6.7 mm/year for SSP5-8.5 (*likely* 2.7 to 12.9 mm/year) by 2100. Under SSP5-8.5 the *low confidence* projections indicate rates could approach ~30 mm/year by 2100, and ~100 mm/year by 2150 (83rd percentile).

3.5 Regional and local sea-level projections

Geographical variations in the projections are largely governed by differences in VLM, GRD effects and the dynamical ocean response play a lesser role. Plots of projected regional RSL changes for 2100 and 2150, relative to the 1995-2014 baseline, are given in Fig. 3.3 and Fig. 3.4. Projected regional RSL *rates* for 2100 are shown in Fig. 3.5. From the envelope of results from all projections (both *medium* and *low confidence* projections, all SSPs, and all projections between the 5th and 95th percentiles) the following statements can be made:

- For 2050, the difference between the lowest and highest projected RSL change along the coast is 0.20-0.25 m. Around two-thirds of locations along the coastline will experience a RSL change within ± 0.05 m of the coastal average change.
- For 2100, the difference between the lowest and highest projected sea-level change along the coast is 0.40-0.55 m. Around two-thirds of locations along the coastline will experience a RSL change within ± 0.10 to ± 0.15 m of the coastal average change.
- For 2150, the difference between the lowest and highest projected sea-level change along the coast is 0.60-1.00 m. Around two-thirds of locations along the coastline will experience a RSL change within ± 0.15 to ± 0.20 m of the coastal average change.

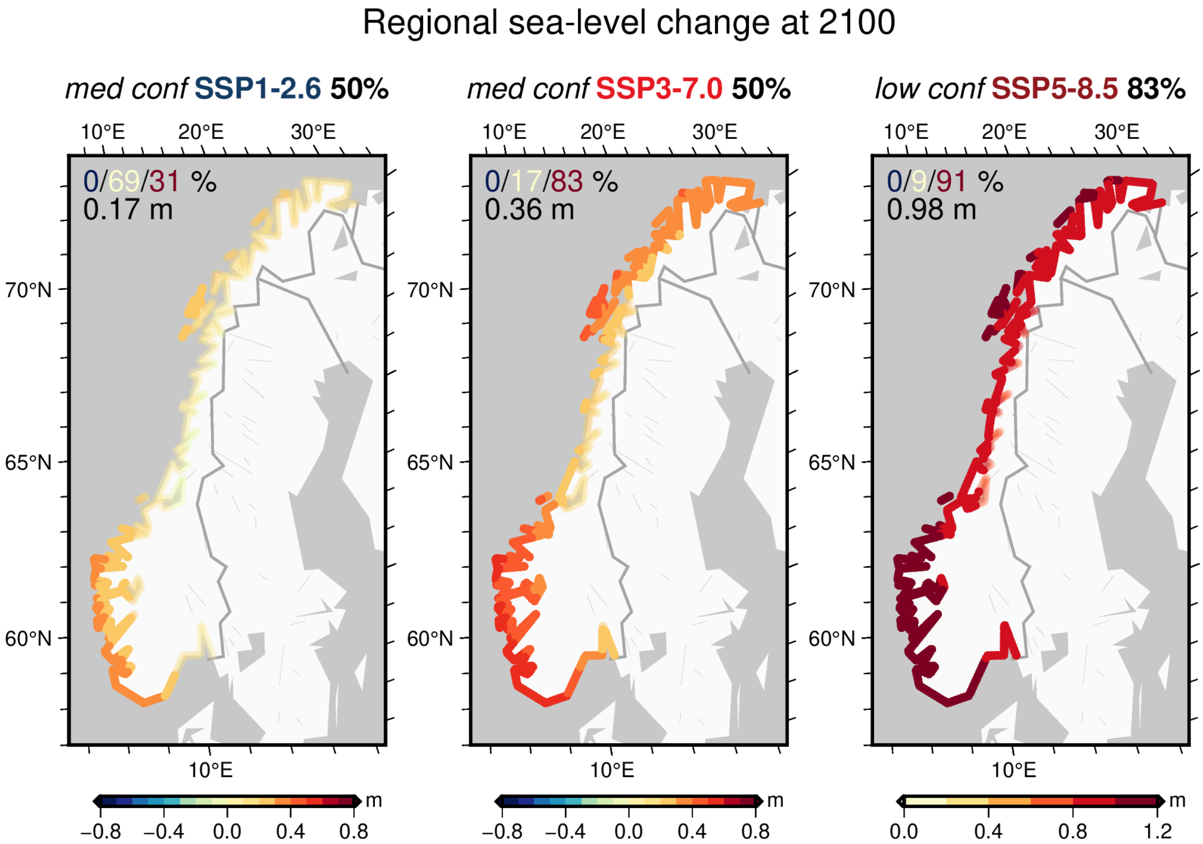

Figure 3.3: From left to right: Projected relative sea-level change at 2100 for the *medium confidence* projections under SSP1-2.6 and 50th percentile (median), *medium confidence* projections under SSP3-7.0 and 50th percentile (median), and *low confidence* projections under SSP5-8.5 and 83rd percentile. Baseline period is 1995-2014. Numbers on the plots show the coastal average relative sea-level change (m) and percentage split of coastline where the spread (17-83%) of the projections is negative/overlaps with zero/positive. Areas where the 17-83% spread overlaps with zero have partially transparent colouring. See Fig. 9.1 for an alternate plot of these data.

Figure 3.3 shows that for the *medium confidence* projections under SSP1-2.6, 31% of the coastline will *likely* experience sea-level rise (the *likely* range is above zero). This shows that Western and Southern Norway, as well as parts of the north, will experience sea-level rise even under a low emission scenario. Whereas for the remaining 69% of the coastline, the *likely* range overlaps with zero, and there is a chance that sea level will be kept stable (marked as partially transparent colours in the plot).

For the *medium confidence* projections under SSP3-7.0, the percentage of coastline *likely* to experience sea-level rise increases to 83%. That is, the majority of the coast. For the remaining 17% of the coastline the *likely* range overlaps with zero. These are the areas between Trondheim and Narvik, and Oslo, where VLM uplift rates are highest. For all SSPs the projections show that no areas of the coast will *likely* experience a sea-level fall (the *likely* range being below zero).

For 2100 the range in the projections along the coast are, from Fig 3.3: For the median value of the *medium confidence* projections under SSP1-2.6 between -0.07 m (lowest) and 0.35 m (highest). For the median value of the *medium confidence* projections under SSP3-7.0 between 0.12 m (lowest) and 0.56 m (highest). And for the 83rd percentile of the *low confidence* projections under SSP5-8.5 between 0.74 m (lowest) and 1.21 m (highest).

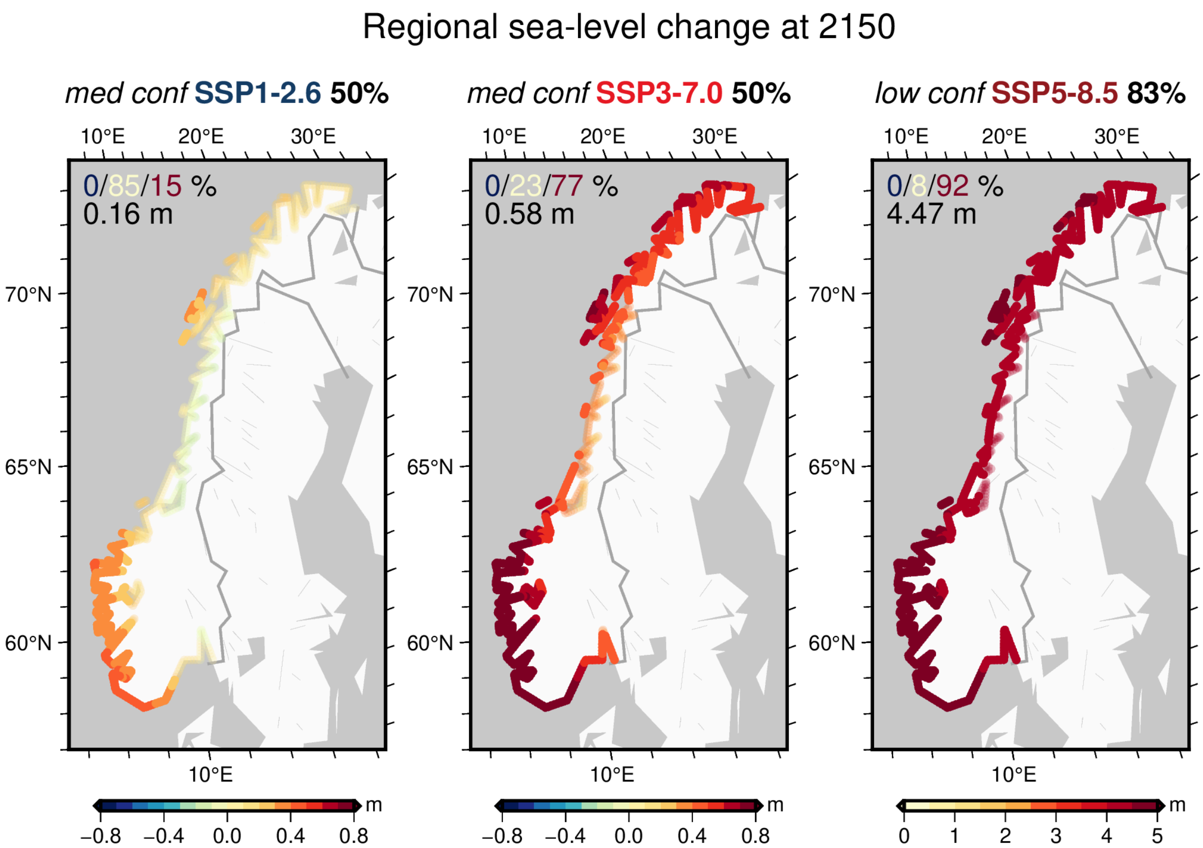

Figure 3.4: From left to right: Projected relative sea-level change at 2150 for the *medium confidence* projections under SSP1-2.6 and 50th percentile (median), *medium confidence* projections under SSP3-7.0 and 50th percentile (median), and *low confidence* projections under SSP5-8.5 and 83rd percentile. Baseline period is 1995-2014. Numbers on the plots show the coastal average relative sea-level change (m) and percentage split of coastline where the spread (17-83%) of the projections is negative/overlaps with zero/positive. Areas where the 17-83% spread overlaps with zero have partially transparent colouring. See Fig. 9.2 for an alternate plot of these data.

For 2150 the range in the projections along the coast are, from Fig 3.4: For the median value of the *medium confidence* projections under SSP1-2.6 between -0.18 m (lowest) and 0.45 m (highest). For the median value of the *medium confidence* projections under SSP3-7.0 between 0.23 m (lowest) and 0.91 m (highest). And for the 83rd percentile of the *low confidence* projections under SSP5-8.5 between 4.09 m (lowest) and 4.83 m (highest).

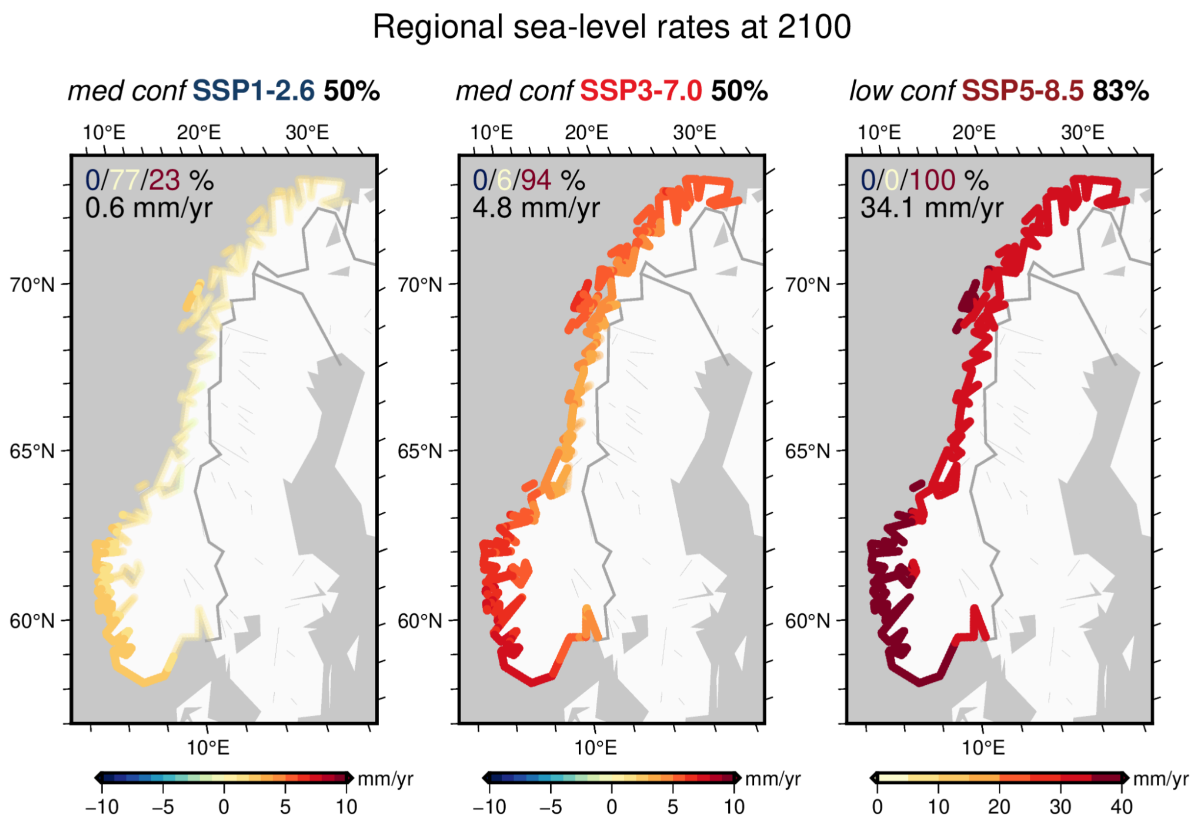

Figure 3.5: From left to right: Projected relative sea-level rates at 2100 for the *medium confidence* projections under SSP1-2.6 and 50th percentile (median), *medium confidence* projections under SSP3-7.0 and 50th percentile (median), and *low confidence* projections under SSP5-8.5 and 83rd percentile. Baseline period is 1995-2014. Numbers on the plots show the coastal average relative sea-level rates (mm/yr) and percentage split of coastline where the spread (17-83%) of the projections is negative/overlaps with zero/positive. Areas where the 17-83% spread overlaps with zero have partially transparent colouring.

For 2100 the range in the projected rates along the coast are, from Fig 3.5: For the median value of the *medium confidence* projections under SSP1-2.6 between -1 mm/yr (lowest) and 2 mm/yr (highest). For the median value of the *medium confidence* projections under SSP3-7.0 between 2 mm/yr (lowest) and 7 mm/yr (highest). And for the 83rd percentile of the *low confidence* projections under SSP5-8.5 between 32 mm/yr (lowest) and 37 mm/yr (highest).

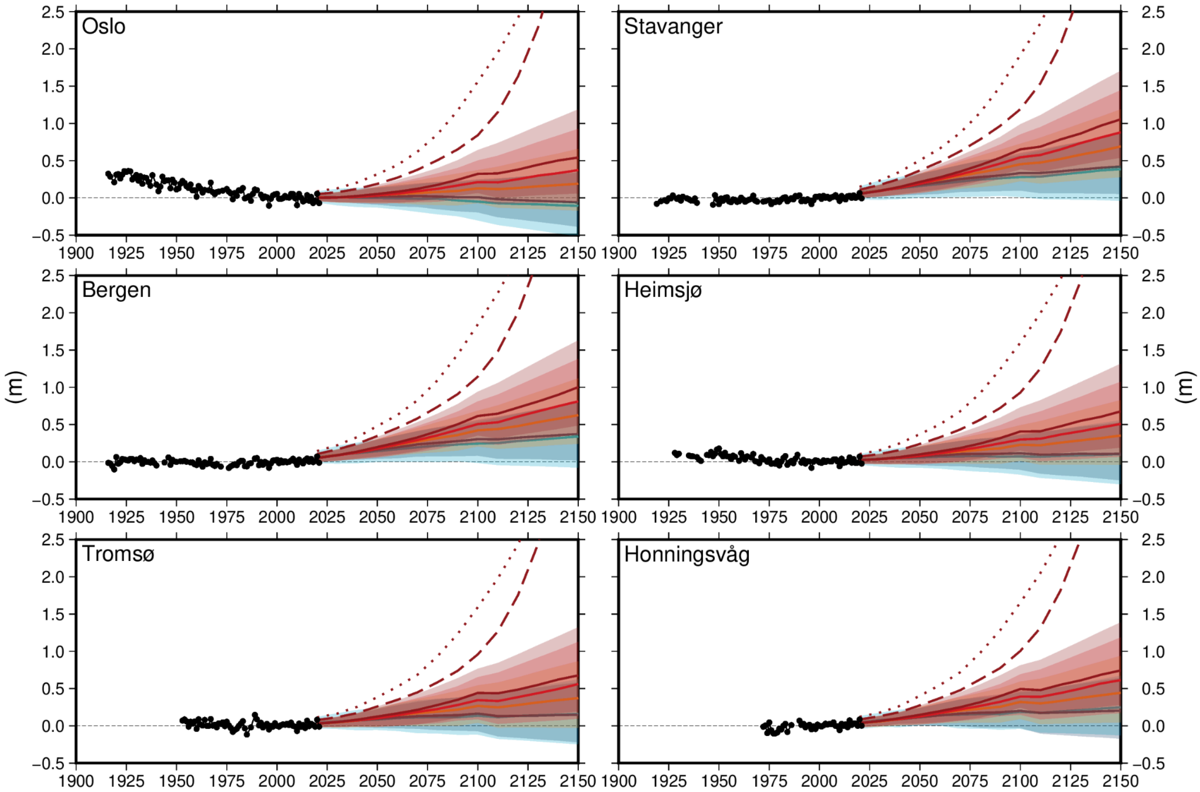

Figure 3.6: Observed and projected RSL change for the different SSP scenarios at six key tide gauge locations. The *medium confidence* projections and their *likely* ranges (17-83%) are shown as shaded. *Low confidence* projections under SSP5-8.5 are shown for the 83rd percentile (dashed line) and 95th percentile (dotted line). See Fig. 3.7 below for colour references for the different SSPs. Baseline period is 1995-2014.

Figure 3.6 shows tide gauge observations alongside projected RSL change for the different SSP scenarios and our six key locations. Some locations show a slight RSL rise while others show falling sea levels over the 20th century (see Chapter 2 for a summary).

As with the coastal average projections, Fig. 3.6 shows the projections across the SSPs are similar and show considerable overlap of their uncertainties up until 2050. After 2050 the projections for the different SSPs begin to diverge. Differences in projected sea-level change at our six key locations can be largely explained by differences in VLM along the Norwegian coast. This essentially explains why Oslo has a lower projected sea-level change than, for example, Bergen and Stavanger on the west coast. GRD effects and the dynamical ocean response play a lesser role in these geographical differences.

Finally, we show the spread in projected sea-level change for 2100 (Fig. 3.7) and 2150 (Fig. 3.8) at our six key locations.

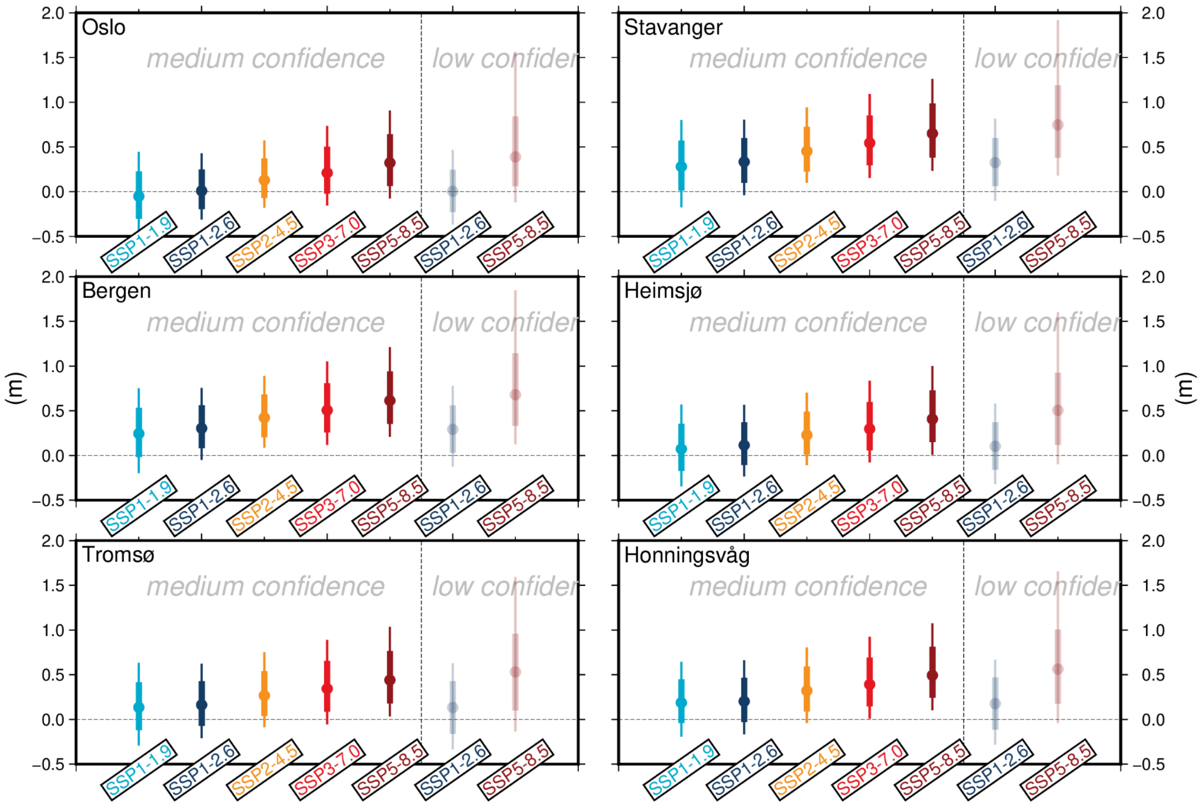

Figure 3.7: Projected RSL change at 2100 for the different SSP scenarios at six key tide gauge locations. Bars show the 17-83% (thick bars) and 5-95% (thinner lines) for the *medium confidence* (solid colours) and *low confidence* (lightly shaded) projections. Baseline period is 1995-2014. See also Tables 9.1 and 9.2 for projected sea-level change (m) and projected sea-level rates (mm/yr) for 2100, respectively.

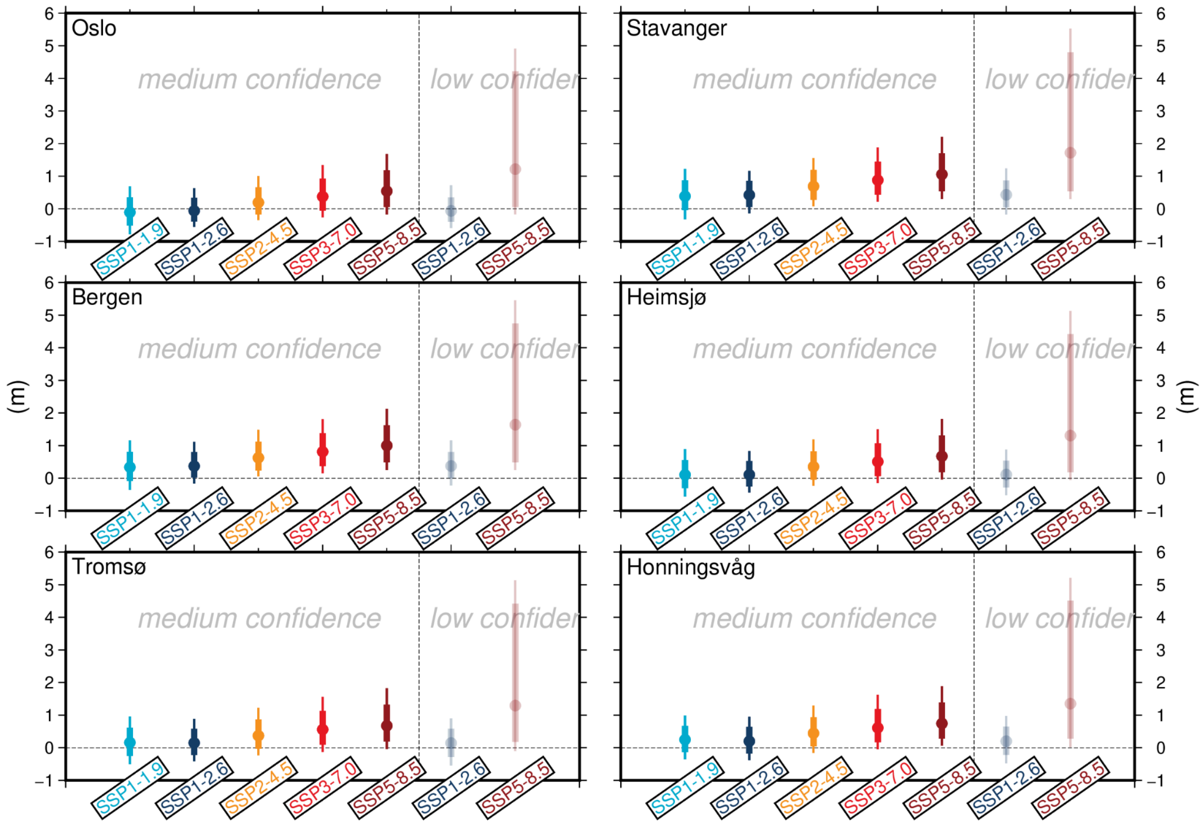

Figure 3.8: Projected RSL change at 2150 for the different SSP scenarios at six key tide gauge locations. Bars show the 17-83% (thick bars) and 5-95% (thinner lines) for the *medium confidence* (solid colours) and *low confidence* (lightly shaded) projections. Baseline period is 1995-2014.

3.6 Uncertainties in the projections

In general there are three sources of uncertainty in climate projections: Emission uncertainty, process uncertainty, and natural variability.

Emission uncertainty is explored by using the different Shared Socioeconomic Pathways (SSPs). SSPs are the greenhouse gas emission scenarios used in IPCC AR6 (Box 1.2). They represent the climate forcing used to produce the sea-level projections presented in this report.

Process uncertainty refers to the uncertainty in the sea-level projections for a specific climate forcing (or emissions scenario). Increases in emissions will cause GMSL to rise because of ice mass loss from glaciers and ice sheets, and ocean thermal expansion. We do not have an exact answer to, for example, how much the Greenland ice sheet will melt for a given level of warming. Instead, a range of outcomes for how much the ice sheet will melt is shown. This means that the physical processes that drive sea-level rise, and for a given climate forcing, have an attached uncertainty. The sea-level projections are therefore presented with a range, for example, the *medium confidence* projections are given with a *likely* range (Box 1.3).

Other possible contributions to process uncertainty are more difficult to quantify. These can come from physical processes that are poorly understood or not included in models (sometimes referred to as deep uncertainty). The *low confidence* sea-level projections attempt to account for such uncertainties by including potential high-end ice sheet contributions, which are driven by processes that are not well understood . These projections include information from a single Antarctic ice sheet model that accounts for marine ice cliff collapse (Deconto et al., 2021), a process that is generally not included in other ice sheet models.

Natural variability refers to the internal variability in the climate system. This can be thought about as noise in the climate system and occurs naturally, i.e., without greenhouse gas emission forcing. Atmospheric variability (e.g. the NAO) and changes in the Norwegian Atlantic Current play an important role in determining the natural variability along the Norwegian coast (see Section 2.5). Natural variability is not directly accounted for in the sea-level projections given in this report.

Over the next few decades, natural variability dominates the overall uncertainty in the sea-level projections. Annual sea level can deviate from mean sea level by up to ± 0.10 m (Section 2.5). This can be an important consideration for stakeholders interested in short timescales. Over longer timescales, that is past 2050, emission and process uncertainty grow and are the main sources of uncertainty in the projections (e.g. Palmer et al., 2020).

3.7 Observation-based projections

Here we explore observation-based extrapolations of RSL for the period 2020 to 2050. Near-term extrapolations serve as a useful comparison to the sea-level projections, and give an indication of the agreement between the projections and the present-day observed RSL trend. This is useful since the projections start in 2020 and we will have to wait some years before they can be evaluated against local RSL records.

Extrapolations are calculated using a similar method to Sweet et al. (2022). Firstly, trends of the individual tide gauge records were estimated by least squares adjustment of the annual tide gauge observations. Data from 1993 to 2020 was used in the regression to ensure the estimated trends represented RSL change from recent decades. To account for serial correlation in the observations, a generalised least squares adjustment with a first order autoregressive (AR1) noise model was applied. The observation-based extrapolations were then calculated for the period 2020 to 2050 by extrapolating the estimated trends into the future.

Initial tests showed that best results were obtained using a basic linear regression model with a constant rate and offset. Tests that tried to account for any acceleration, by including quadratic terms, lead to spurious results: significant positive accelerations at some tide gauges but negative accelerations at others, and some unrealistic extrapolations. Uncertainties on the extrapolations account for (1) the uncertainty of the rate estimate and (2) the year-to-year natural variability of the annual tide gauge measurements.

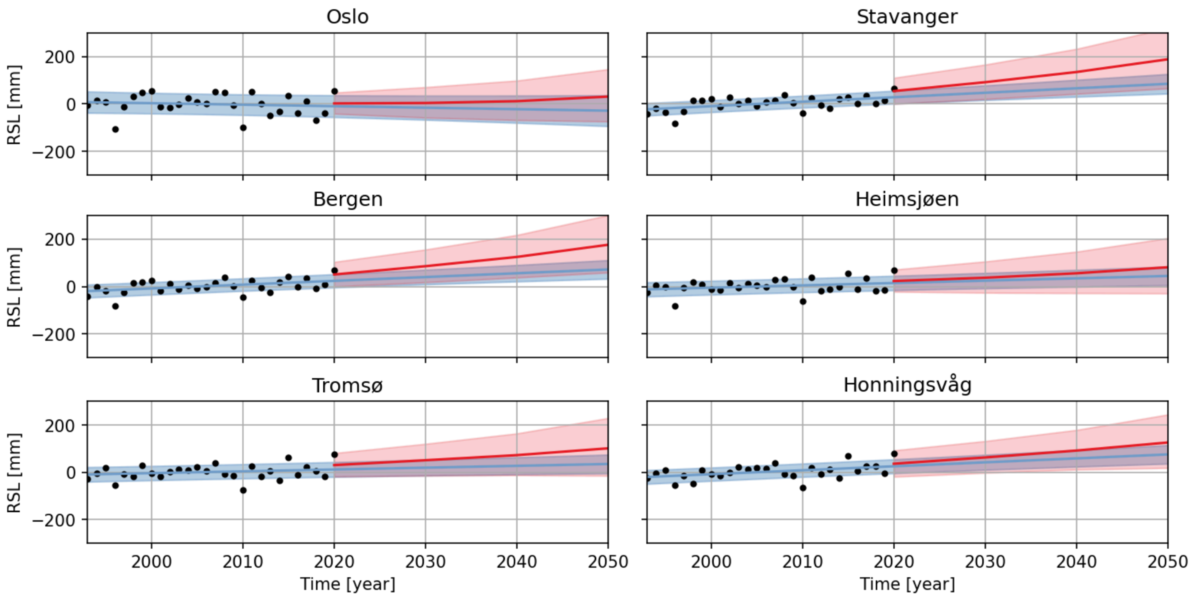

Figure 3.9: Tide gauge observations (black markers) and observation-based extrapolations (blue). *Medium confidence* RSL projections showing the median (red line) and *likely* ranges (red shaded) for SSP3-7.0. Baseline period is 1995-2014.

The RSL projections are very similar across the SSPs in the near-term (2020 to 2050) so only projections for SSP3-7.0 are shown in Fig. 3.9. The observation-based extrapolations sit within the uncertainties of the projections, and their respective uncertainties overlap. In the near-term, therefore, projected RSL does not deviate significantly from the present-day observed RSL trends. That said, at all tide gauges we note that the median projected RSL change is somewhat higher than the median of the extrapolated rates. The largest differences are found at Stavanger and Bergen, where the projections are 27 and 104 mm higher than the extrapolations in 2020 and 2050, respectively.

This difference could simply be because both observed and projected RSL shows an acceleration whereas the extrapolations assume constant sea-level rates. However, examination of the contributions to projected RSL also indicates that the ocean dynamic component to be higher than expected (figure not shown). We suggest that this issue could be the focus of future work. It is important to stress that any data-model mismatch over shorter timescales does not necessarily mean the projections are biassed in the long term, because different physical processes dominate over different timescales.

Tide gauge	Median (mm)	Lower (mm)	Upper (mm)	Δ_{2020} (mm)	Δ_{2050} (mm)	a (mm/yr^2)
Oslo	-28	-94	38	12	59	0.08
Stavanger	85	44	126	27	104	0.13
Bergen	73	34	112	27	104	0.13
Heimsjøen	45	6	84	8	37	0.05
Tromsø	35	-4	74	19	66	0.08
Honningsvåg	75	36	115	11	51	0.06

Table 3.4: Median observation-based extrapolations in 2050 and associated lower and upper uncertainty bounds. Δ_{2020} and Δ_{2050} show the difference between the projections and the extrapolations at 2020 and 2050, respectively, and *a* is the acceleration necessary to bring observations in line with projections by 2050.

By how much would the median of the observed rates (1993 to 2022) have to increase to match the median projected RSL change in 2050? We estimate that it would require an acceleration of between 0.05 to 0.13 mm/yr^2 (Table 3.4). In other words, an increase similar to the GMSL acceleration (0.084 ± 0.025 mm/yr^2) found from satellite altimetry over 1993 to 2017 (Nerem et al., 2018). A modest acceleration in RSL rise therefore has the potential to bring observed sea level in line with projections by 2050. To summarise, the observation-based extrapolations provide a reality check for projections in the near-term. And give some guidance as to how future sea level might deviate from the rates we observe today.

3.8 Long-term sea-level rise, thresholds, and commitment

Owing to the long response times of the oceans and ice sheets, global sea-level rise will continue beyond 2100 and for many centuries to come (Fox-Kemper et al., 2021). Furthermore, sea level is expected to remain elevated over thousands of years. In AR6 it is estimated that, if emissions were to be stopped today, the sea level commitment would be 0.7-1.1 m up to 2300. This is a lower bound on the global sea-level rise that we can expect in the next few hundred years.

Our *low confidence* regional projections suggest coastal average relative sea-level change for Norway under SSP1-2.6 will be between -0.75 and 1.4 m by 2300 (17 to 83 percentiles). Under SSP5-8.5, coastal average relative sea-level change is projected to be between 0.4 and 16 m by 2300. When excluding Marine Ice Cliff Instability (MICI) the spread of projections under SSP5-8.5 is reduced with a high end of ~6 m (Fox-Kemper et al., 2021).

As previously touched upon, both Greenland and Antarctica have tipping points and critical thresholds (see Box 3.1). If global temperatures are sustained over a threshold, the ice sheets become committed to large ice mass losses in the long-term (thousands of years). Committed GMSL rise over 2000 years is estimated in AR6 and given in Table 3.5. These estimates, alongside new evidence (e.g. McKay et al., 2022; Höning et al., 2023), suggest that the ice sheets are very close to or may even have crossed some thresholds. This implies that we are committed to a multiple metre GMSL rise in the long term.

Peak warming (above 1850-1900)	Committed GMSL rise
1.5 °C	2 to 3 m
2.0 °C	2 to 6 m
3.0 °C	4 to 10 m
4.0 °C	12 to 16 m
5.0 °C	19 to 22 m

Table 3.5: Peak warming (above 1850-1900 baseline) and committed GMSL rise over 2000 years as estimated in IPCC AR6 (Fox-Kemper et al., 2021).

It is also possible tipping points in the climate system can interact with each other (e.g. McKay et al., 2022). This can lead to cascading effects, where one tipping point can cause another tipping point to be triggered. For example, a tipping point in Greenland ice sheet melt and large freshwater input could increase the chance of a second tipping point; a collapse of the Atlantic overturning circulation. Cascading effects have implications for sea level and sea level extremes in Norway, but are not further discussed in this report.

3.9 Comparison to projections from previous national sea level report (SLC2015)

Here we compare the regional sea-level projections presented in this national report based on IPCC AR6 with those from the previous report for Norway (SLC2015; Simpson et al., 2015) based on IPCC AR5 (Church et al., 2013). We compare the *likely* ranges of the *medium confidence* projections. These are given as the 5-95% model spread in IPCC AR5, but as the 17-83% percentile ranges in IPCC AR6. This can be confusing for some users but reflects a distinct change in the method for projecting sea level between the IPCC assessments.

The SLC2015 projections were given with respect to the reference period 1986 to 2005. To make a comparison to the IPCC AR6 based projections, we therefore apply a correction (not larger than a few centimetres) so that SLC2015 projections have a baseline reference period of 1996 to 2014 as used in this report.

	Projected relative sea-level change for 2090 (m)			
	RCP2.6/SSP1-2.6		**RCP8.5/SSP5-8.5**	
	SLC2015 AR5	SLR2024 AR6	SLC2015 AR5	SLR2024 AR6
Oslo	-0.08 (-0.32 to 0.15)	0.01 (-0.18 to 0.22)	0.19 (-0.10 to 0.47)	0.24 (0.03 to 0.51)
Stavanger	0.23 (0.01 to 0.44)	0.30 (0.09 to 0.54)	0.49 (0.23 to 0.75)	0.54 (0.31 to 0.82)
Bergen	0.19 (-0.01 to 0.38)	0.28 (0.08 to 0.51)	0.45 (0.22 to 0.69)	0.50 (0.29 to 0.77)
Heimsjø	0.06 (-0.14 to 0.25)	0.11 (-0.09 to 0.33)	0.31 (0.07 to 0.55)	0.32 (0.10 to 0.59)
Tromsø	0.04 (-0.12 to 0.21)	0.14 (-0.06 to 0.38)	0.29 (0.06 to 0.54)	0.35 (0.11 to 0.64)
Honningsvåg	0.14 (-0.11 to 0.40)	0.18 (-0.02 to 0.42)	0.40 (0.08 to 0.73)	0.40 (0.17 to 0.68)

Table 3.6: Comparison of projected sea-level changes for 2090 from SLC2015 (IPCC AR5) and this report SLR2024 (IPCC AR6). Baseline period is 1995-2014.

Table 3.6 shows that the *likely* ranges of the *medium confidence* projections are similar within uncertainties for SLC2015 (IPCC AR5) and this report SLR2024 (IPCC AR6). Averaging across our six key locations, the median projected sea-level change presented in this report and based on IPCC AR6 is 7 cm higher for RCP2.6/SSP1-2.6 and 4 cm higher for RCP8.5/SSP5-8.5 than the projections given in SLC2015. We conclude that the projections for Norway are generally now slightly higher (differences less than 0.1 m for 2090) but these changes are within uncertainties. The projected *likely* ranges in SLR2024 and SLC2015 are therefore broadly similar.

SLC2015 also explored sea level projections outside the *likely* ranges for Norway. In line with IPCC AR5, here it was assumed that only a collapse of the marine-based sectors of the Antarctic ice sheet could cause GMSL to rise substantially above the *likely* range. This extra contribution was stated to be some tens of centimetres. Using a sampling approach, and assuming a lognormal distribution for Antarctica, SLC2015 stated that a sea-level rise in Norway upwards of ~0.5 m above the *likely* ranges was a plausible but low probability event for the 21st century. But stressed that the amounts and timing of these potential ice sheet contributions are very uncertain.

4 Present-day extreme still water levels (ESWLs)

In this chapter we start by discussing how the tides and storm surges contribute to extreme sea levels and vary along the Norwegian coast. We go on to present updated ESWLs for Norway which are important for coastal planning decisions. These levels give a statistical estimate of the present-day risk for today's climate. We show differences between the official ESWLs from 2015 and the most recent update from 2024.

A new high-end ESWL for use in planning is introduced (øvre estimat vannstand). This is of particular relevance for buildings and infrastructure that are important for regional or national emergency response and preparedness. Finally, evidence on changes in the size and frequency of ESWLs is discussed.

4.1 Key points

- Present-day extreme still water levels (ESWLs) have been updated to 2024. Tides and storm surges are the two main contributions to the ESWLs; wave effects are not included. The ESWLs are calculated using statistical analysis (extreme value analysis) of the tide gauge data. They give an estimate of the present-day risk in today's climate.
- The ESWLs are extrapolated to other parts of the coast using observations and a model to quantify the tidal regime in areas away from the permanent tide gauges. In this manner, the Norwegian coastline is divided into tidal zones, and ESWLs are given per zone.
- For our preferred extreme value analysis method and the 2024 update; the 1-in-200 year ESWL has an average uncertainty (5 to 95% confidence interval) of 0.21 m for the tide gauge network. ESWL uncertainties are mostly determined by the extreme value analysis, but there will also be uncertainties introduced in the extrapolation of the ESWLs to other parts of the coast away from the permanent tide gauges.
- There are generally very small changes in the ESWLs between the 2015 report and 2024 updates. The change in the 1-in-200 year ESWL at the tidal zones is generally less than ±0.05 m. An exception to this is the area close to the Andenes tide gauge, which shows a reduction in the height of the 1-in-200 year ESWL of between 0.10 and 0.15 m. Changes in ESWLs from 2015 to 2024 are generally within uncertainties (5 to 95% confidence interval).
- Differences in the ESWLs between 2015 and 2024 can be explained by (1) having 8 years of additional data for the extreme value analysis and (2) improvements to the observations and model used to quantify the tidal regime in areas away from the permanent tide gauges.

- From a user perspective, a major change is that the 2024 ESWLs are provided in the tidal zone format, whereas, in 2015, the ESWLs were given as one (or a few) numbers per coastal municipality.
- Users have raised the need for a high-end extreme still water level. This is of relevance for buildings and infrastructure that are important for regional or national emergency response and preparedness. We provide a new high-end ESWL for use in planning; an estimate of a very rare event when the maximum tide coincides with a very large surge.
- Although sea-level rise has been the major driver of changes to extreme sea levels, some evidence points towards changes in the size and frequency of extremes themselves (i.e. changes in storminess).

4.2 How tides and storm surges vary along the Norwegian coast

For coastal management decisions, it is important to know which water level to be concerned about. Changes in mean sea level represent a long-term trend that we need to adapt to, whereas, in the context of impact, it is the short-term water level changes that need to be taken into account. Although tides are predominantly diurnal, their height (amplitude) varies on a range of time scales from fortnightly to much longer periods due to different tidal constituents. Tidal amplitudes also vary significantly along the coast. Storm surges occur when a low-pressure weather system approaches the coast and its increased surface wind stress and lower pressure acts to push up water levels along the coast. For coastal impacts and preparedness, it is the combination of tides, storm surges, and waves (collectively known as extreme sea levels) that need to be considered.

For coastal planning in Norway, the heights of extreme still water levels (ESWLs) are estimated from tide gauge measurements using extreme value analysis. (This is a standard approach and widely practised in other countries). ESWLs are typically expressed as return frequencies and do not include the effects of waves - waves are discussed separately in Chapter 6. The main contributions to the ESWLs are therefore tides and storm surges. Below we broadly outline how tides and storm surges act and vary along the Norwegian coast (see also Fig. 4.1).

Starting with surges, we first note that Norway's long coastline faces mostly to the west and northwest. As most low-pressure systems move from west to east in the mid-latitudes, this orientation means that coastal communities are prone to a combination of the two main effects of cyclones on water level: (1) the wind effect, or so-called *Ekman transport*, by which the friction of the wind and the earth's rotation leads to a transport of water in the upper part of the ocean which is 90 degrees to the right of the downwind direction (Ekman, 1905). As the water is pushed up against a coastline, a gradual rise in sea level over hours occurs. In addition, the interplay with the earth's rotation sets up a so-called *Kelvin wave* as the piled-up water builds up a pressure gradient and tries to flow back towards the ocean. This results in a wave which travels, like the tidal wave, with the coast to its right in the northern hemisphere at the speed of shallow water waves ($\sqrt{gH}$, where g is the gravitational acceleration and H is the local water depth). An important point here is that this can lead to water level variations far from where the wind pushed up against the coastline. (2) in response to the lower-than-average sea level pressure, the water will rise. This is known as the *inverse barometer effect*. As a rule of thumb, a drop in pressure of 1 hPa leads to an increase of approximately 1 cm in water level.

The combination of Ekman transport and the inverse barometric effect will tend to contribute to particularly high water levels along the western coast of Norway during the passage of cyclones from southwest. Conversely, *northerly* wind situations will tend to set up Kelvin waves in the North Sea. These waves, famously responsible for the 1953 flooding in England and The Netherlands, typically start with a pile-up of water along the east coast of Scotland (Ekman transport to the right of the northerly wind) before progressing towards the south along the east coast of England and eventually northwards along the European coast. An example of such an event is the one in December 2013 which led to severe flooding along the east coast of England and in the German Bight (Staneva et al., 2017; Hewson et al., 2014; Bonaduce et al., 2020). However, such storm surges usually attenuate before reaching the coast of southern Norway, in part because of the deep Norwegian Trench off the south-western coast of Norway. Note also that the *local effect* of northerly winds along the west coast of Norway will be to *lower* the water level through Ekman transport *away* from the coast (Gjevik and Røed, 1976).

The astronomical tides are generally well understood and can be accurately predicted. The tidal regime varies considerably along Norway's coast. The tidal range is smallest along the southern coast and towards the Swedish border. In these regions the ESWLs are largely determined by the storm surges; i.e., the weather effect dominates the astronomical tide, and a storm surge event will have consequences regardless of the tides. For the northern part of Norway and most of the western coast, the amplitude of the astronomical tide is much larger. In these areas the ESWLs are tidally dominated and a storm surge event occurring during low tide has little or no impact.

High tides are higher (and low tides are lower) in the days around a full or new moon (called the spring period) than in the days around a half moon (neap period). In northern Norway it is generally only storm surges that occur in a spring period high tide that will have large consequences. A storm surge during a neap period will typically result in a water level comparable to a normal high tide in a spring period.

This can be seen in Figure 4.1 where Vestfjorden and Ofotfjorden south of the Lofoten islands stand out with both tides and surge among the highest in Norway. See Gjevik (2009) for more information on the tidal differences and variation of extreme still water levels along the Norwegian coast.

4.3 Present-day extreme still water levels and tidal zones

Knowledge of extreme high and low water levels is important for planning purposes, coastal management, and for informing the public. As mentioned, ESWLs are typically expressed in terms of return frequencies. Following Norwegian planning law, residential buildings, for example, need to be built above or protected from the 1-in-200 year ESWL (Fig 4.1). A 1-in-200 year ESWL will on average occur once every 200 years. Alternatively, it has a 0.5% annual probability or an expected rate of 0.005 events/year. The Norwegian Mapping Authority (NMA) is responsible for Norway's official water levels, including the ESWLs.

A challenge with coastal risk management is that although we are interested in historically rare events, like the 1-in-200 or even 1-in-1000 year ESWL, the observational records are typically shorter than 100 years long. However, extreme value analysis allows us to estimate ESWLs with return periods that are longer than the observational records. Different extreme value analysis methods can be used to estimate ESWLs from tide gauge data and these give different results (e.g. Wahl et al., 2017). Currently, Norway's official ESWLs are based on extreme value analysis performed using the Average Conditional Exceedance Rate (ACER) method (Borck and Ravndal, 2024). The ACER method has been shown to be well suited to the Norwegian tide gauge data (Skjong et al., 2013) and it has been possible to automate its application to the entire coast. It is not a true 'peak over threshold' method as recommended by Arns et al. (2013) but is closely related. The ACER method is performed using hourly data where a linear trend has been removed (see Borck and Ravndal (2024) for details). Only tide gauges with at least 35 years of data are analysed - as is generally recommended for extreme value analysis.

Since the amplitude and time of the tide vary significantly along the Norwegian coast, the ESWLs calculated for a particular tide gauge cannot simply be applied to another point of the coastline. Hence, we need to be able to extrapolate these extreme water levels along the coast. In addition to the permanent tide gauges, the NMA also has several hundred shorter data series available from temporary tide gauges, dating from the beginning of the 20th century to present-day. These data series are analysed so that the relationship between the tidal behaviour in the area of the temporary tide gauge and that of the permanent tide gauge can be quantified. Oceanographic and local knowledge is also taken into account in the extrapolation. Following this procedure, the Norwegian coastline has been divided into zones of similar tidal properties (Fig. 4.1). When extrapolating the water level to a point away from the permanent tide gauge, the astronomical tide is first determined using the tidal zones as described above, and then added to the meteorological effect on the water level as seen at the closest permanent tide gauge.

Note that the quality of this extrapolated water level will differ along the coast. The tidal part is locally adapted and thus in general of high quality, except for the coast from Lista to Sirevåg (southern part of Jæren where the tides are very weak) and some smaller basins. As the meteorological effect on the water level is extrapolated from the closest permanent tide gauge, the quality will be reduced with increasing distance from the tide gauge, and in particular when extrapolating into a fjord. The extrapolation model is continuously improved, but only the improvements of the tidal part influences the ESWLs as we need 35 years of observations for these analyses.

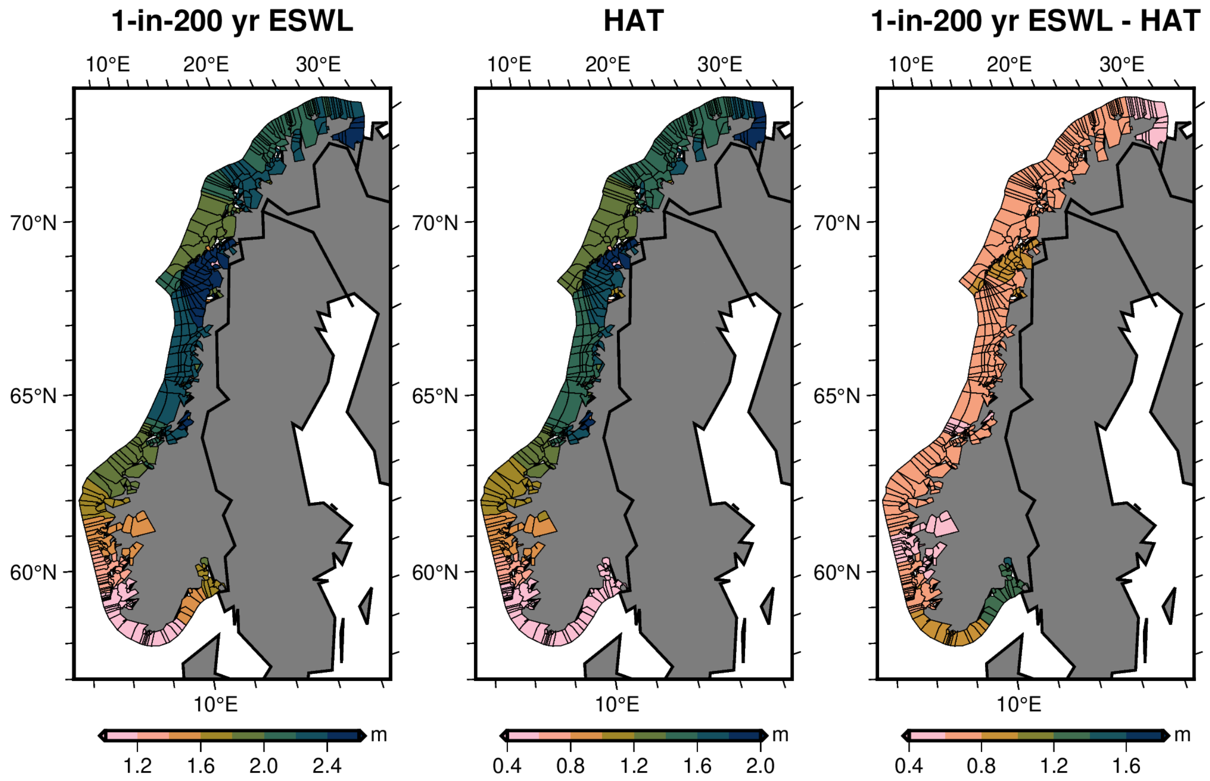

Figure 4.1: Left panel: The height of 1-in-200 year ESWL above mean sea level (1996 to 2014). Central panel: The height of the Highest Astronomical Tide (HAT; the highest possible tidal level, not including weather effects) above mean sea level (1996 to 2014). Right panel: The height of the 1-in-200 year ESWL above HAT. For climate adaptation and planning work, water levels given in Norway's vertical reference frame NN2000 should be used (see Chapter 8).

4.3.1 Differences between ESWLs in SLR2024 and SLC2015

The ESWLs normally undergo a major update by NMA every ~5 years. This ensures that changes in (1) the frequency and height of the sea level extremes, as well as (2) the mean RSL change are taken into account. As a practical consideration, updating the levels every ~5 years also means they are kept stable enough to be used by the general public and by the local and national authorities. The revisions include reviewing the method used, the selection of data, as well as including additional years of still water level observations since the last major analysis. Furthermore, major updates have been performed to coincide with this sea level report series. Note that independent of the major reports, minor updates to the official water levels are done when required (typically whenever better data becomes available for locations where we do not have permanent tide gauges).

The previous major update was done in 2015 (Ravndal and Sande, 2016) at the same time as SLC2015. A major update was planned for 2020 but postponed (at the time it was assessed that the 2015 ESWLs were still valid). The most recent major update was released in 2024 (Borck and Ravndal, 2024) and done to coincide with the current report (SLR2024).

For the major update in 2024 the same methodology is used for calculating the ESWLs as in 2015 (i.e. ACER). For the 2024 update, however, there are 8 years of additional data that go into the analysis. Several minor revisions have also been performed since 2015, mostly concerned with improvements to the model used to estimate still water levels for locations away from the permanent tide gauges. Figure 4.2 shows the ESWLs at the permanent tide gauges and from the 2015 (Ravndal and Sande, 2016) and 2024 (Borck and Ravndal, 2024) updates. General features of the ESWLs show that rarer events (which are larger than the more frequent events) have larger uncertainties.

There are generally very small differences between the ESWLs in the 2015 and 2024 updates. Only Andenes shows a change in the 1-in-200 year ESWL that exceeds ±0.05 m. For the majority of tide gauges, adding 8 years of high-quality observations (2015 to 2022) results in a reduction of the uncertainties (5 to 95% confidence intervals). It is expected that uncertainties on the ESWLs will be smaller the longer the data record they are based on, but other factors impact this too. The average uncertainty for the 1-in-200 year ESWL was 0.23 m for 2015 and is 0.21 m for 2024 (a 0.02 m reduction). However, for tide gauges established in the late 1980s or early 1990s, the reduction has been somewhat larger.

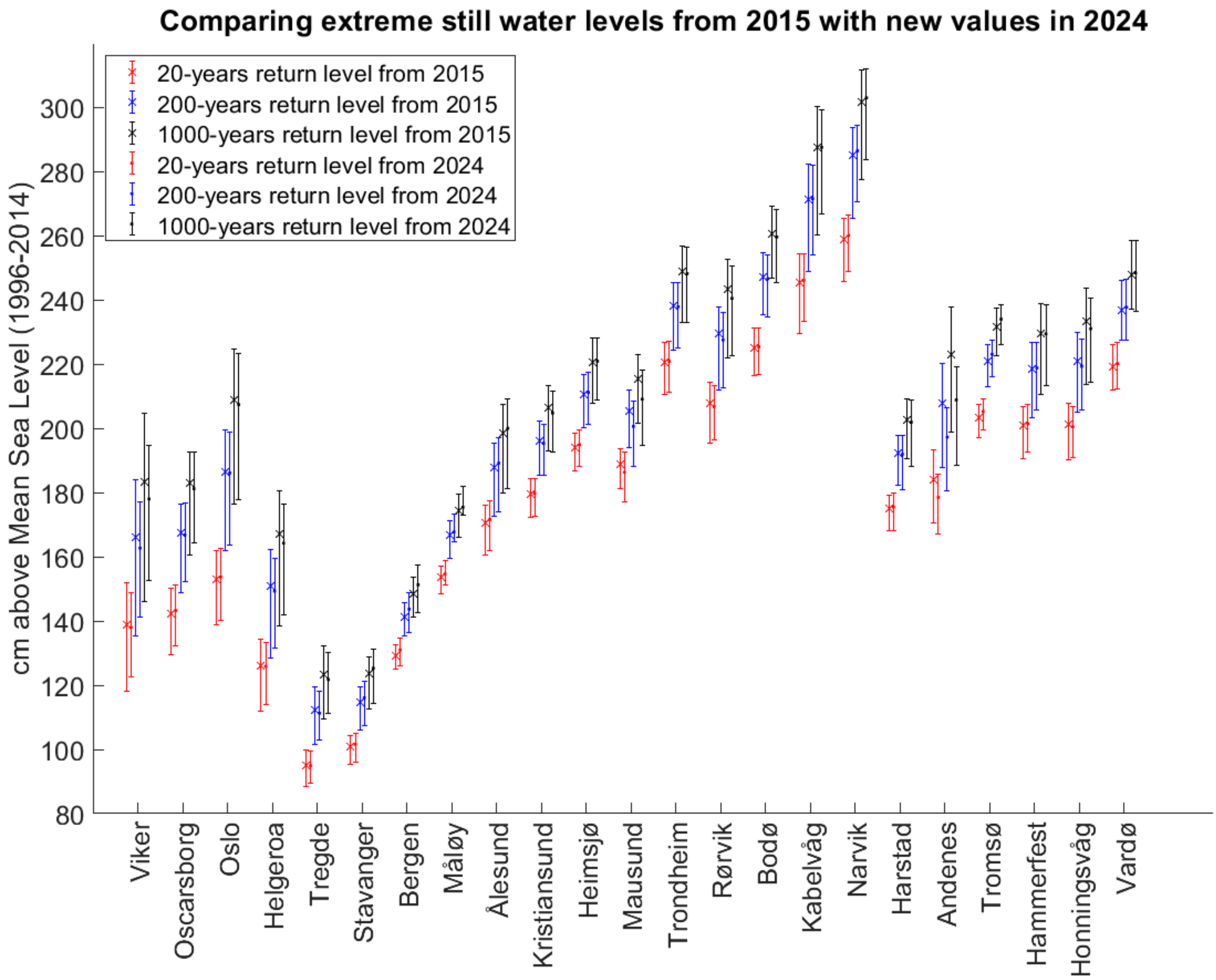

Figure 4.2: The 1-in-20, 1-in-200 and 1-in-1000 year ESWLs at the permanent tide gauges and from the 2015 (Ravndal and Sande, 2016) and 2024 (Borck and Ravndal, 2024) updates.[4] Bars show the 5 and 95% confidence intervals. For climate adaptation and planning work, water levels given in Norway's vertical reference frame NN2000 should be used (see Chapter 8).

For the ESWLs estimated at the tidal zones, changes from 2015 to 2024 can be explained by (1) having 8 years of additional data for the extreme value analysis and (2) improvements to the observations and model used to quantify the tidal regime in areas away from the permanent tide gauges (see Borck and Ravndal (2024) for details). Adding more data has resulted in largest changes close to Andenes; see Figure 4.3 showing a reduction in the height of the 1-in-200 year ESWL of between 0.10 and 0.15 m (including only improvements to the model after 2022).

[4] Mausund was not available for the 2015 analysis. The 2015 ESWLs for Mausund are therefore based on the Heimsjø tide gauge record.

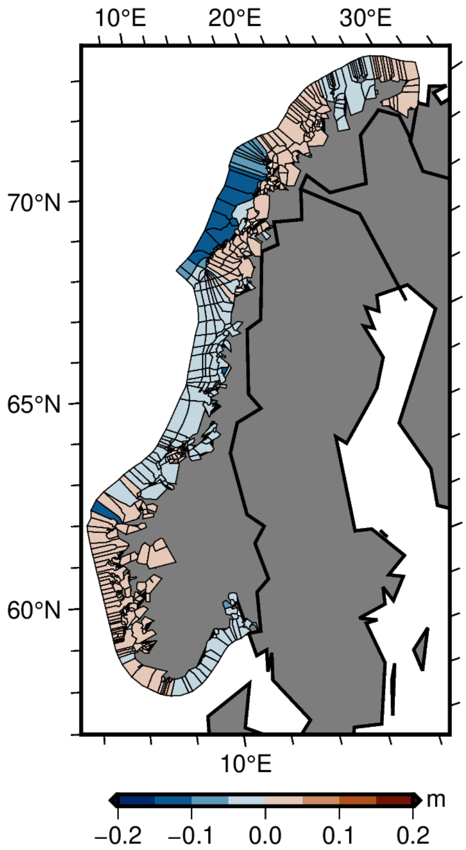

Figure 4.3: Difference between the 1-in-200 year ESWL from the 2024 and 2015 updates. For this comparison, the ESWLs from 2015 have been updated to the tidal zones of 2022.

From a user perspective, a major change in SLR2024 is that the ESWL data products from NMA are provided in the tidal zone format. Whereas, in SLC2015, the ESWLs were extracted as one (or a few) numbers per coastal municipality. This change in format is preferable for the application of the ESWLs in planning at local levels (see also Chapter 8).

4.4 A high-end extreme still water level for use in planning

In addition to the ESWLs described above, users and the authorities have highlighted the need for a high-end extreme still water level (øvre estimat vannstand). This is of particular relevance for buildings and infrastructure that are important for regional or national emergency response and preparedness. In addition, defining such low-likelihood, high-impact events is important for vulnerability testing.

Following SLC2015, when the Norwegian Directorate for Civil Protection (DSB) was working on guidelines for use of sea level information in municipality planning (DSB, 2017), the need for a high-end ESWL was raised. In a first attempt to define a high-end ESWL, it was decided to simply add a 1 m safety margin to the 1-in-1000 year ESWLs from 2015. This high-end estimate was higher than the highest astronomical tide added to the highest observed surge at all of the permanent tide gauges. In other words, it was an estimate of a very rare event when the maximum tide coincides with a very large surge. A drawback of this approach, however, is that a fixed safety margin does not reflect regional differences along the coast. It is a reasonable estimate for west and north of Norway, where the ESWLs are tidally dominated, but likely an overestimate for the surge dominated parts of the south.

How might we better define a high-end ESWL? As noted by Arns et al. (2015), direct methods used for analysing the total observed still water level may underperform in tidally dominated regions. An upper bound from traditional extreme value analysis (e.g. the 1-in-10,000 year ESWL) is therefore likely to have similar challenges as a fixed safety margin. An alternative approach is to use indirect methods (e.g. Wolf et al., 2023); these methods analyse the tidal and surge parts separately. For estimating a high-end ESWL this approach can work well both for tidally dominated and surge dominated areas. It will likely not result in overestimates in the surge dominated areas, but will still account for the very rare possibility that a very large surge could coincide with the maximum tides.

We therefore propose a new high-end ESWL for use in planning; defined as the 1-in-1000 year surge added to the maximum tide (Highest Astronomical Tide, HAT). HAT can be calculated for any given location with high-quality tidal predictions. Thus, the model used to provide water level data for the tidal zones also gives the best available estimates of HAT along the coast. For the surge component we use observations from the permanent tide gauge network for the period from 1992 to 2022. The observed surge is calculated by subtracting high-quality tidal predictions, including the predictable seasonal weather effect, from the high quality observed water level. The resulting time series are then analysed using the same methodology as for the ESWLs, that is, using the ACER method. More details can be found in Borck and Ravndal (2024).

We use the observed surge, often referred to as the (surge) residuals, even though the skew surge is normally used in extreme value analysis of still water levels by indirect methods. The skew surge is the difference between the maximum observed water level and the nearby predicted high-water and is thus not as sensitive to the quality of the observations or the tidal predictions (Bousquet and Bernardara, 2021). Errors in the timing of observations are a common problem for the pre-modern data, but by using only the modern tide gauge data from 1992 onwards we avoid this issue. We also have locally adapted high-quality tidal predictions, typically not available when doing regional or global analyses of ESWLs. The observed surge may still be influenced by some tide-surge interactions, as discussed by Horsburgh and Wilson (2007), where they found it was unlikely that the maximum surge residual would coincide with the high tides. Skew surge has thus been argued to be the best choice in tidal dominated regions (Williams et al., 2016). However, finding the skew surge in areas with small tides or with double high tides is challenging and likely to introduce other artefacts. Since our high-end ESWL will cover both tidal and surge dominated regions, we choose to use the observed surge for the analysis and limit the period to the modern data (Borck and Ravndal, 2024). This will give more consistent results along the Norwegian coast, with smoother changes where the tide gauge of influence changes from one to another.

The resulting high-end ESWL, defined as the 1-in-1000 year surge added to maximum tide (HAT), is shown for the permanent tide gauges in Figure 4.4. We also show the height of the high-end ESWL at the tidal zones, plotted with respect to mean sea level (Fig. 4.5, left panel) and the 1-in-1000 year ESWL (Fig. 4.5, central panel). The difference between the high-end ESWL presented in this report, SLR2024, and that from 2015 is also shown (Fig. 4.5, right panel). This indicates that the high-end ESWL from 2015 was an overestimate for southern parts of Norway and also the area north of Lofoten.

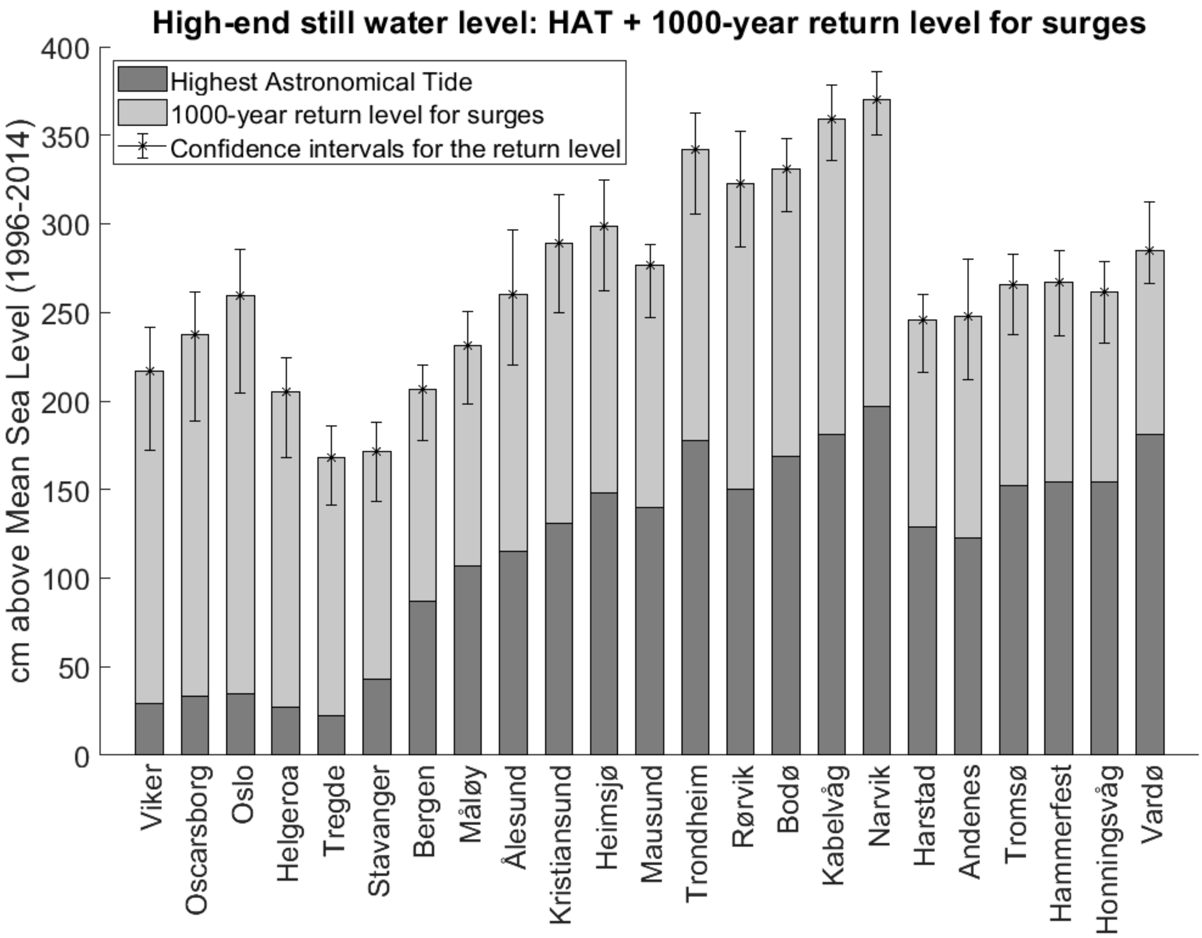

Figure 4.4: A high-end ESWL, defined as the 1-in-1000 year surge added to maximum tide (HAT), at the permanent tide gauges. For climate adaptation and planning work, water levels

given in Norway's vertical reference frame NN2000 should be used (see Chapter 8).

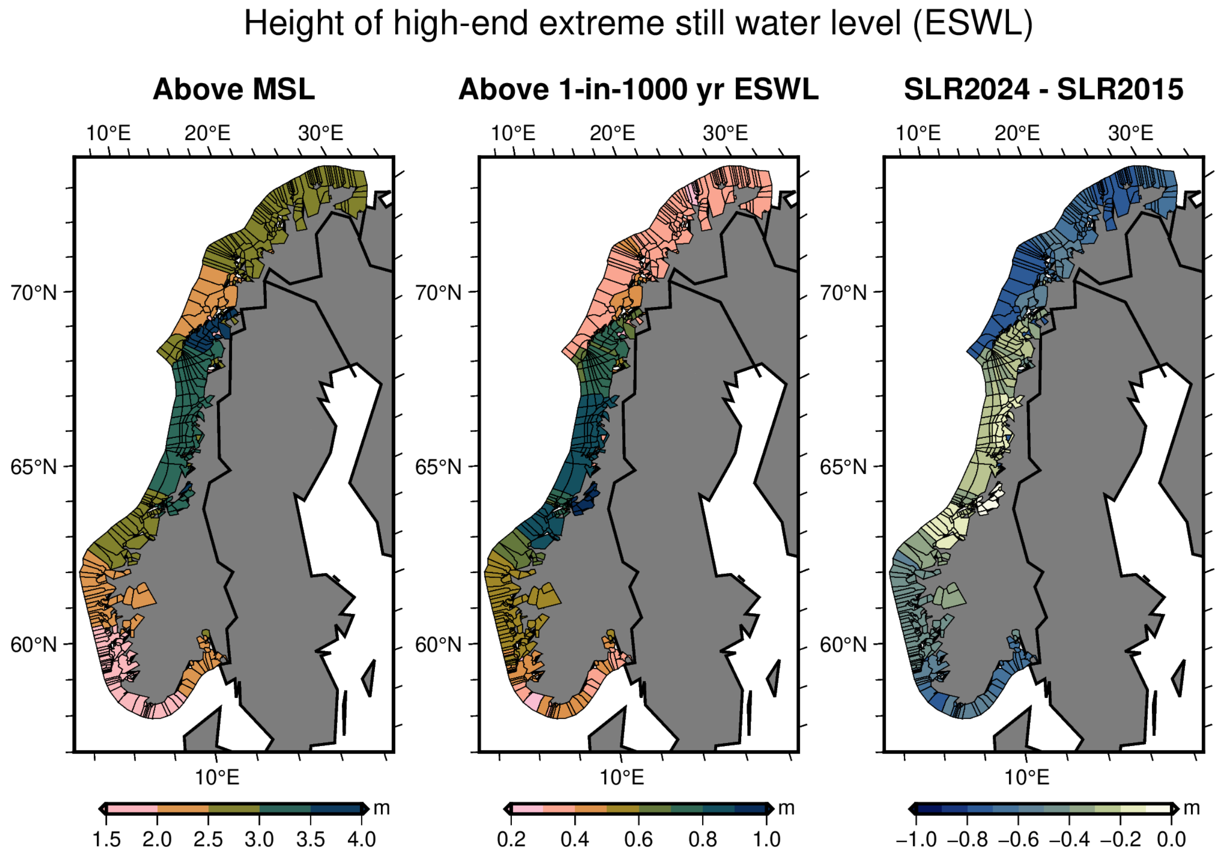

Figure 4.5: Left panel: Height of the high-end ESWL above mean sea level (1996 to 2014). Central panel: Height of the high-end ESWL above the 1-in-1000 year ESWL. Right panel: The difference between the high-end ESWL presented in this report, SLR2024, and that from 2015. For climate adaptation and planning work, water levels given in Norway's vertical reference frame NN2000 should be used (see Chapter 8).

4.5 Evidence on changes in the size and frequency of sea level extremes

The ESWLs presented above and used in Norwegian planning law assume that extreme sea levels do not change over time. But is there any evidence that indicates that the size and frequency of sea level extremes are changing?

Tide gauge observations generally show that mean sea-level rise has been the major driver of increases in the height of extreme sea levels globally (e.g. Menéndez and Woodworth, 2010; Marcos and Woodworth, 2017). The same analyses also show regionally coherent trends in the extremes, with links to large-scale climate modes (e.g. NAO). Results from such regional or global studies show a mixed picture for the Norwegian tide gauge network: Some tide gauges show a small but statistically positive trend in sea level extremes, while others indicate a negative or insignificant trend (these are trends in the extremes after the removal of the mean sea-level trend). More recent work has challenged the view that mean sea-level rise has been the major driver of trends in the extremes. Calafat et al. (2022) find that trends in the extremes and sea-level rise have made *comparable* contributions to the overall change in extreme sea levels in Europe since 1960.

In summary, although sea-level rise has been the major driver of changes to extreme sea levels, some evidence points towards changes in the size and frequency of extremes themselves. This conclusion is drawn from global or regional studies that have included Norway - there has been no dedicated study of observed changes to sea level extremes for the Norwegian coast.

5 Future flood risk changes and storm surge projections

In this chapter we look at two approaches to projecting changes to extreme sea levels, these are: (1) the *static*, or mean sea level offset, approach. Here the projected mean sea-level change is added to the static ESWLs. (2) the *dynamic* approach. Here numerical models are used to project changes to storm surges, waves, and/or tides.

We first show, using the static approach, how sea-level rise can drive dramatic increases in the frequency of flooding. The timing and extent of future flooding frequency changes are also shown. In the second part of the chapter projected changes to storm surges are reviewed.

5.1 Key points

- Sea-level rise will increase flood risk in Norway by pushing up the height of sea level extremes, which will reach higher and further inland.
- Small height differences (0.3 to 0.6 m depending on location) separate the 1-in-200 year ESWL and the once-a-year event. This shows that, in some areas of the coast, only a few decimeters of sea-level rise are required to drive a 200-fold increase in flooding frequency. Sea-level rise will therefore cause the height of historically rare extreme sea level events to be reached annually or more frequently in the future.
- There are large differences in the timing and extent of flooding frequency changes depending on projected sea level. For higher emission scenarios and thus faster and larger future sea-level rises, flooding frequency increases occur earlier and are more widespread. Western and Southern Norway will experience increases in flooding frequency first.
- Projected changes to sea level extremes are primarily determined by the projected mean sea-level change. Changes to the strength and frequency of storms are of secondary importance. There is generally low confidence in projected changes to wind extremes.
- Projections indicate that the mean wind speed for the Norwegian coast may decrease, but the variance can get larger. This suggests that some of the most extreme storm surge events will become more severe in future. There is low confidence in these projected changes.

5.2 Changes in extreme still water levels (ESWLs) due to projected sea-level change - the *static* approach

Here we use the *static*, or mean sea level offset, approach. Following this approach the projected mean sea-level change (Chapter 3) is added to the historical distribution of the extremes (typically expressed as present-day ESWLs, Chapter 4). This assumes that the sea level extremes themselves do not change over time, i.e., they are static. This is a fairly standard approach to dealing with sea-level rise at the national planning level and is current practice in Norway.

Sea-level rise will increase flood risk in Norway by pushing up the height of sea level extremes, which will reach higher and further inland. Furthermore, it is expected to drive dramatic increases in the frequency of flooding (e.g. Fox-Kemper et al., 2021; Sweet et al., 2022). As RSL rises along the coast, this acts to push up the ESWLs. A result of this is that the *height* of historically rare extreme sea level events will be exceeded far more frequently in the future. Changes in the frequency of flooding are typically known as “amplification factors”. The above changes also mean the duration of flooding events will increase.

In SLC2015 it was noted that even small changes to RSL can lead to hundred- to thousand-fold increases in the frequency of exceedance. The *height* of today’s 1-in-100 year extreme still water level (1% annual probability or an expected rate of 0.01 events/year) can in the future be exceeded as often as once a year or more at many locations along the Norwegian coast. Changes in the frequency of exceedance are dependent on projected sea-level change and the spread of the ESWLs.

Firstly we here ask: How much sea-level rise is needed so that the heights of today’s extreme water levels are, on average, exceeded once a year? This is shown in Fig. 5.1. See also e.g. Hermans et al. (2023). The 1-in-20, 1-in-200, and 1-in-1000 year events are chosen as these return frequencies are used in Norwegian planning law. Note that the 1-in-20, 1-in-200 and 1-in-1000 year return frequencies correspond to the 5%, 0.5%, and 0.1% annual probabilities or an expected rate of 0.05, 0.005, and 0.001 events/year.

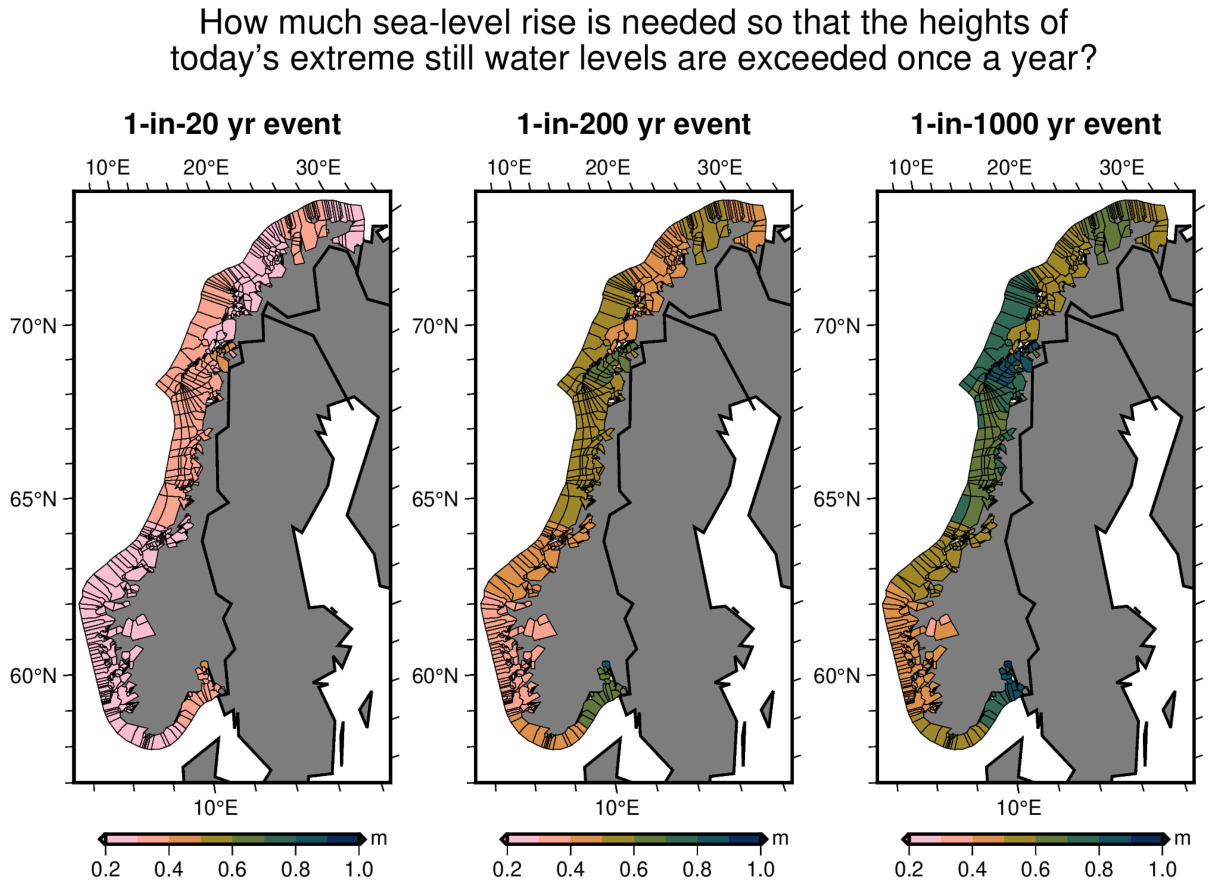

Figure 5.1: Difference in height between historically rare ESWLs and the height which is, on average, exceeded once a year.

The height difference between the ESWLs used in planning and the once-a-year event is largest in Oslo and the north of Norway, around Lofoten. In these locations upwards of 0.6 m sea-level rise is required to change the 1-in-200 year ESWL to a once-a-year event. Smallest differences are in west Norway, where only 0.3-0.4 m sea-level rise is needed. The *spread* between the ESWLs is also smallest in west Norway.

Secondly, we examine when the height of historically rare ESWLs will be exceeded once-a-year given projected sea-level change. For example, when will the 1-in-200 year ESWL be exceeded once a year on average? This is again calculated for the ESWLs used in planning law. The timing of this frequency change for the 1-in-200 year event is shown in (Fig. 5.2). Corresponding figures for the 1-in-20 and 1-in-1000 year ESWL are given in the Appendix; Fig. 9.3 and Fig. 9.4.

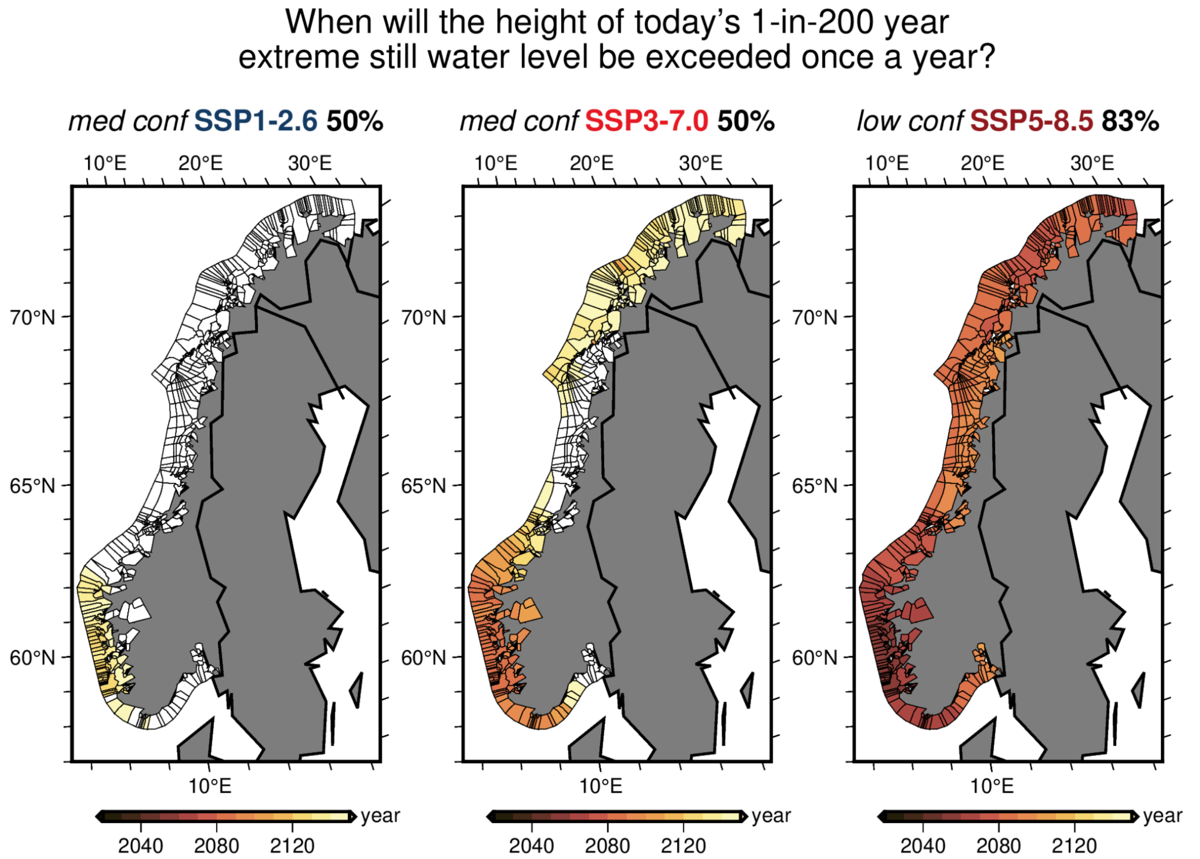

Figure 5.2: Timing of when the height of today's 1-in-200 ESWL will be on average flooded once a year for, from left to right; the *medium confidence* projections under SSP1-2.6 and 50th percentile (median), *medium confidence* projections under SSP3-7.0 and 50th percentile (median), and *low confidence* projections under SSP5-8.5 and 83rd percentile. White areas indicate areas where this frequency change does not occur by 2150.

There are large differences in the timing and extent of the flooding frequency changes depending on projected sea level (Fig 5.2). A feature common to all projections is that Western and Southern Norway will experience increases in flooding frequency first. For SSP1-2.6, the median of the *medium confidence* projections shows the height of today's 1-in-200 year ESWL will be exceeded annually by 2120-2130 in parts of Western and Southern Norway. Other areas are projected to experience a frequency change less than a 200-fold increase, or have a negative projected sea-level change by 2150. For SSP5-8.5, the 83rd percentile of the *low confidence* projections (a low-likelihood high-impact storyline of rapid ice-sheet mass loss) shows all of Norway will experience a 200-fold increase in flooding frequency by 2150. Western and Southern Norway will experience this frequency change first around 2050.

5.3 Projected changes to storm surges - the *dynamic* approach

Following the *dynamic* approach, numerical models are used to project changes to storm surges, waves, and/or tides (e.g. Vousdoukas et al., 2018). These can then be combined with the projected mean sea-level change. The dynamic approach is computationally expensive. There is generally low confidence in projected changes to extremes and there are relatively few studies examining such changes (Fox-Kemper et al., 2021). Furthermore, projected changes to the size and frequency of the extremes (i.e. changes in storminess) are broadly thought to be of secondary importance when compared to the projected sea-level change (Vousdoukas et al., 2018; Muis et al., 2020).

In this subchapter we focus solely on projected changes to the storm surges, whereas Chapter 6 focusses on projected changes to the wave climate. Although surges and waves are driven by the same meteorological conditions, from a user perspective it can be preferable to present these processes separately. This is maybe because of the different time and spatial scales surges and waves act on (surges cause broad regional-scale increases in water levels, whereas waves are a more local effect). The modelling approaches for storm surges and waves are also different.

The frequency of midlatitude storms is expected to change, primarily following a poleward shift of the storm tracks (Seneviratne et al., 2021). Also, a decrease in the pole-to-equator temperature gradient is likely as the Arctic amplification acts to warm the polar regions faster than equatorial regions (Seneviratne et al., 2021). There is medium confidence that changes in the dynamical intensity (e.g., wind speeds) of mid-latitude storms will be small, although changes in the location of storm tracks can lead to substantial changes in local extreme wind speeds (Zappa et al., 2013; Seneviratne et al., 2021). This may then lead to a decrease in average wind speeds in the mid latitudes. However, as shown by Aarnes et al (2017) and others, the variance from one year to another may still increase, and thus the upper percentiles of the wind speed may increase. This is what ultimately drives the most extreme storm surges.

Hydrodynamical models can be used to simulate changes in storm surges due to changes in atmospheric pressure and the wind field in climate simulations. For the European coastline, Vousdouskas et al. (2018) showed increases of storm surges and waves of up to 10%, compared to historical water levels. However, this is part of a global study, and there is low confidence in the projected changes for the Norwegian coast. Box 5.1 shows an assessment of the impact on the Norwegian coastline based on these methods.

Extreme value estimates and storm surge projections are still affected by large uncertainties. The scarcity of regional modelling frameworks capable of resolving extreme events in climate simulations, reduces our capabilities to project storm surges with adequate accuracy. There are only a few studies looking at changes to storm surge climate and, among those, there is little agreement.

Box 5.1: Changes in the 1-in-100 year extreme sea level event

Vousdoukas et al. (2018) assessed changes to the 1-in-100 year event based on CMIP5 scenarios up to 2100 by partitioning the extreme signal into the storm surge and wave set-up components along the world's coastlines. Figure 5.3 shows, based on their results, the 1-in-100 year event due to the combined effect of storm surges and wave setup along the Norwegian coast. Changes in the 95th percentile by 2050 (left panels) and 2100 (right panels) and for the intermediate (RCP4.5; upper panels) and very high (RCP8.5; lower panels) emission scenarios are shown, relative to the period 1980-2014. The figure gives a mixed picture of the potential changes and their sign, but suggests that the 1-in-100 year event could increase by up to 0.5 m for some parts of the Norwegian coast by the end of the century. As we show changes for the upper end of the projections (95%), this is a low likelihood outcome, but can be of relevance for users with low risk tolerance.

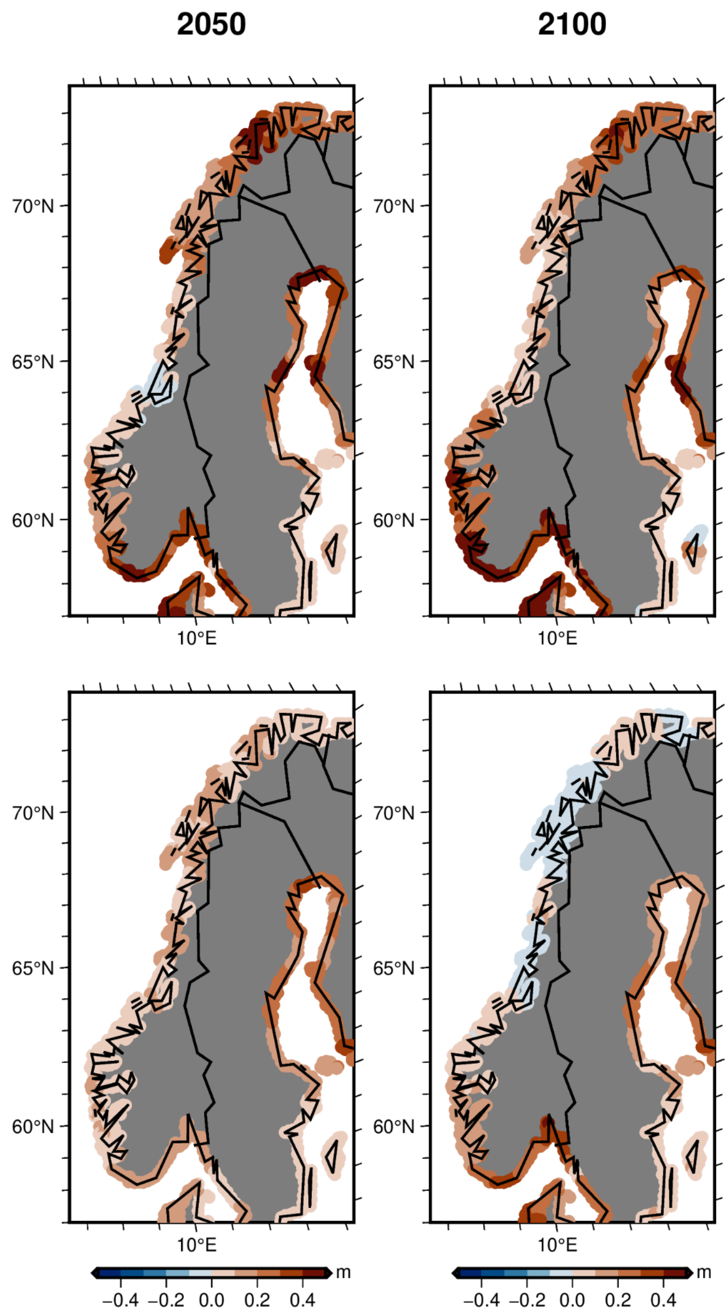

Figure 5.3: Projected changes to the 1-in-100 year extreme sea level event (only contributions from storm surges and wave set-up, see also Chapter 6 for a presentation of projected changes to the wave climate). Projections show the change in the 95th percentile by 2050 (left panels) and 2100 (right panels), relative to the baseline period 1980-2014. Upper panels: RCP4.5. Lower panels: RCP8.5. Data from Vousdoukas et al. (2018).

6 Present-day and future wave climate

In this chapter we first look at the present-day wave climate in the open ocean areas close to Norway. We go on to look at the most important factors users should account for when considering the local wave climate along the coast. Including an example of how the combination of waves and storm surges can impact a coastal site. Finally, projected changes to waves are reviewed.

6.1 Key points

- The coastal wave climate is controlled by the orientation of the coastline, the amount of sheltering provided by islands, and the type of coastline. Determining the local wave climate requires fine-scale wave modelling.
- The combined effect of storm surges and the wave field is determined by the orientation of the coastline and the prevailing wind direction.
- Arctic sea ice is receding and projections indicate that, for all emission scenarios, this will lead to a more severe wave climate in the Barents Sea and along the coasts of Northern Norway due to increased fetch (especially along north-facing coastlines).
- Projections indicate that the mean wind speed for the Norwegian coast may decrease, but the variance can get larger. This suggests that some of the most extreme wave events will become more severe in future. There is low confidence in these projected changes.

6.2 The present-day wave climate

Waves integrate the effect of winds over the stretch of ocean they blow across (Bricheno and Wolf, 2018). This is known as the *fetch* and is influenced by changes in sea ice extent due to global warming (Wolf and Woolf, 2006). This is particularly evident in the northern Norwegian Sea and the Barents Sea, where a large reduction in sea ice cover is expected and wave heights will increase (Bricheno and Wolf, 2018, Aarnes et al., 2017).

The wave climate of the Norwegian Sea is dominated by the progression of low pressure systems from the southwest.[5] Thus, wave extremes in the eastern Norwegian Sea will tend to have an easterly direction of propagation (Reistad et al, 2011, Aarnes et al, 2012, Erikson et al., 2022). The North Sea, on the other hand,

[5] We here define the wave climate in terms of the significant wave height which is traditionally defined as the average of the highest third of individual waves (measured from the trough to the crest) over a period of 20-30 minutes. From wave models, we estimate the significant wave height from the full two-dimensional wave spectrum.

having Great Britain to its west, tends to see the highest waves with northerly winds, which gives the wave field a very long fetch. This difference in the wave climate of the North Sea and the Norwegian Sea is illustrated in Fig. 6.1, where the 99th percentile of the significant wave height modelled with the wave model NORA3WAM is shown.

Extremes in significant wave height, here defined as 1-in-100-year return values, range from 13 m in the central North Sea (Aarnes et al., 2012; Breivik et al., 2013, 2014; Meucci et al., 2018, Bohlinger et al., 2023) to as much as 17 m in the Haltenbanken area (Aarnes et al., 2012). As the Norwegian coastline is mostly rocky with steep bathymetry, little wave attenuation from shallow waters is found, except very close to shore. This means that extremes of more than 14 m can occur close to or on the coastline.

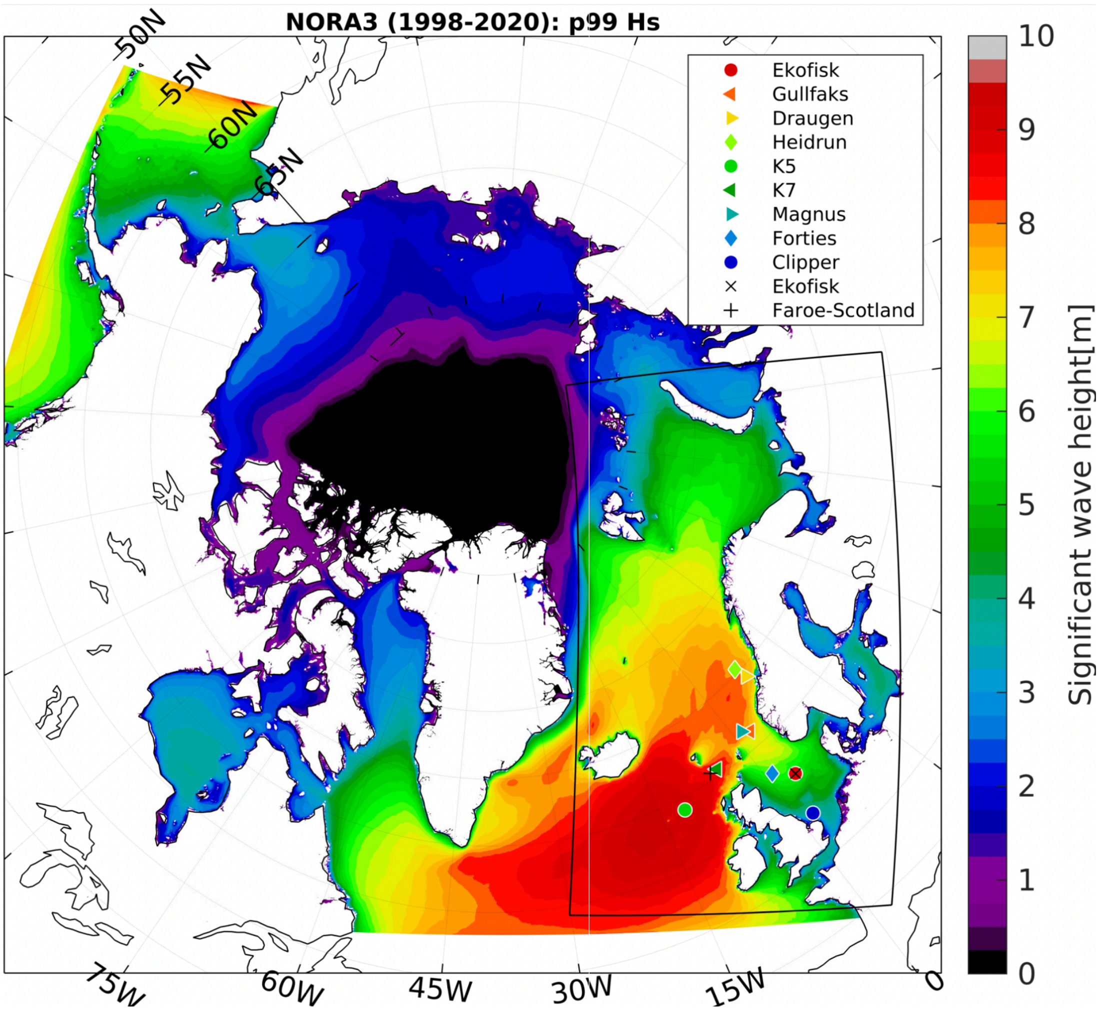

Figure 6.1: The 99 percentile significant wave height from NORA3 (1998-2020). Adapted from Breivik et al. (2022).

One important distinction between waves and storm surges is that the wave field will be effectively reduced inside fjords and behind islands whereas the water level will rise everywhere. This means that the wave field puts higher demands on resolution (higher even than the wind field) to achieve a realistic representation of the local wave conditions and wave climatology. Historical hindcast archives such as NORA3 are only applicable for open ocean conditions, but are a useful starting point for high-resolution studies (see Box 6.1).

Box 6.1: The combined impact of waves and storm surges on a coastal site

Waves and storm surges can pose a double threat to vulnerable infrastructure along the coast. In cases with southwesterly winds, the Ekman transport combined with the inverse barometer effect will tend to lead to higher than normal water level. Under such synoptic situations high waves will coincide with strong winds *and* a higher than normal water level. On the other hand, situations with northerly winds will tend to be associated with lower than normal or average water level, and waves will tend to follow the coastline, thus their impact on coastal infrastructure will be smaller.

The combined impact of waves and storm surges involves long-term (several years) simulations of the wave field and the water level. The most important factors to take into account are:

- Directional exposure (i.e., whether infrastructure is facing west and north, where the strongest winds typically come from)
- Fetch (the stretch of water available for creating waves in sheltered seas)
- Width of the fjord/bay (wider means the wind has more lateral room to work)
- Orientation of the stretch of coastline in question (i.e. the degree of exposure to a combination of storm surges and waves)
- Coastline features (e.g., beaches will experience wave runup, whereas cliffs will not)

To illustrate the combined effect of waves and water level we look at the case of Stavanger harbour (from the report by Aarnes et al., 2020) as shown in Fig. 6.2. In a sheltered area with a north-facing inlet, such as Stavanger harbour (shown in the right hand panel), the waves will be lower than normal (the blue arrow) when the wind is southerly, due to the short fetch (i.e. sheltering by land). Thus, the waves are *low* when the water level is *high*. On the contrary, for northerly winds, the waves are *high* due to the long fetch over the Boknafjord. However, as shown in the left panel, the water level will be *lower than average* in such cases due to the Ekman transport away from the coast (see Chapter 4). This demonstrates the importance of the local orientation of the coastline, which in the case of Stavanger harbour works to its advantage.

On the other hand, a harbour facing south west would experience higher than normal water levels simultaneously with high waves. This also explains why most harbours in Norway are not facing south west.

Figure 6.2: Waves and storm surges in combination can yield a very different total impact depending on the wind direction. Left panel: A wind from the south leads to Ekman transport to the right toward the coast (grey arrow). This leads to an increase in water level (red arrow). On the contrary, northerly winds (upper wind barb) leads to Ekman transport toward the open ocean (grey arrow pointing west). This leads to a decrease in water level (blue arrow). Right panel: Stavanger harbour faces north. This means it experiences high waves in the long fetch of northerly winds (red arrow means higher than normal waves) and low waves in southerly winds due to the short fetch (blue arrow indicates lower than normal waves).

6.3 Future wave climate

It is estimated that 50% of the world's coastlines are at risk from wave climate change (Morim et al., 2019). Although ocean waves are an important component of the Earth's climate system, as they control the interaction between the ocean and the atmosphere (Hemer et al., 2013; Breivik et al., 2019), the vast majority of Earth System Models (CMIP5/CMIP6) do not incorporate wave models. In ESMs the wave-induced processes are primarily parameterized by the wind.

However, as shown by Fan and Griffies (2014) and Belcher et al. (2012), the coupled wave-atmosphere-ocean effects are important to get the right heat exchange across the ocean surface. Although this does not affect the water level directly, it has an indirect effect as it modifies the wind field. The direct effect is that waves also enhance the surface roughness, leading to a stronger drag on the water surface. This in turn affects the water level (Staneva et al., 2017) both in the open ocean and in coastal areas (Bonaduce et al., 2020).

Aarnes et al. (2017) used wind field ensembles from six CMIP5 models to force wave model time slices of the northeast Atlantic over the last three decades of the 20th and the 21st centuries with RCP4.5 and RCP8.5 emission scenarios. They found the future wave climate in the period 2071-2100, relative to 1971-2000, to have a lower mean significant wave height in the northeast Atlantic. However, they found a small increase in the future extremes (Aarnes et al, 2017) in certain regions along the coast of Norway from Stad and northwards (with low confidence). Bonaduce et al. (2019), investigating the wave climate in the North Sea under a very high emission scenario, also found an increase in the extreme significant wave height by the end of the century for the same areas. Recent findings by Meucci et al. (2023), who performed global wind-wave simulations over 140 years under two different emission scenarios (SSP1–2.6 and SSP5–8.5) found that changes in wave climate are projected to be most significant in the North Pacific, the North Atlantic, and the Southern Ocean due to changes in the wind field, while in the Arctic the large sea ice retreat triggers a sharp increase in the projected wave heights.

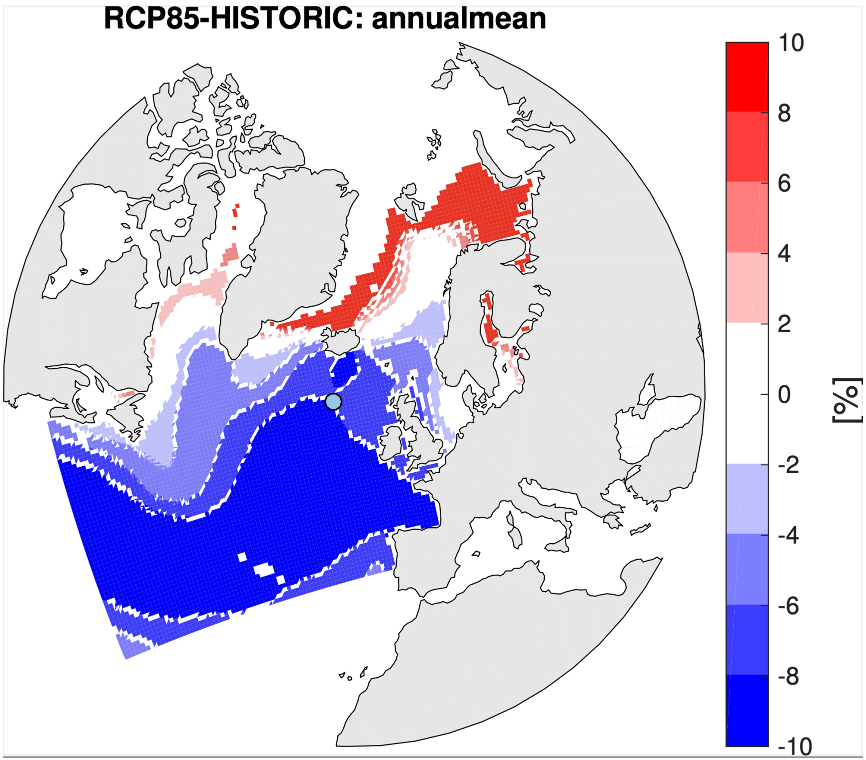

Figure 6.3: The difference in annual mean significant wave height between an ensemble of historical (1971-2000) climate model integrations and future (2071-2100) climate projections under the RCP8.5 scenario. An increase of up to 10% is expected in the Barents Sea and the north-western part of the Norwegian Sea due to receding ice cover. Modified from Fig. 3b by Aarnes et al. (2017).

The Norwegian Sea lies between the zone of receding sea ice and the North Atlantic and is expected to see both increases in its northern part and a decrease in its southern part, see Fig. 6.3 (modified from Aarnes et al., 2017) which shows the impact of receding ice cover on the wave field. Here, red marks regions where the future wave annual mean wave height is expected to increase, mainly due to receding ice cover. What is also clear from the figure is that there is an expected decrease in annual mean wave height further south (the regions marked blue). This is due to a general reduction in average wind speed in the region. It is important to note, however, that although the mean decreases, the spread between the lowest and highest percentiles appears to increase (Aarnes et al., 2017). This suggests that some of the most extreme wave events will become more severe in future (low confidence).

7 Acknowledgements

This report went through an informal review process. We are very thankful to Jan Even Øie Nilsen, Matt Palmer, Tom Howard, Anita Verpe Dyrrdal, the Norwegian Environment Agency and the project’s reference group for useful feedback and discussions. We thank Gökhan Aslan and John Dehls for providing the InSAR figure and helpful advice. ØB is grateful to the Research Council of Norway for funding through the StormRisk project (grant no 300608), which partially funded MET Norway's production of the NORA3 and NORA-Surge atmosphere, wave and water level hindcast archives.

We thank the projection authors for developing and making the sea-level rise projections available, multiple funding agencies for supporting the development of the projections, and the NASA Sea-Level Change Team for developing and hosting the IPCC AR6 Sea-Level Projection Tool.

8 Data availability and vertical reference levels

For coastal municipalities there are two main data products for local planning that can be used “off-the-shelf”:

1. Sea level allowances (klimapåslag) based on IPCC AR6 projections.
2. Updated ESWLs for the return frequencies used in Norwegian planning law (1-in-20, 1-in-200, and 1-in-1000 year ESWLs corresponding to the F1, F2, and F2 safety classes). A new addition to this dataset is an estimated high-end ESWL (øvre estimat vannstand).

These datasets, adapted for local planning and available via Geonorge.no, are described in Section 8.1 and, for more in-depth analyses, in Section 8.3. Sea-level projections and extreme still water levels can also be viewed on the Norwegian Mapping Authority’s (Kartverket) website Sehavnivå.no. Guidelines for how to use these data products in municipal planning will be given in a separate document and are the responsibility of The Norwegian Directorate for Civil Protection (DSB).

Section 8.2 deals with vertical reference levels (or datums) which are vital for local planning and climate adaptation work. There are different types of geodetic and tidal vertical reference levels users need to be aware of. NN2000 is, for example, the national vertical reference frame currently in use in Norway. Finally, Section 8.3 lists data that can be used for more in-depth analyses.

8.1 Data products for use in local planning

DOK-datasets (Det offentlige kartgrunnlaget – publicly available geodata for use in planning) are available at Geonorge.no and are the official data products that coastal municipalities should use in local planning.

For integrating sea-level rise and storm surge information in local planning, use the DOK-dataset “Storm surges and sea-level rise” (“Stormflo og havnivå”). This is a geospatial dataset with layers showing the flooded area for a given water level: It contains the 1-in-20, 1-in-200, and 1-in-1000 year ESWLs corresponding to the F1, F2, and F2 safety classes (TEK17), plus an estimated high-end ESWL (øvre estimat vannstand). It also includes layers for the mean high water level; which is the level used to identify areas that will be permanently inundated by seawater. These water levels are available both in combination with (1) current sea level and (2) the sea level allowance (klimapåslag) as recommended in DSB’s guidelines. All layers are given in Norway’s vertical reference frame, NN2000. These flooding layers can also be viewed using a webtool called “Se havnivå i kart”.

These data products have a number of limitations that users should be aware of. One significant limitation, for example, is that the water level datasets do not include wave effects. Other general limitations are listed in Section 1.1, and more details of the underlying datasets and their limitations can be found in Chapters 3 and 4.

8.2 Vertical geodetic and tidal reference levels

Vertical reference levels are vital for local planning and climate adaptation work along the coast. A vertical reference level (or datum) is a surface with zero elevation. There are a number of different vertical reference levels and understanding these, and how they relate to each other, is crucial for compatibility and consistency when working with geospatial data (Fig. 8.1).

When working with water level information the most important reference levels are mean sea level (middelvann), mean high water (middel høyvann), the highest and lowest astronomical tide, the chart datum, and normalnull 2000 (NN2000). These are briefly explained below.

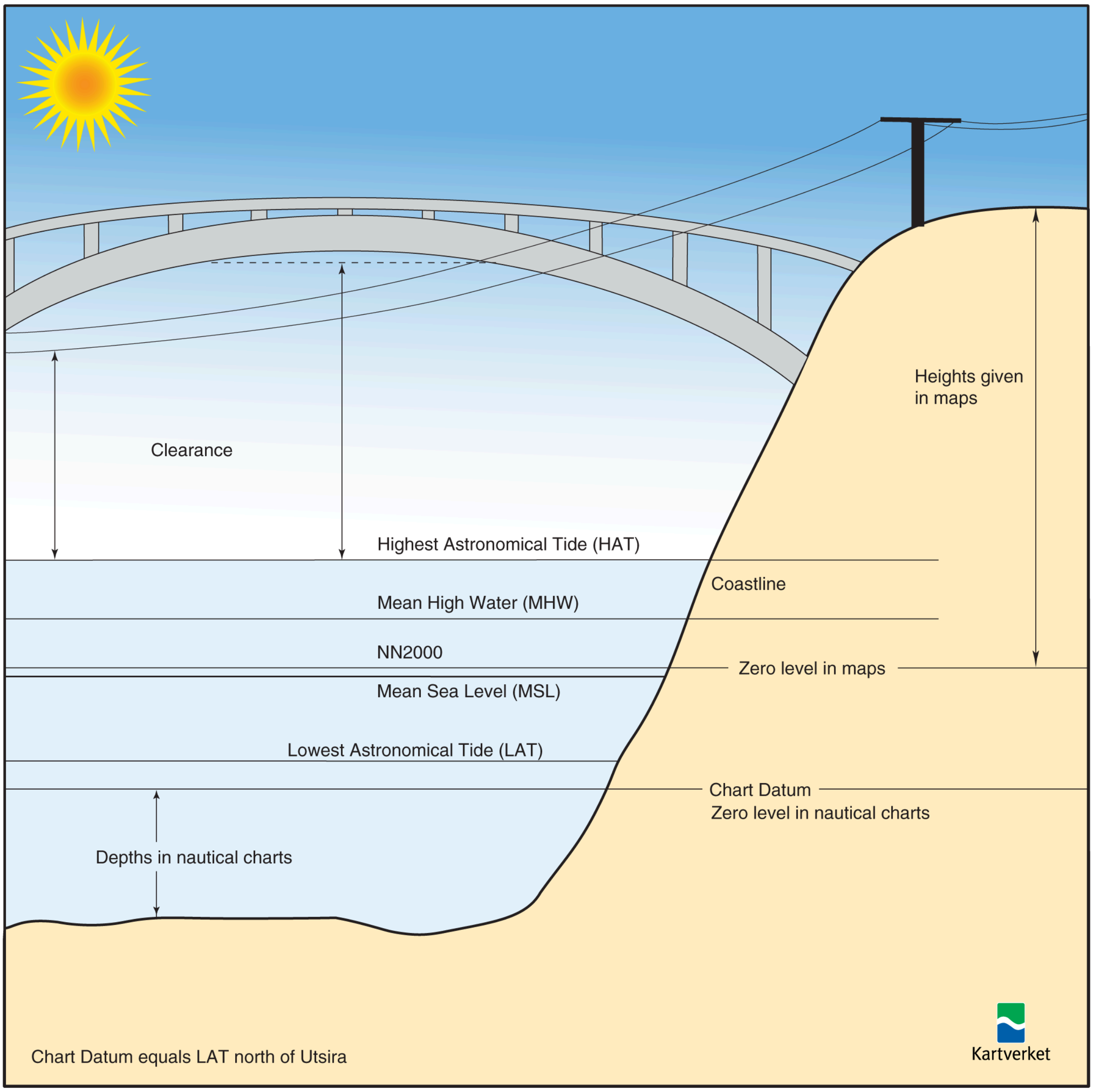

Figure 8.1: The relationship between different vertical geodetic and tidal reference levels.

Mean sea level (MSL) is the average height of the observed surface of the sea over a 19-year period. The official MSL for Norway is currently for the period 1996 to 2014. As sea level changes over time and as measurements of MSL have improved, the official MSL reference level is occasionally updated, the last time being September 2015.

The ESWLs shown in this report are given with respect to observed MSL (1996-2014). Whereas the baseline period for the sea-level projections is 1995 to 2014. The period used for the official MSL for Norway (1996-2014) and the baseline period for the sea-level projections (1995-2014) are therefore essentially the same. Any differences between these periods are negligible and can be ignored for practical purposes.

Mean High Water (MHW) is the average of all the high water heights observed over a 19-year period. MHW defines the coastline boundary on both land maps and nautical charts, and is the tidal datum used to define areas that are permanently inundated by seawater.

The **Highest Astronomical Tide** (HAT) is defined by the International Hydrographic Organisation as being “the highest tidal level which can be predicted to occur under average meteorological conditions and under any combination of astronomical conditions” (IHO, 2014). In practice, HAT is determined by taking the highest predicted tide over a period of 19 years, which ensures that all combinations of astronomical conditions are considered. HAT is thus the highest possible tide when ignoring the effect of storm surges. HAT is useful for defining clearance under bridges or power lines.

The **Lowest Astronomical Tide** (LAT) is the lowest predictable tide under any combination of astronomical conditions. Like HAT, LAT is determined by taking the lowest predicted tide over a period of 19 years.

Chart Datum is the zero level of nautical charts to which all depths are given. For safety reasons, Chart Datum is defined to be a level that the water level seldom sinks below. North of Utsira, Chart Datum is equal to LAT. For the southern and southeastern coast, where the water level can be dominated by the weather effects, Chart Datum is defined to be 20 or 30 cm below LAT.

Normalnull 2000 (NN2000) is the name of the national vertical reference frame currently in use in Norway (Lysaker and Vestøl, 2020). NN2000 is the datum typically used for basic maps of Norway, local planning and climate adaptation work, and surveying.

Users need to be able to transform geospatial data referenced to these different vertical geodetic and tidal reference levels into a common system. This allows users to mesh different geospatial datasets together – and is vital for consistency. Users should be aware that offsets between vertical reference levels vary significantly depending on location. For example, the height of mean sea level in NN2000 varies by approximately 40 cm along the coast (Fig. 8.2).

Vertical transformations can be performed using height conversion models (Separasjonsmodeller) available at Geonorge. These conversion models contain dynamic data, i.e., they will be periodically updated as new methods and data become available. For the DOK-datasets used in local planning, all data has been transformed to NN2000 for ease of use. DOK-datasets are automatically updated to make use of the most up-to-date height conversion models.

Users should also be aware that the offsets between the different vertical reference levels are only well known close to the permanent tide gauges; they are less well defined in other parts of the coast. The uncertainty associated with the height of mean sea level in NN2000 can be up to 30 cm in certain areas - due to errors in NN2000 and uncertainty related to the mapping of variations in dynamic ocean topography (Kartverket, 2021). Hence, transforming data from mean sea level to NN2000 introduces additional errors.

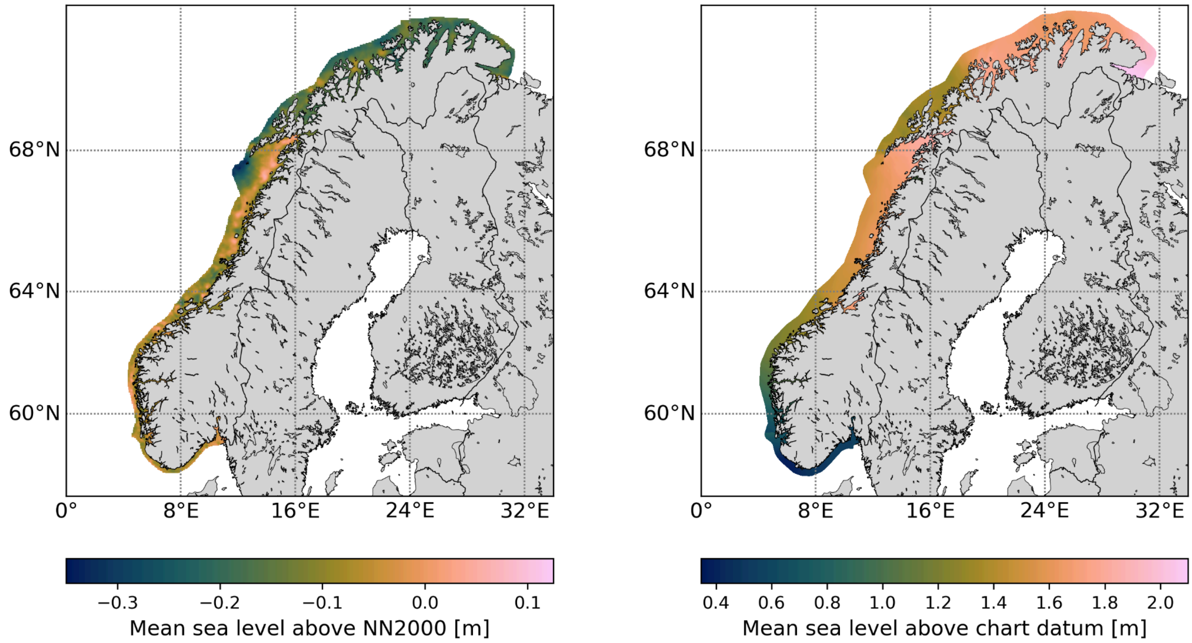

Figure 8.2: The height of mean sea level (1996-2014) above NN2000 (left) and above the Chart Datum (right) along the Norwegian coast.

8.3 Data for in-depth analysis

8.3.1 Sea-level projections based on IPCC AR6

Sea-level projections are available as gridded data in netCDF version 4 format here (Simpson, 2024). The variables in the gridded netCDF data are described below (Table 8.1).

quantile	Quantiles of the distribution of the sea-level change variable. Quantiles from 0.01 to 0.99 in 0.01 increments are available. In addition, the quantiles 0.001, 0.005, 0.167, 0.833, 0.995, and 0.999 are included. (total of 105 quantiles). Multiply by 100 to get the equivalent percentile values.
year	Years at which projection data are available. The *medium confidence* projections are available from 2020 to 2150 in 10-year increments (14 time steps). The low *confidence* projections are available from 2020 to 2300 in 10-year increments (29 time steps).
lat	Latitudes from 49 to 75 degrees north in 1/12 degree increments (313 values).
lon	Longitudes from 0 to 50 degrees east in 1/6 degree increments (301 values).
sea_level_change (sea_level_change_rate)	Projected sea-level change (rate) with respect to the reference period 1995-2014. Units are millimeters (millimeters per year).

Table 8.1: Variables given in the gridded netCDF data for the sea-level projections.

8.3.2 Extreme still water levels, tidal reference levels, and sea-level observations

Relevant datasets used or presented in this report that can be viewed or accessed for more in-depth analysis include:

- Extreme still water levels (Chapter 4).
- Water levels and tidal reference levels (Chapter 4).
- Observed monthly and annual sea level from the permanent tide gauges (Chapter 2.3)
- Vertical land movement rates (Chapter 2.2).

These datasets can be viewed using the website Sehavnivå.no and accessed using an API (requests based on location). Read more about the datasets and the API at Geonorge.

An overview of the permanent tide gauges and their data availability can be found here. Water level data from Norway's permanent network of tide gauges can also be found at PSMSL (Permanent Service for Mean Sea Level) and the Copernicus Marine Service. In-situ data from the temporary tide gauges are available upon request from NMA (Kartverket).

8.3.3 Modelled historical extreme surge climate

The NORA3 Storm Surge Hindcast, called NORA-Surge is a barotropic ocean model integration on 4 km resolution. The Regional Ocean Model System (ROMS, see Kristensen et al., 2023; Shchepetkin and McWilliams, 2005) forced with mean sea level pressure and 10 m wind from the NORA3 hindcast archive (Breivik et al., 2022; Haakenstad et al., 2021; Haakenstad and Breivik, 2022) has been used to produce a continuous water level archive (without tides) from 1979 to the present. The NORA-Surge water level hindcast can be found on the Norwegian Meteorological Institute's thredds server here.

Fig. 8.3 shows the maximum storm surge modelled in the NORA-SS hindcast, where the model indicates a maximum of up to 4.21 m above mean sea level (excluding tides) in the German Bight.

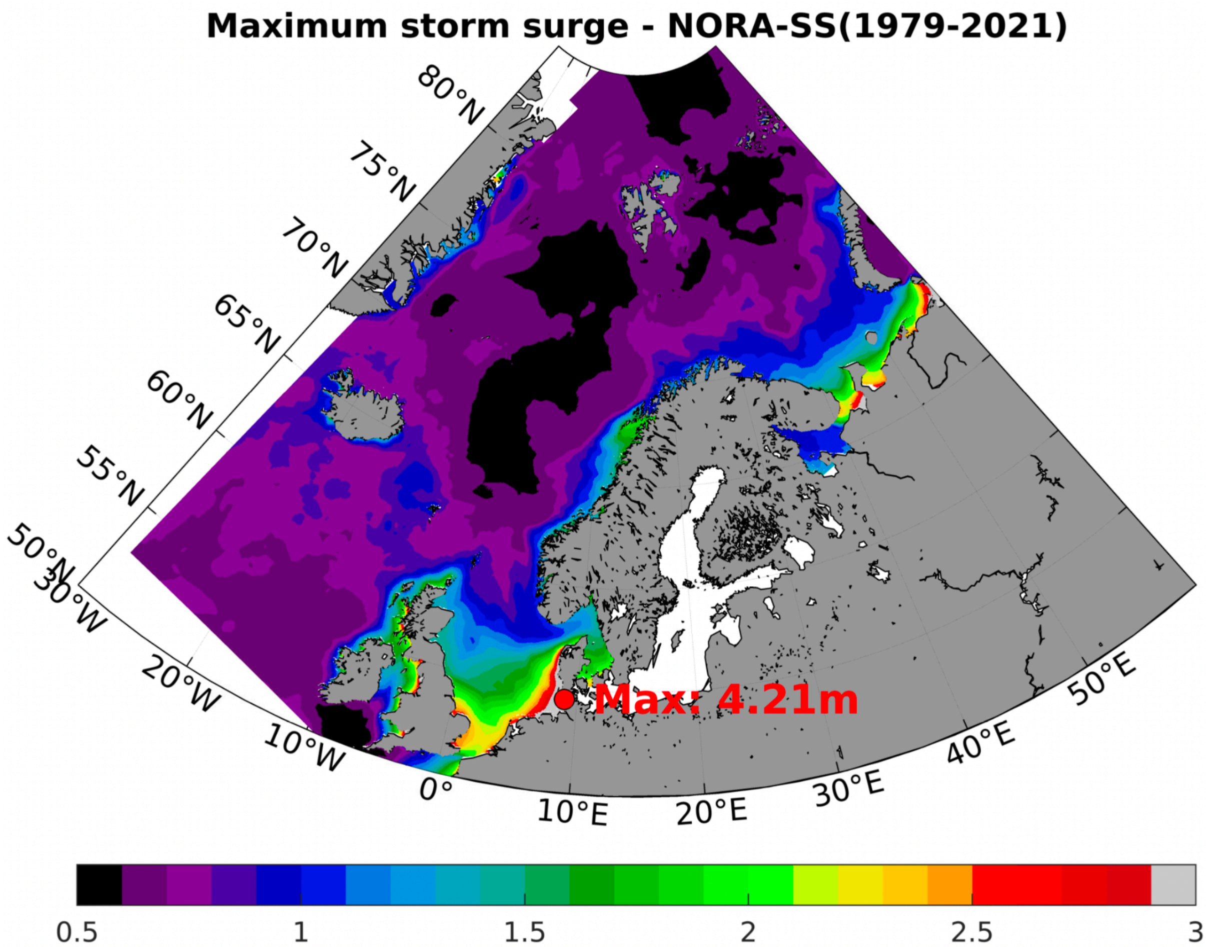

Figure 8.3: The maximum storm surge in a 42-year hindcast period modelled with a 4 km barotropic ocean model forced with NORA3 pressure and wind fields.

8.3.4 Modelled historical wave climate

NORA3WAM (Breivik et al, 2022) is a 3 km resolution wave hindcast forced with winds from the NORA3 atmospheric hindcast (Haakenstad et al., 2021). The archive covers the period from 1979 to the present. This resolution is sufficient to provide realistic estimates of the wave conditions at the mouths of the major fjords and along the coast, but is insufficient for assessing wave conditions inside fjords. For this, local downscaling is required, typically to a resolution of about 500 m or less (Christakos et al., 2020, 2021a, 2021b).

The NORA3WAM hindcast archive can be found on the Norwegian Meteorological Institute's thredds server here. Whereas, the NORA3 atmospheric hindcast archive used as wind forcing for NORA3WAM and for wind and surface pressure forcing for NORA-Surge can be found here.

9 Appendix

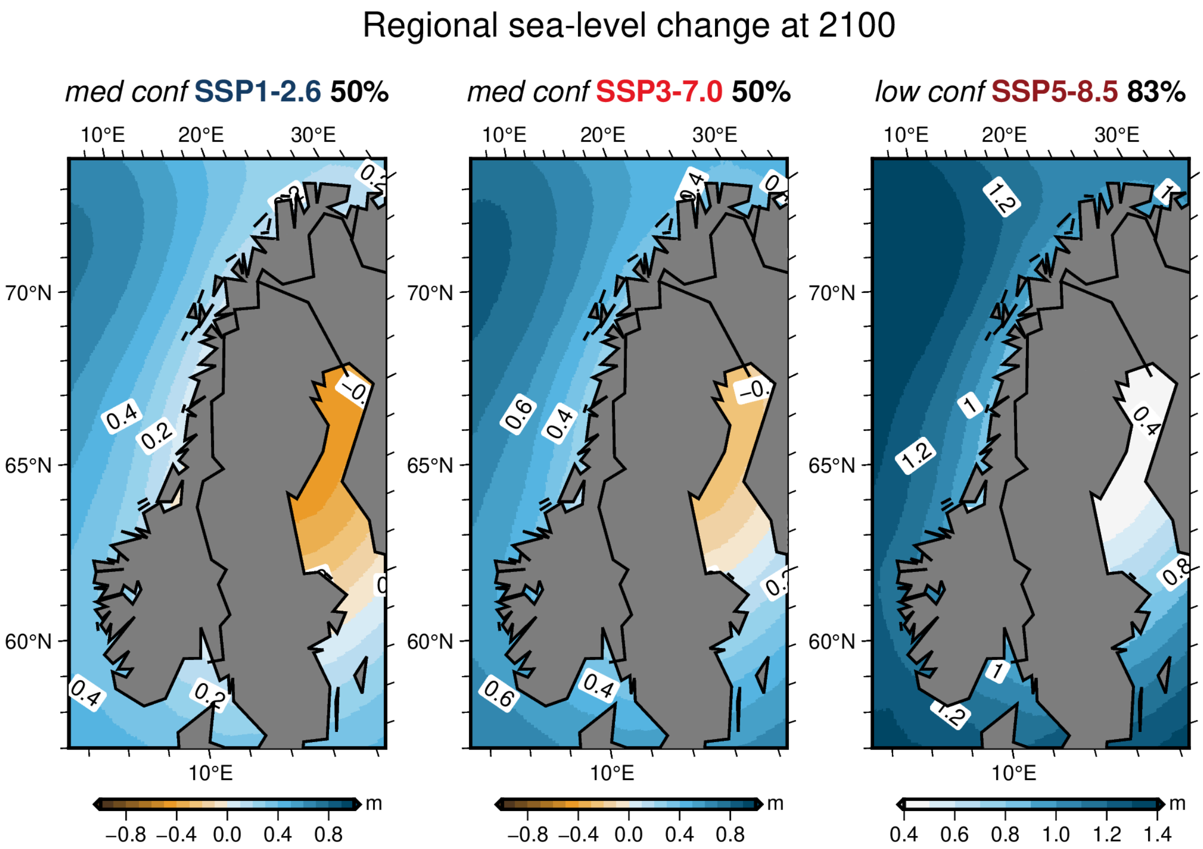

Figure 9.1: From left to right: Projected relative sea-level change at 2100 for the *medium confidence* projections under SSP1-2.6 and 50th percentile (median), *medium confidence* projections under SSP3-7.0 and 50th percentile (median), and *low confidence* projections under SSP5-8.5 and 83rd percentile. Baseline period is 1995-2014.

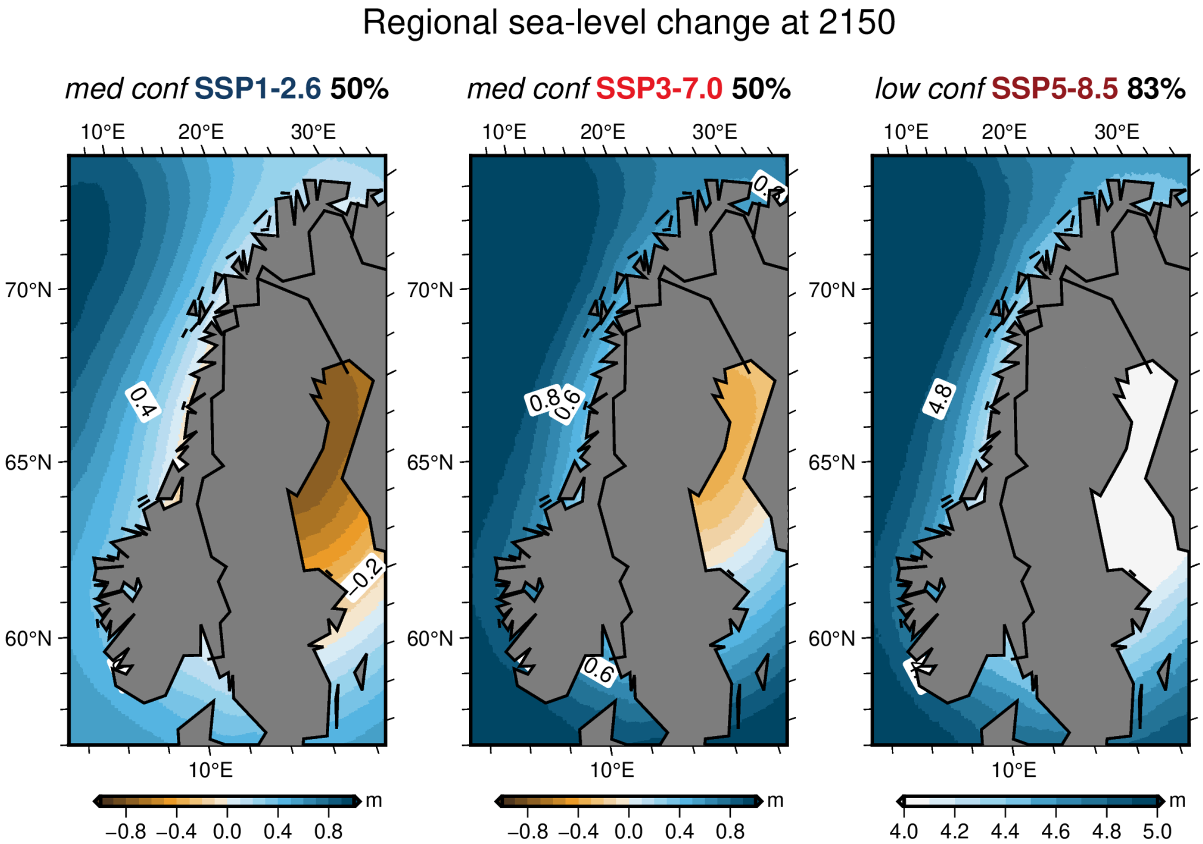

Figure 9.2: From left to right: Projected relative sea-level change at 2150 for the *medium confidence* projections under SSP1-2.6 and 50th percentile (median), *medium confidence* projections under SSP3-7.0 and 50th percentile (median), and *low confidence* projections under SSP5-8.5 and 83rd percentile. Baseline period is 1995-2014.

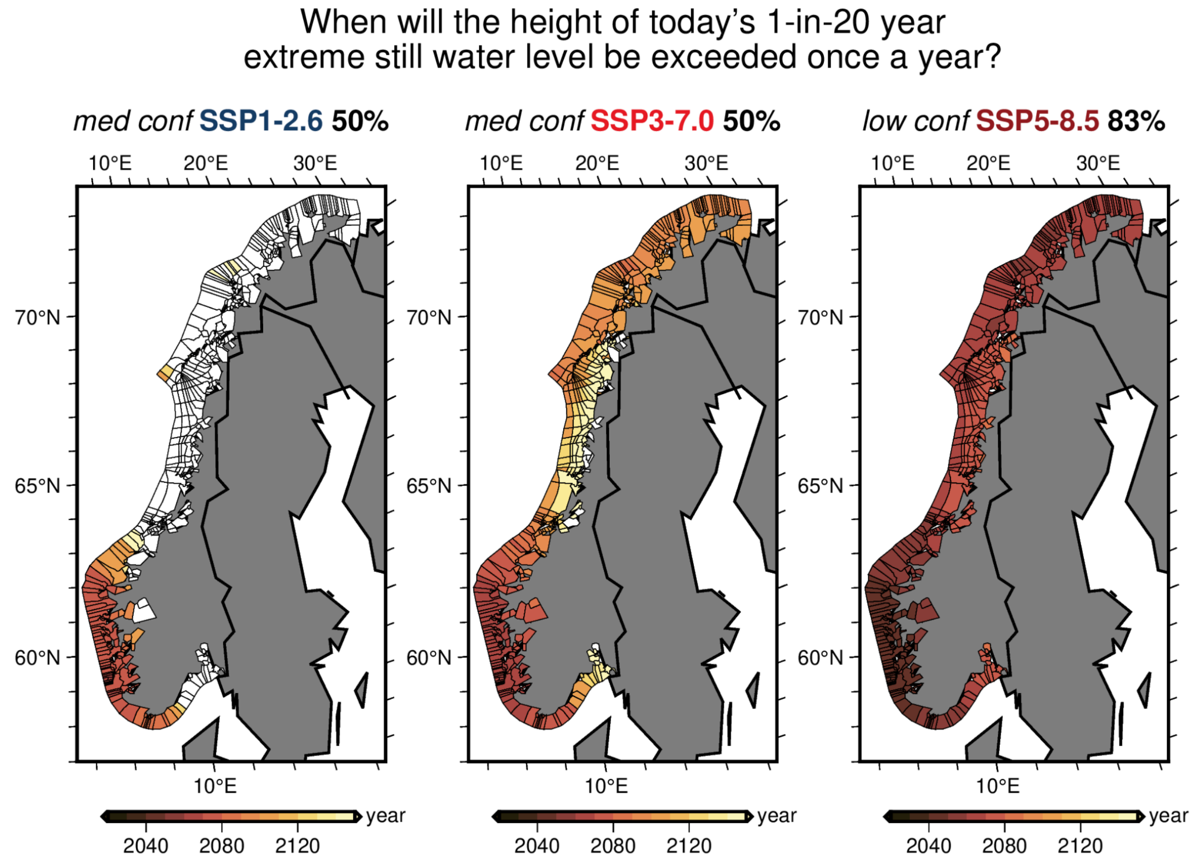

Figure 9.3: Timing of when the height of today's 1-in-20 ESWL will be on average flooded once a year for, from left to right; the *medium confidence* projections under SSP1-2.6 and 50th percentile (median), *medium confidence* projections under SSP3-7.0 and 50th percentile (median), and *low confidence* projections under SSP5-8.5 and 83rd percentile. White areas indicate areas where this frequency change does not occur by 2150.

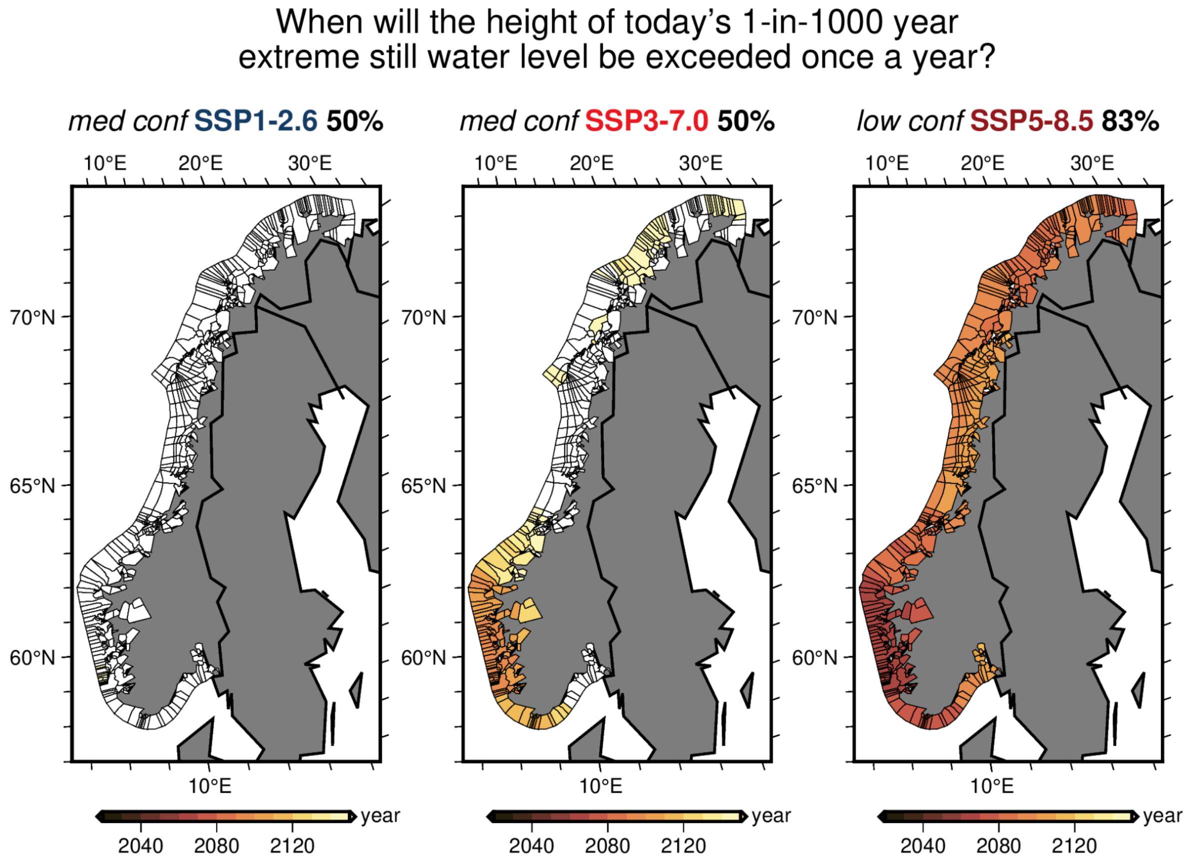

Figure 9.4: Timing of when the height of today's 1-in-1000 ESWL will be on average flooded once a year for, from left to right; the *medium confidence* projections under SSP1-2.6 and 50th percentile (median), *medium confidence* projections under SSP3-7.0 and 50th percentile (median), and *low confidence* projections under SSP5-8.5 and 83rd percentile. White areas indicate areas where this frequency change does not occur by 2150.

		Medium confidence					*Low confidence*	
	%	SSP1-1.9	SSP1-2.6	SSP2-4.5	SSP3-7.0	SSP5-8.5	SSP1-2.6	SSP5-8.5
Oslo	95	0.45	0.43	0.57	0.74	0.91	0.46	1.56
	83	0.23	0.25	0.37	0.5	0.64	0.25	0.84
	50	-0.05	0.01	0.13	0.21	0.32	0	0.39
	17	-0.3	-0.19	-0.07	-0.02	0.07	-0.23	0.06
	5	-0.48	-0.31	-0.18	-0.15	-0.07	-0.37	-0.12
Stavanger	95	0.8	0.8	0.94	1.09	1.26	0.82	1.92
	83	0.57	0.6	0.73	0.85	0.99	0.6	1.19
	50	0.28	0.33	0.45	0.55	0.65	0.33	0.75
	17	0.02	0.1	0.23	0.3	0.38	0.06	0.38
	5	-0.17	-0.04	0.1	0.16	0.24	-0.1	0.18
Bergen	95	0.75	0.76	0.89	1.05	1.21	0.78	1.85
	83	0.53	0.56	0.68	0.81	0.94	0.56	1.14
	50	0.25	0.3	0.42	0.51	0.61	0.29	0.68
	17	-0.02	0.08	0.21	0.26	0.35	0.03	0.33
	5	-0.2	-0.05	0.09	0.12	0.21	-0.12	0.13
Heimsjø	95	0.57	0.57	0.7	0.84	1	0.58	1.6
	83	0.35	0.37	0.49	0.6	0.73	0.37	0.93
	50	0.07	0.12	0.23	0.3	0.41	0.1	0.51
	17	-0.17	-0.11	0.01	0.06	0.15	-0.16	0.12
	5	-0.34	-0.23	-0.11	-0.08	0.01	-0.32	-0.1
Tromsø	95	0.63	0.62	0.75	0.89	1.04	0.63	1.59
	83	0.42	0.43	0.54	0.65	0.77	0.43	0.96
	50	0.14	0.16	0.27	0.34	0.44	0.13	0.53
	17	-0.12	-0.07	0.04	0.09	0.18	-0.16	0.1
	5	-0.29	-0.21	-0.09	-0.06	0.04	-0.33	-0.13
Honningsvåg	95	0.64	0.66	0.81	0.92	1.08	0.67	1.65
	83	0.45	0.47	0.59	0.69	0.81	0.47	1.01
	50	0.19	0.2	0.32	0.39	0.49	0.18	0.56
	17	-0.04	-0.03	0.09	0.15	0.24	-0.11	0.18
	5	-0.19	-0.17	-0.04	0.01	0.11	-0.28	-0.04

Table 9.1: Projected RSL change (m) at 2100 for the different SSP scenarios at six key tide gauge locations. Baseline period is 1995-2014.

	%	SSP1-1.9 (Medium confidence)	SSP1-2.6 (Medium confidence)	SSP2-4.5 (Medium confidence)	SSP3-7.0 (Medium confidence)	SSP5-8.5 (Medium confidence)	SSP1-2.6 (Low confidence)	SSP5-8.5 (Low confidence)
Oslo	95	5.0	5.0	9.0	13.0	17.0	7.0	43.0
	83	2.0	2.0	6.0	9.0	12.0	2.0	33.0
	50	-1.0	0.0	2.0	3.0	6.0	0.0	11.0
	17	-5.0	-2.0	0.0	0.0	1.0	-3.0	1.0
	5	-7.0	-3.0	-1.0	-2.0	0.0	-5.0	-1.0
Stavanger	95	8.0	8.0	12.0	16.0	20.0	10.0	47.0
	83	5.0	6.0	9.0	12.0	16.0	6.0	36.0
	50	1.0	2.0	5.0	7.0	9.0	2.0	14.0
	17	-1.0	0.0	2.0	3.0	4.0	-1.0	4.0
	5	-3.0	-1.0	1.0	1.0	2.0	-3.0	2.0
Bergen	95	8.0	8.0	12.0	16.0	20.0	10.0	46.0
	83	5.0	5.0	8.0	12.0	15.0	5.0	36.0
	50	1.0	2.0	4.0	6.0	9.0	2.0	13.0
	17	-1.0	0.0	2.0	2.0	4.0	-1.0	4.0
	5	-3.0	-1.0	1.0	0.0	2.0	-4.0	1.0
Heimsjø	95	7.0	6.0	10.0	14.0	18.0	8.0	43.0
	83	4.0	4.0	7.0	10.0	13.0	4.0	34.0
	50	0.0	0.0	3.0	5.0	6.0	0.0	11.0
	17	-2.0	-2.0	0.0	0.0	2.0	-3.0	2.0
	5	-4.0	-3.0	0.0	-1.0	0.0	-6.0	0.0
Tromsø	95	7.0	7.0	10.0	15.0	17.0	8.0	43.0
	83	5.0	4.0	7.0	10.0	12.0	4.0	34.0
	50	1.0	0.0	3.0	5.0	6.0	0.0	11.0
	17	-1.0	-2.0	0.0	0.0	3.0	-3.0	2.0
	5	-3.0	-3.0	0.0	-1.0	1.0	-6.0	-1.0
Honningsvåg	95	8.0	7.0	11.0	15.0	17.0	9.0	44.0
	83	6.0	5.0	8.0	11.0	13.0	5.0	34.0
	50	2.0	1.0	4.0	5.0	7.0	1.0	12.0
	17	0.0	-1.0	1.0	1.0	3.0	-2.0	3.0
	5	-2.0	-3.0	0.0	-1.0	2.0	-5.0	0.0

Table 9.2: Projected RSL rates (mm/yr) at 2100 for the different SSP scenarios at six key tide gauge locations. Baseline period is 1995-2014.

10 References

Aarnes, O.J., Breivik, Ø., Reistad, M., 2012. Wave Extremes in the Northeast Atlantic. Journal of Climate 25, 1529–1543. https://doi.org/10.1175/JCLI-D-11-00132.1

Aarnes, O.J., Reistad, M., Bohlinger, P., 2020. Samtidighet av høy vannstand og høye bølger for Stavanger kommune, MET internal report., n.d.

Aarnes, O.J., Reistad, M., Breivik, Ø., Bitner-Gregersen, E., Ingolf Eide, L., Gramstad, O., Magnusson, A.K., Natvig, B., Vanem, E., 2017. Projected changes in significant wave height toward the end of the 21st century: Northeast Atlantic. Journal of Geophysical Research: Oceans 122, 3394–3403. https://doi.org/10.1002/2016JC012521

Abulaitijiang, A., Andersen, O.B., Stenseng, L., 2015. Coastal sea level from inland CryoSat-2 interferometric SAR altimetry. Geophysical Research Letters 42, 1841–1847. https://doi.org/10.1002/2015GL063131

Altamimi, Z., Collilieux, X., Métivier, L., 2011. ITRF2008: an improved solution of the international terrestrial reference frame. J Geod 85, 457–473. https://doi.org/10.1007/s00190-011-0444-4

Armstrong McKay, D.I., Staal, A., Abrams, J.F., Winkelmann, R., Sakschewski, B., Loriani, S., Fetzer, I., Cornell, S.E., Rockström, J., Lenton, T.M., 2022. Exceeding 1.5°C global warming could trigger multiple climate tipping points. Science 377, eabn7950. https://doi.org/10.1126/science.abn7950

Arns, A., Dangendorf, S., Jensen, J., Talke, S., Bender, J., Pattiaratchi, C., 2017. Sea-level rise induced amplification of coastal protection design heights. Sci Rep 7, 40171. https://doi.org/10.1038/srep40171

Arns, A., Wahl, T., Haigh, I.D., Jensen, J., 2015. Determining return water levels at ungauged coastal sites: a case study for northern Germany. Ocean Dynamics 65, 539–554. https://doi.org/10.1007/s10236-015-0814-1

Arns, A., Wahl, T., Haigh, I.D., Jensen, J., Pattiaratchi, C., 2013. Estimating extreme water level probabilities: A comparison of the direct methods and recommendations for best practise. Coastal Engineering 81, 51–66. https://doi.org/10.1016/j.coastaleng.2013.07.003

Aunan, K., Romstad, B., 2008. Strong Coasts and Vulnerable Communities: Potential Implications of Accelerated Sea-Level Rise for Norway. coas 2008, 403–409. https://doi.org/10.2112/07A-0013.1

Bamber, J.L., Oppenheimer, M., Kopp, R.E., Aspinall, W.P., Cooke, R.M., 2019. Ice sheet contributions to future sea-level rise from structured expert judgment. Proceedings of the National Academy of Sciences 116, 11195–11200. https://doi.org/10.1073/pnas.1817205116

Belcher, S.E., Grant, A.L.M., Hanley, K.E., Fox-Kemper, B., Van Roekel, L., Sullivan, P.P., Large, W.G., Brown, A., Hines, A., Calvert, D., Rutgersson, A., Pettersson, H., Bidlot, J.-R., Janssen, P.A.E.M., Polton, J.A., 2012. A global perspective on Langmuir turbulence in the ocean surface boundary layer. Geophysical Research Letters 39. https://doi.org/10.1029/2012GL052932

Benveniste, J., Mandea, M., Melet, A., Ferrier, P., 2020. Earth Observations for Coastal Hazards Monitoring and International Services: A European Perspective. Surv Geophys 41, 1185–1208. https://doi.org/10.1007/s10712-020-09612-6

Bevacqua, E., Maraun, D., Vousdoukas, M.I., Voukouvalas, E., Vrac, M., Mentaschi, L., Widmann, M., 2019. Higher probability of compound flooding from precipitation and storm surge in Europe under anthropogenic climate change. Science Advances 5, eaaw5531. https://doi.org/10.1126/sciadv.aaw5531

Bohlinger, P., Economou, T., Aarnes, O.J., Malila, M., Breivik, Ø., 2023. A general framework to obtain seamless seasonal–directional extreme individual wave heights—Showcase Ekofisk. Ocean Engineering 270, 113535. https://doi.org/10.1016/j.oceaneng.2022.113535

Bonaduce, A., Staneva, J., Behrens, A., Bidlot, J.-R., Wilcke, R.A.I., 2019. Wave Climate Change in the North Sea and Baltic Sea. Journal of Marine Science and Engineering 7, 166. https://doi.org/10.3390/jmse7060166

Bonaduce, A., Staneva, J., Grayek, S., Bidlot, J.-R., Breivik, Ø., 2020. Sea-state contributions to sea-level variability in the European Seas. Ocean Dynamics 70, 1547–1569. https://doi.org/10.1007/s10236-020-01404-1

Borck, H.S., Ravndal, O.R., 2024. Extreme water levels for Norway: Updated extreme value analysis based on data series up to 2022. Kartverkets rapportserie, 19/04811-19. ISBN: 978-82-7945-477-9, n.d.

Bousquet, N. and Bernardara, P., 2021. Extreme Value Theory with Applications to Natural Hazards. Springer International Publishing., n.d.

Breili, K., 2022. Evolution of sea-level trends along the Norwegian coast from 1960 to 2100. Ocean Dynamics 72, 115–136. https://doi.org/10.1007/s10236-021-01492-7

Breili, K., Simpson, M.J.R., Klokkervold, E., Roaldsdotter Ravndal, O., 2020. High-accuracy coastal flood mapping for Norway using lidar data. Natural Hazards and Earth System Sciences 20, 673–694. https://doi.org/10.5194/nhess-20-673-2020

Breivik, Ø., Aarnes, O.J., Abdalla, S., Bidlot, J.-R., Janssen, P.A.E.M., 2014. Wind and wave extremes over the world oceans from very large ensembles. Geophysical Research Letters 41, 5122–5131. https://doi.org/10.1002/2014GL060997

Breivik, Ø., Aarnes, O.J., Bidlot, J.-R., Carrasco, A., Saetra, Ø., 2013. Wave Extremes in the Northeast Atlantic from Ensemble Forecasts. Journal of Climate 26, 7525–7540. https://doi.org/10.1175/JCLI-D-12-00738.1

Breivik, Ø., Carrasco, A., Haakenstad, H., Aarnes, O.J., Behrens, A., Bidlot, J.-R., Björkqvist, J.-V., Bohlinger, P., Furevik, B.R., Staneva, J., Reistad, M., 2022. The Impact of a Reduced High-Wind Charnock Parameter on Wave Growth With Application to the North Sea, the Norwegian Sea, and the Arctic Ocean. Journal of Geophysical Research: Oceans 127, e2021JC018196. https://doi.org/10.1029/2021JC018196

Breivik, Ø., Carrasco, A., Staneva, J., Behrens, A., Semedo, A., Bidlot, J.-R., Aarnes, O.J., 2019. Global Stokes Drift Climate under the RCP8.5 Scenario. Journal of Climate 32, 1677–1691. https://doi.org/10.1175/JCLI-D-18-0435.1

Bricheno, L.M., Wolf, J., 2018. Future Wave Conditions of Europe, in Response to High-End Climate Change Scenarios. Journal of Geophysical Research: Oceans 123, 8762–8791. https://doi.org/10.1029/2018JC013866

Calafat, F.M., Wahl, T., Tadesse, M.G., Sparrow, S.N., 2022. Trends in Europe storm surge extremes match the rate of sea-level rise. Nature 603, 841–845. https://doi.org/10.1038/s41586-022-04426-5

Cazenave, A., Nerem, R.S., 2004. Present-day sea level change: Observations and causes. Reviews of Geophysics 42. https://doi.org/10.1029/2003RG000139

Chafik, L., Nilsen, J.E.Ø., Dangendorf, S., 2017. Impact of North Atlantic Teleconnection Patterns on Northern European Sea Level. Journal of Marine Science and Engineering 5, 43. https://doi.org/10.3390/jmse5030043

Chafik, L., Nilsen, J.E.Ø., Dangendorf, S., Reverdin, G., Frederikse, T., 2019. North Atlantic Ocean Circulation and Decadal Sea Level Change During the Altimetry Era. Sci Rep 9, 1041. https://doi.org/10.1038/s41598-018-37603-6

Chen, D., M. Rojas, B.H. Samset, K. Cobb, A. Diongue Niang, P. Edwards, S. Emori, S.H. Faria, E. Hawkins, P. Hope, P. Huybrechts, M. Meinshausen, S.K. Mustafa, G.-K. Plattner, and A.-M. Tréguier, 2021: Framing, Context, and Methods. In Climate Change 2021: The Physical Science Basis. Contribution of Working Group I to the Sixth Assessment Report of the Intergovernmental Panel on Climate Change [Masson-Delmotte, V., P. Zhai, A. Pirani, S.L. Connors, C. Péan, S. Berger, N. Caud, Y. Chen, L. Goldfarb, M.I. Gomis, M. Huang, K. Leitzell, E. Lonnoy, J.B.R. Matthews, T.K. Maycock, T. Waterfield, O. Yelekçi, R. Yu, and B. Zhou (eds.)]. Cambridge University Press, Cambridge, United Kingdom and New York, NY, USA, pp. 147–286, doi:10.1017/9781009157896.003.

Christakos, K., Björkqvist, J.-V., Breivik, Ø., Tuomi, L., Furevik, B.R., Albretsen, J., 2021a. The impact of surface currents on the wave climate in narrow fjords.

Ocean Modelling 168, 101894. https://doi.org/10.1016/j.ocemod.2021.101894

Christakos, K., Björkqvist, J.-V., Tuomi, L., Furevik, B.R., Breivik, Ø., 2021b. Modelling wave growth in narrow fetch geometries: The white-capping and wind input formulations. Ocean Modelling 157, 101730. https://doi.org/10.1016/j.ocemod.2020.101730

Christakos, K., Furevik, B.R., Aarnes, O.J., Breivik, Ø., Tuomi, L., Byrkjedal, Ø., 2020. The importance of wind forcing in fjord wave modelling. Ocean Dynamics 70, 57–75. https://doi.org/10.1007/s10236-019-01323-w

Church, J.A., P.U. Clark, A. Cazenave, J.M. Gregory, S. Jevrejeva, A. Levermann, M.A. Merrifield, G.A. Milne, R.S. Nerem, P.D. Nunn, A.J. Payne, W.T. Pfeffer, D. Stammer and A.S. Unnikrishnan, 2013: Sea Level Change. In: Climate Change 2013: The Physical Science Basis. Contribution of Working Group I to the Fifth Assessment Report of the Intergovernmental Panel on Climate Change [Stocker, T.F., D. Qin, G.-K. Plattner, M. Tignor, S.K. Allen, J. Boschung, A. Nauels, Y. Xia, V. Bex and P.M. Midgley (eds.)]. Cambridge University Press, Cambridge, United Kingdom and New York, NY, USA, n.d.

Collilieux, X., Altamimi, Z., Argus, D.F., Boucher, C., Dermanis, A., Haines, B.J., Herring, T.A., Kreemer, C.W., Lemoine, F.G., Ma, C. and MacMillan, D.S., 2014. External evaluation of the terrestrial reference frame: report of the task force of the IAG sub-commission 1.2. In Earth on the Edge: Science for a Sustainable Planet: Proceedings of the IAG General Assembly, Melbourne, Australia, June 28-July 2, 2011 (pp. 197-202). Springer Berlin Heidelberg., n.d.

Coulson, S., Lubeck, M., Mitrovica, J.X., Powell, E., Davis, J.L., Hoggard, M.J., 2021. The Global Fingerprint of Modern Ice-Mass Loss on 3-D Crustal Motion. Geophysical Research Letters 48, e2021GL095477. https://doi.org/10.1029/2021GL095477

DeConto, R.M., Pollard, D., Alley, R.B., Velicogna, I., Gasson, E., Gomez, N., Sadai, S., Condron, A., Gilford, D.M., Ashe, E.L., Kopp, R.E., Li, D., Dutton, A., 2021. The Paris Climate Agreement and future sea-level rise from Antarctica. Nature 593, 83–89. https://doi.org/10.1038/s41586-021-03427-0

DSB, 2017. Integrating Sea Level Rise and Storm Surges in Local Planning. ISBN 978-82-7768-447-5., n.d.

Ekman, V. W., 1905. On the influence of the earth's rotation on ocean currents, Ark. Mat. Astron. Fys., 2, 1–53., n.d.

Erikson, L., Morim, J., Hemer, M., Young, I., Wang, X.L., Mentaschi, L., Mori, N., Semedo, A., Stopa, J., Grigorieva, V., Gulev, S., Aarnes, O., Bidlot, J.-R., Breivik, Ø., Bricheno, L., Shimura, T., Menendez, M., Markina, M., Sharmar, V., Trenham, C., Wolf, J., Appendini, C., Caires, S., Groll, N., Webb, A., 2022. Global ocean wave fields show consistent regional trends between 1980 and 2014 in a multi-product ensemble. Commun Earth Environ 3, 1–16. https://doi.org/10.1038/s43247-022-00654-9

Fan, Y., Griffies, S.M., 2014. Impacts of Parameterized Langmuir Turbulence and Nonbreaking Wave Mixing in Global Climate Simulations. Journal of Climate 27, 4752–4775. https://doi.org/10.1175/JCLI-D-13-00583.1

Fox-Kemper, B., H.T. Hewitt, C. Xiao, G. Aðalgeirsdóttir, S.S. Drijfhout, T.L. Edwards, N.R. Golledge, M. Hemer, R.E. Kopp, G. Krinner, A. Mix, D. Notz, S. Nowicki, I.S. Nurhati, L. Ruiz, J.-B. Sallée, A.B.A. Slangen, and Y. Yu, 2021: Ocean, Cryosphere and Sea Level Change. In Climate Change 2021: The Physical Science Basis. Contribution of Working Group I to the Sixth Assessment Report of the Intergovernmental Panel on Climate Change [Masson-Delmotte, V., P. Zhai, A. Pirani, S.L. Connors, C. Péan, S. Berger, N. Caud, Y. Chen, L. Goldfarb, M.I. Gomis, M. Huang, K. Leitzell, E. Lonnoy, J.B.R. Matthews, T.K. Maycock, T. Waterfield, O. Yelekçi, R. Yu, and B. Zhou (eds.)]. Cambridge University Press, Cambridge, United Kingdom and New York, NY, USA, pp. 1211–1362, doi:10.1017/9781009157896.011.

Frederikse, T., Riva, R., Kleinherenbrink, M., Wada, Y., van den Broeke, M., Marzeion, B., 2016. Closing the sea level budget on a regional scale: Trends and variability on the Northwestern European continental shelf. Geophysical Research Letters 43, 10,864-10,872. https://doi.org/10.1002/2016GL070750

Gjevik, B., 2009. Flo og fjære langs kysten av Norge og Svalbard. Farleia., n.d.

Gjevik, B., Røed, L.P., 1976. Storm surges along the Western coast of Norway. Tellus 28, 166–182. https://doi.org/10.1111/j.2153-3490.1976.tb00664.x

Global Ocean Along Track L 3 Sea Surface Heights Reprocessed 1993 Ongoing Tailored For Data Assimilation. E.U. Copernicus Marine Service Information (CMEMS). Marine Data Store (MDS). DOI: 10.48670/moi-00146

Gomez-Enri, J., Vignudelli, S., Quartly, G.D., Gommenginger, C.P., Cipollini, P., Challenor, P.G., Benveniste, J., 2010. Modeling Envisat RA-2 Waveforms in the Coastal Zone: Case Study of Calm Water Contamination. IEEE Geoscience and Remote Sensing Letters 7, 474–478. https://doi.org/10.1109/LGRS.2009.2039193

Gregory, J.M., Griffies, S.M., Hughes, C.W., Lowe, J.A., Church, J.A., Fukimori, I., Gomez, N., Kopp, R.E., Landerer, F., Cozannet, G.L., Ponte, R.M., Stammer, D., Tamisiea, M.E., van de Wal, R.S.W., 2019. Concepts and Terminology for Sea Level: Mean, Variability and Change, Both Local and Global. Surv Geophys 40, 1251–1289. https://doi.org/10.1007/s10712-019-09525-z

Haakenstad, H., Breivik, Ø., 2022. NORA3. Part II: Precipitation and Temperature Statistics in Complex Terrain Modeled with a Nonhydrostatic Model. Journal of Applied Meteorology and Climatology 61, 1549–1572. https://doi.org/10.1175/JAMC-D-22-0005.1

Haakenstad, H., Breivik, Ø., Furevik, B.R., Reistad, M., Bohlinger, P., Aarnes, O.J., 2021. NORA3: A Nonhydrostatic High-Resolution Hindcast of the North Sea, the Norwegian Sea, and the Barents Sea. Journal of Applied Meteorology and Climatology 60, 1443–1464. https://doi.org/10.1175/JAMC-D-21-0029.1

Haasnoot, M., Kwadijk, J., Alphen, J. van, Bars, D.L., Hurk, B. van den, Diermanse, F., Spek, A. van der, Essink, G.O., Delsman, J., Mens, M., 2020. Adaptation to uncertain sea-level rise; how uncertainty in Antarctic mass-loss impacts the coastal adaptation strategy of the Netherlands. Environ. Res. Lett. 15, 034007. https://doi.org/10.1088/1748-9326/ab666c

Haasnoot, M., Kwakkel, J.H., Walker, W.E., ter Maat, J., 2013. Dynamic adaptive policy pathways: A method for crafting robust decisions for a deeply uncertain world. Global Environmental Change 23, 485–498. https://doi.org/10.1016/j.gloenvcha.2012.12.006

Hemer, M.A., Fan, Y., Mori, N., Semedo, A., Wang, X.L., 2013. Projected changes in wave climate from a multi-model ensemble. Nature Clim Change 3, 471–476. https://doi.org/10.1038/nclimate1791

Hermans, T.H.J., Malagón-Santos, V., Katsman, C.A., Jane, R.A., Rasmussen, D.J., Haasnoot, M., Garner, G.G., Kopp, R.E., Oppenheimer, M., Slangen, A.B.A., 2023. The timing of decreasing coastal flood protection due to sea-level rise. Nat. Clim. Chang. 13, 359–366. https://doi.org/10.1038/s41558-023-01616-5

Hermans, T.H.J., Tinker, J., Palmer, M.D., Katsman, C.A., Vermeersen, B.L.A., Slangen, A.B.A., 2020. Improving sea-level projections on the Northwestern European shelf using dynamical downscaling. Clim Dyn 54, 1987–2011. https://doi.org/10.1007/s00382-019-05104-5

Hewson, T.D., Magnusson, L., Breivik, O., Prates, F., Tsonevsky, I., de Vries, J.W., 2014. Windstorms in northwest Europe in late 2013. ECMWF Newsletter, Volume: 139, 22-28., n.d.

Hinkel, J., Church, J.A., Gregory, J.M., Lambert, E., Le Cozannet, G., Lowe, J., McInnes, K.L., Nicholls, R.J., van der Pol, T.D., van de Wal, R., 2019. Meeting User Needs for Sea Level Rise Information: A Decision Analysis Perspective. Earth's Future 7, 320–337. https://doi.org/10.1029/2018EF001071

Holgate, S.J., Matthews, A., Woodworth, P.L., Rickards, L.J., Tamisiea, M.E., Bradshaw, E., Foden, P.R., Gordon, K.M., Jevrejeva, S., Pugh, J., 2013. New Data Systems and Products at the Permanent Service for Mean Sea Level. coas 29, 493–504. https://doi.org/10.2112/JCOASTRES-D-12-00175.1

Höning, D., Willeit, M., Calov, R., Klemann, V., Bagge, M., Ganopolski, A., 2023. Multistability and Transient Response of the Greenland Ice Sheet to Anthropogenic CO2 Emissions. Geophysical Research Letters 50, e2022GL101827. https://doi.org/10.1029/2022GL101827

Horsburgh, K.J., Wilson, C., 2007. Tide-surge interaction and its role in the distribution of surge residuals in the North Sea. Journal of Geophysical Research: Oceans 112. https://doi.org/10.1029/2006JC004033

IPCC, 2021: Climate Change 2021: The Physical Science Basis. Contribution of Working Group I to the Sixth Assessment Report of the Intergovernmental Panel on Climate Change [Masson-Delmotte, V., P. Zhai, A. Pirani, S.L. Connors, C. Péan, S. Berger, N. Caud, Y. Chen, L. Goldfarb, M.I. Gomis, M. Huang, K. Leitzell, E. Lonnoy, J.B.R. Matthews, T.K. Maycock, T. Waterfield, O. Yelekçi, R. Yu, and B. Zhou (eds.)]. Cambridge University Press, Cambridge, United Kingdom and New York, NY, USA, 2391 pp. doi:10.1017/9781009157896.

Kartverket, 2021. Utredning av Norges framtidige høydereferanseramme. Utarbeidet av Olav Vestøl (redaktør), Kristian Breili, Eirik Mysen, Ove Omang og Karoline Arnfinnsdatter Skår. Kartverkets rapportserie, 10-04811-8., n.d.

Kierulf, H.P., 2017. Analysis strategies for combining continuous and episodic GNSS for studies of neo-tectonics in Northern-Norway. Journal of Geodynamics 109, 32–40. https://doi.org/10.1016/j.jog.2017.07.002

Kierulf, H.P., Steffen, H., Barletta, V.R., Lidberg, M., Johansson, J., Kristiansen, O., Tarasov, L., 2021. A GNSS velocity field for geophysical applications in Fennoscandia. Journal of Geodynamics 146, 101845. https://doi.org/10.1016/j.jog.2021.101845

Kopp, R. E. (2021). IPCC AR6 Relative Sea Level Projections without Background Component (Version 20210809) [Data set]. Zenodo. https://doi.org/10.5281/zenodo.5967269, n.d.

Kopp, R.E., Garner, G.G., Hermans, T.H.J., Jha, S., Kumar, P., Slangen, A.B.A., Turilli, M., Edwards, T.L., Gregory, J.M., Koubbe, G., Levermann, A., Merzky, A., Nowicki, S., Palmer, M.D., Smith, C., 2023. The Framework for Assessing Changes To Sea-level (FACTS) v1.0-rc: A platform for characterizing parametric and structural uncertainty in future global, relative, and extreme sea-level change. EGUsphere 1–34. https://doi.org/10.5194/egusphere-2023-14

Kopp, R.E., Gilmore, E.A., Little, C.M., Lorenzo-Trueba, J., Ramenzoni, V.C., Sweet, W.V., 2019. Usable Science for Managing the Risks of Sea-Level Rise. Earth's Future 7, 1235–1269. https://doi.org/10.1029/2018EF001145

Kopp, R.E., Horton, R.M., Little, C.M., Mitrovica, J.X., Oppenheimer, M., Rasmussen, D.J., Strauss, B.H., Tebaldi, C., 2014. Probabilistic 21st and 22nd century sea-level projections at a global network of tide-gauge sites. Earth's Future 2, 383–406. https://doi.org/10.1002/2014EF000239

Kristensen, N.M., Røed, L.P., Sætra, Ø., 2023. A forecasting and warning system of storm surge events along the Norwegian coast. Environ Fluid Mech 23, 307–329. https://doi.org/10.1007/s10652-022-09871-4

Lawrence, J., Bell, R., Blackett, P., Stephens, S., Allan, S., 2018. National guidance for adapting to coastal hazards and sea-level rise: Anticipating change, when and how to change pathway. Environmental Science & Policy 82, 100–107. https://doi.org/10.1016/j.envsci.2018.01.012

Ludwigsen, C.B., Andersen, O.B., Rose, S.K., 2022. Components of 21 years (1995–2015) of absolute sea level trends in the Arctic. Ocean Science 18, 109–127. https://doi.org/10.5194/os-18-109-2022

Lysaker, D.I. and Vestøl, O., 2020. The Norwegian vertical reference frame NN2000. Technical report of the Norwegian Mapping Authority 19-04811-4, ISBN 978-82-7945-247-8, n.d.

Mangini, F., Chafik, L., Bonaduce, A., Bertino, L., Nilsen, J.E.Ø., 2022. Sea-level variability and change along the Norwegian coast between 2003 and 2018 from satellite altimetry, tide gauges, and hydrography. Ocean Science 18, 331–359. https://doi.org/10.5194/os-18-331-2022

Mangini, F., Chafik, L., Madonna, E., Li, C., Bertino, L., Nilsen, J.E.Ø., 2021. The relationship between the eddy-driven jet stream and northern European sea level variability. Tellus A: Dynamic Meteorology and Oceanography 73, 1–15. https://doi.org/10.1080/16000870.2021.1886419

Marcos, M., Woodworth, P.L., 2017. Spatiotemporal changes in extreme sea levels along the coasts of the North Atlantic and the Gulf of Mexico. Journal of Geophysical Research: Oceans 122, 7031–7048. https://doi.org/10.1002/2017JC013065

Menéndez, M., Woodworth, P.L., 2010. Changes in extreme high water levels based on a quasi-global tide-gauge data set. Journal of Geophysical Research: Oceans 115. https://doi.org/10.1029/2009JC005997

Meucci, A., Young, I.R., Breivik, Ø., 2018. Wind and Wave Extremes from Atmosphere and Wave Model Ensembles. Journal of Climate 31, 8819–8842. https://doi.org/10.1175/JCLI-D-18-0217.1

Meucci, A., Young, I.R., Hemer, M., Trenham, C., Watterson, I.G., 2023. 140 Years of Global Ocean Wind-Wave Climate Derived from CMIP6 ACCESS-CM2 and EC-Earth3 GCMs: Global Trends, Regional Changes, and Future Projections. Journal of Climate 36, 1605–1631. https://doi.org/10.1175/JCLI-D-21-0929.1

Mitrovica, J.X., Gomez, N., Clark, P.U., 2009. The Sea-Level Fingerprint of West Antarctic Collapse. Science 323, 753–753. https://doi.org/10.1126/science.1166510

Morim, J., Hemer, M., Wang, X.L., Cartwright, N., Trenham, C., Semedo, A., Young, I., Bricheno, L., Camus, P., Casas-Prat, M., Erikson, L., Mentaschi, L., Mori, N., Shimura, T., Timmermans, B., Aarnes, O., Breivik, Ø., Behrens, A., Dobrynin, M., Menendez, M., Staneva, J., Wehner, M., Wolf, J., Kamranzad, B., Webb, A., Stopa, J., Andutta, F., 2019. Robustness and uncertainties in global multivariate wind-wave climate projections. Nat. Clim. Chang. 9, 711–718. https://doi.org/10.1038/s41558-019-0542-5

Muis, S., Apecechea, M.I., Dullaart, J., de Lima Rego, J., Madsen, K.S., Su, J., Yan, K., Verlaan, M., 2020. A High-Resolution Global Dataset of Extreme Sea Levels, Tides, and Storm Surges, Including Future Projections. Front. Mar. Sci. 7, 512955. https://doi.org/10.3389/fmars.2020.00263

Nerem, R.S., Beckley, B.D., Fasullo, J.T., Hamlington, B.D., Masters, D., Mitchum, G.T., 2018. Climate-change–driven accelerated sea-level rise detected in the altimeter era. Proceedings of the National Academy of Sciences 115, 2022–2025. https://doi.org/10.1073/pnas.1717312115

Olesen, O., Pascal Kierulf, H., Brönner, M., Dalsegg, E., Fredin, O. and Solbakk, T., 2013. Deep weathering, neotectonics and strandflat formation in Nordland, northern Norway. Norwegian Journal of Geology/Norsk Geologisk Forening, 93., n.d.

Oppenheimer, M., B.C. Glavovic , J. Hinkel, R. van de Wal, A.K. Magnan, A. Abd-Elgawad, R. Cai, M. Cifuentes-Jara, R.M. DeConto, T. Ghosh, J. Hay, F. Isla, B. Marzeion, B. Meyssignac, and Z. Sebesvari, 2019: Sea Level Rise and Implications for Low-Lying Islands, Coasts and Communities. In: IPCC Special Report on the Ocean and Cryosphere in a Changing Climate [H.-O. Pörtner, D.C. Roberts, V. Masson-Delmotte, P. Zhai, M. Tignor, E. Poloczanska, K. Mintenbeck, A. Alegría, M. Nicolai, A. Okem, J. Petzold, B. Rama, N.M. Weyer (eds.)]. Cambridge University Press, Cambridge, UK and New York, NY, USA, pp. 321-445. https://doi.org/10.1017/9781009157964.006

Palmer, M.D., Gregory, J.M., Bagge, M., Calvert, D., Hagedoorn, J.M., Howard, T., Klemann, V., Lowe, J.A., Roberts, C.D., Slangen, A.B.A., Spada, G., 2020. Exploring the Drivers of Global and Local Sea-Level Change Over the 21st Century and Beyond. Earth's Future 8, e2019EF001413. https://doi.org/10.1029/2019EF001413

Ranger, N., Reeder, T., Lowe, J., 2013. Addressing 'deep' uncertainty over long-term climate in major infrastructure projects: four innovations of the Thames Estuary 2100 Project. EURO J Decis Process 1, 233–262. https://doi.org/10.1007/s40070-013-0014-5

Ravndal, O.R.; Sande, B.H. Ekstremverdianalyse av Vannstandsdata Langs Norskekysten; Technical Report NDDF 16-1; Norwegian Mapping Authority, Hydrographic Service: Stavanger, Norway, January 2016; p. 26., n.d.

Reistad, M., Breivik, Ø., Haakenstad, H., Aarnes, O.J., Furevik, B.R., Bidlot, J.-R., 2011. A high-resolution hindcast of wind and waves for the North Sea, the Norwegian Sea, and the Barents Sea. Journal of Geophysical Research: Oceans 116. https://doi.org/10.1029/2010JC006402

Richter, K., Nilsen, J.E.Ø., Drange, H., 2012. Contributions to sea level variability along the Norwegian coast for 1960–2010. Journal of Geophysical Research: Oceans 117. https://doi.org/10.1029/2011JC007826

Richter, K., Riva, R. e. m., Drange, H., 2013. Impact of self-attraction and loading effects induced by shelf mass loading on projected regional sea level rise. Geophysical Research Letters 40, 1144–1148. https://doi.org/10.1002/grl.50265

Seneviratne, S.I., X. Zhang, M. Adnan, W. Badi, C. Dereczynski, A. Di Luca, S. Ghosh, I. Iskandar, J. Kossin, S. Lewis, F. Otto, I. Pinto, M. Satoh, S.M. Vicente-Serrano, M. Wehner, and B. Zhou, 2021: Weather and Climate Extreme Events in a Changing Climate. In Climate Change 2021: The Physical Science Basis. Contribution of Working Group I to the Sixth Assessment Report of the Intergovernmental Panel on Climate Change [Masson-Delmotte, V., P. Zhai, A. Pirani, S.L. Connors, C. Péan, S. Berger, N. Caud, Y. Chen, L. Goldfarb, M.I. Gomis, M. Huang, K. Leitzell, E. Lonnoy, J.B.R. Matthews, T.K. Maycock, T. Waterfield, O. Yelekçi, R. Yu, and B. Zhou (eds.)]. Cambridge University Press, Cambridge, United Kingdom and New York, NY, USA, pp. 1513–1766, doi:10.1017/9781009157896.013.

Shchepetkin, A.F., McWilliams, J.C., 2005. The regional oceanic modeling system (ROMS): a split-explicit, free-surface, topography-following-coordinate oceanic model. Ocean Modelling 9, 347–404. https://doi.org/10.1016/j.ocemod.2004.08.002

Simpson, M. J. R. (2024). Relative sea-level projections for Norway based on IPCC AR6 [Data set]. Zenodo. https://doi.org/10.5281/zenodo.10793963

Simpson, M. J. R., J. E. Ø. Nilsen, O. R. Ravndal, K. Breili, H. Sande, H. P. Kierulf, H. Steffen, E. Jansen, M. Carson and O. Vestøl (2015). Sea Level Change for Norway: Past and Present Observations and Projections to 2100. Norwegian Centre for Climate Services report 1/2015, ISSN 2387-3027, Oslo, Norway., n.d.

Simpson, M.J.R., Breili, K., Kierulf, H.P., 2014. Estimates of twenty-first century sea-level changes for Norway. Clim Dyn 42, 1405–1424. https://doi.org/10.1007/s00382-013-1900-z

Simpson, M.J.R., Ravndal, O.R., Sande, H., Nilsen, J.E.Ø., Kierulf, H.P., Vestøl, O., Steffen, H., 2017. Projected 21st Century Sea-Level Changes, Observed Sea Level Extremes, and Sea Level Allowances for Norway. Journal of Marine Science and Engineering 5, 36. https://doi.org/10.3390/jmse5030036

Skjong, M., Naess, A., Næss, O.E.B., 2013. Statistics of Extreme Sea Levels for Locations along the Norwegian Coast. coas 29, 1029–1048. https://doi.org/10.2112/JCOASTRES-D-12-00208.1

Slangen, A.B.A., Palmer, M.D., Camargo, C.M.L., Church, J.A., Edwards, T.L., Hermans, T.H.J., Hewitt, H.T., Garner, G.G., Gregory, J.M., Kopp, R.E., Santos, V.M., Wal, R.S.W. van de, 2023. The evolution of 21st century sea-level projections from IPCC AR5 to AR6 and beyond. Cambridge Prisms: Coastal Futures 1, e7. https://doi.org/10.1017/cft.2022.8

Staneva, J., Alari, V., Breivik, Ø., Bidlot, J.-R., Mogensen, K., 2017. Effects of wave-induced forcing on a circulation model of the North Sea. Ocean Dynamics 67, 81–101. https://doi.org/10.1007/s10236-016-1009-0

Sweet, W.V., B.D. Hamlington, R.E. Kopp, C.P. Weaver, P.L. Barnard, D. Bekaert, W. Brooks, M. Craghan, G. Dusek, T. Frederikse, G. Garner, A.S. Genz, J.P. Krasting, E. Larour, D. Marcy, J.J. Marra, J. Obeysekera, M. Osler, M. Pendleton, D. Roman, L. Schmied, W. Veatch, K.D. White, and C. Zuzak, 2022: Global and Regional Sea Level Rise Scenarios for the United States: Updated Mean Projections and Extreme Water Level Probabilities Along U.S. Coastlines. NOAA Technical Report NOS 01. National Oceanic and Atmospheric Administration, National Ocean Service, Silver Spring, MD, 111 pp. https://oceanservice.noaa.gov/hazards/sealevelrise/noaa-nostechrpt01-global-regional-SLR-scenarios-US.pdf

Taburet, G., Sanchez-Roman, A., Ballarotta, M., Pujol, M.-I., Legeais, J.-F., Fournier, F., Faugere, Y., Dibarboure, G., 2019. DUACS DT2018: 25 years of reprocessed sea level altimetry products. Ocean Science 15, 1207–1224. https://doi.org/10.5194/os-15-1207-2019

van de Wal, R.S.W., Nicholls, R.J., Behar, D., McInnes, K., Stammer, D., Lowe, J.A., Church, J.A., DeConto, R., Fettweis, X., Goelzer, H., Haasnoot, M., Haigh, I.D., Hinkel, J., Horton, B.P., James, T.S., Jenkins, A., LeCozannet, G., Levermann, A., Lipscomb, W.H., Marzeion, B., Pattyn, F., Payne, A.J., Pfeffer, W.T., Price, S.F., Seroussi, H., Sun, S., Veatch, W., White, K., 2022. A High-End Estimate of Sea Level Rise for Practitioners. Earth's Future 10, e2022EF002751. https://doi.org/10.1029/2022EF002751

Vestøl, O., Ågren, J., Steffen, H., Kierulf, H., Tarasov, L., 2019. NKG2016LU: a new land uplift model for Fennoscandia and the Baltic Region. J Geod 93, 1759–1779. https://doi.org/10.1007/s00190-019-01280-8

Vousdoukas, M.I., Mentaschi, L., Voukouvalas, E., Verlaan, M., Jevrejeva, S., Jackson, L.P., Feyen, L., 2018. Global probabilistic projections of extreme sea levels show intensification of coastal flood hazard. Nat Commun 9, 2360. https://doi.org/10.1038/s41467-018-04692-w

Wahl, T., Haigh, I.D., Nicholls, R.J., Arns, A., Dangendorf, S., Hinkel, J., Slangen, A.B.A., 2017. Understanding extreme sea levels for broad-scale coastal impact and adaptation analysis. Nat Commun 8, 16075. https://doi.org/10.1038/ncomms16075

Williams, J., Horsburgh, K.J., Williams, J.A., Proctor, R.N.F., 2016. Tide and skew surge independence: New insights for flood risk. Geophysical Research Letters 43, 6410–6417. https://doi.org/10.1002/2016GL069522

Wolf, J., Woolf, D.K., 2006. Waves and climate change in the north-east Atlantic. Geophysical Research Letters 33. https://doi.org/10.1029/2005GL025113

Wolf, T., Outten, S., Mangini, F., Chen, L., Nilsen, J.E.Ø., 2023. Analysis of storm surge events along the Norwegian coast. Frontiers in Earth Science 11.

Zappa, G., Shaffrey, L.C., Hodges, K.I., 2013. The Ability of CMIP5 Models to Simulate North Atlantic Extratropical Cyclones. Journal of Climate 26, 5379–5396. https://doi.org/10.1175/JCLI-D-12-00501.1

The following institutions have contributed to this report and its associated data products:

Citation:

Simpson, M.J.R., Bonaduce, A., Borck, H.S., Breili, K., Breivik, Ø., Ravndal, O.R., Richter, K., 2024. Sea-Level Rise and Extremes in Norway: Observations and Projections Based on IPCC AR6. Norwegian Centre for Climate Services report 1/2024, ISSN 2704-1018, Oslo, Norway.